GAS SENSOR MICROSYSTEMS BASED ON NANOSTRUCTURED LAYERS VIA ANODIC OXIDATION

Raúl Calavia Boldú

Dipòsit Legal: T. 1428-2012

ADVERTIMENT. L'accés als continguts d'aquesta tesi doctoral i la seva utilització ha de respectar els drets de la persona autora. Pot ser utilitzada per a consulta o estudi personal, així com en activitats o materials d'investigació i docència en els termes establerts a l'art. 32 del Text Refós de la Llei de Propietat Intel·lectual (RDL 1/1996). Per altres utilitzacions es requereix l'autorització prèvia i expressa de la persona autora. En qualsevol cas, en la utilització dels seus continguts caldrà indicar de forma clara el nom i cognoms de la persona autora i el títol de la tesi doctoral. No s'autoritza la seva reproducció o altres formes d'explotació efectuades amb finalitats de lucre ni la seva comunicació pública des d'un lloc aliè al servei TDX. Tampoc s'autoritza la presentació del seu contingut en una finestra o marc aliè a TDX (framing). Aquesta reserva de drets afecta tant als continguts de la tesi com als seus resums i índexs.

ADVERTENCIA. El acceso a los contenidos de esta tesis doctoral y su utilización debe respetar los derechos de la persona autora. Puede ser utilizada para consulta o estudio personal, así como en actividades o materiales de investigación y docencia en los términos establecidos en el art. 32 del Texto Refundido de la Ley de Propiedad Intelectual (RDL 1/1996). Para otros usos se requiere la autorización previa y expresa de la persona autora. En cualquier caso, en la utilización de sus contenidos se deberá indicar de forma clara el nombre y apellidos de la persona autora y el título de la tesis doctoral. No se autoriza su reproducción u otras formas de explotación efectuadas con fines lucrativos ni su comunicación pública desde un sitio ajeno al servicio TDR. Tampoco se autoriza la presentación de su contenido en una ventana o marco ajeno a TDR (framing). Esta reserva de derechos afecta tanto al contenido de la tesis como a sus resúmenes e índices.

WARNING. Access to the contents of this doctoral thesis and its use must respect the rights of the author. It can be used for reference or private study, as well as research and learning activities or materials in the terms established by the 32nd article of the Spanish Consolidated Copyright Act (RDL 1/1996). Express and previous authorization of the author is required for any other uses. In any case, when using its content, full name of the author and title of the thesis must be clearly indicated. Reproduction or other forms of for profit use or public communication from outside TDX service is not allowed. Presentation of its content in a window or frame external to TDX (framing) is not authorized either. These rights affect both the content of the thesis and its abstracts and indexes.

UNIVERSITAT ROVIRA I VIRGILI
GAS SENSOR MICROSYSTEMS BASED ON NANOSTRUCTURED LAYERS VIA ANODIC OXIDATION
Raúl Calavia Boldú
Dipòsit Legal: T. 1428-2012

Raúl Calavia Boldú

GAS SENSOR MICROSYSTEMS BASED ON NANOSTRUCTURED LAYERS VIA ANODIC OXIDATION

DOCTORAL THESIS

Supervised by **Dr. Eduard Llobet Valero** and **Dr. Alexander Mozalev**

Department of

Electronic, Electrical & Automation Control Engineering

UNIVERSITAT ROVIRA I VIRGILI

Tarragona

2012

UNIVERSITAT ROVIRA I VIRGILI
GAS SENSOR MICROSYSTEMS BASED ON NANOSTRUCTURED LAYERS VIA ANODIC OXIDATION
Raúl Calavia Boldú
Dipòsit Legal: T. 1428-2012

UNIVERSITAT
ROVIRA I VIRGILI

ESCOLA TÈCNICA SUPERIOR D'ENGINYERIA
DEPARTAMENT D'ENGINYERIA ELECTRONICA, ELÈCTRICA I AUTOMÀTICA

Avinguda dels Països Catalans, 26
Campus sescelades
43007 Tarragona
Tel. (977) 55 96 10
Fax (977) 55 96 05
e-mail: secelec@etse.urv.es
http://www.etse.urv.es/DEEEA/

I HEREBY CONFIRM that this thesis entitled "Gas sensor microsystems based on nanostructured layers via anodic oxidation", presented by Raúl Calavia Boldú for being awarded the Doctorate Degree has been conducted under my supervisión at the Department of Electronic, Electrical and Automation Engineering of this University.

Tarragona, the june 15th 2012

Thesis supervisors

Dr. Eduard Llobet Valero   Dr. Alexander Mozalev

UNIVERSITAT ROVIRA I VIRGILI
GAS SENSOR MICROSYSTEMS BASED ON NANOSTRUCTURED LAYERS VIA ANODIC OXIDATION
Raúl Calavia Boldú
Dipòsit Legal: T. 1428-2012

UNIVERSITAT ROVIRA I VIRGILI
GAS SENSOR MICROSYSTEMS BASED ON NANOSTRUCTURED LAYERS VIA ANODIC OXIDATION
Raúl Calavia Boldú
Dipòsit Legal: T. 1428-2012

Dedicado

a mis padres, Alfredo y María Dolores

a mi hermano, Francisco Javier

y a Mercè

UNIVERSITAT ROVIRA I VIRGILI
GAS SENSOR MICROSYSTEMS BASED ON NANOSTRUCTURED LAYERS VIA ANODIC OXIDATION
Raúl Calavia Boldú
Dipòsit Legal: T. 1428-2012

UNIVERSITAT ROVIRA I VIRGILI
GAS SENSOR MICROSYSTEMS BASED ON NANOSTRUCTURED LAYERS VIA ANODIC OXIDATION
Raúl Calavia Boldú
Dipòsit Legal: T. 1428-2012

Agradecimientos

Me gustaría agradecer a la Universitat Rovira i Virgili la posibilidad de haber realizado esta tesis doctoral y a todas aquellas personas que directa o indirectamente me han ayudado durante los años que he estado dedicado al desarrollo de la misma.

En primer lugar me gustaría dar mi más sincero agradecimiento a mis directores Eduard Llobet Valero y Alexander Mozalev por su incondicional ayuda en el desarrollo del presente trabajo, sin la cual habría sido imposible desarrollarlo.

También me gustaría agradecer a Xavier Vilanova y Xavier Correig su ayuda en todos los momentos en los que la he necesitado.

Durante los años que he estado haciendo este trabajo he conocido mucha gente que me ha ayudado mucho tanto a nivel profesional como personal, por ello me gustaría dar un especial agradecimiento a Rosa María Vázquez, Fernando Blanco, Stella Vallejos, Pierrick Clement, Fatima Ezahara, Lukas Vojkuvka, Alexander Vergara, Toni Stoycheva, Trifon Trifonov, Edwin Espinosa…

Durante este tiempo han habido momentos buenos y malos, por lo que me gustaría hacer un especial agradecimiento a Roser Ingles, Mariona Vinaixa, Serena Pujol y Mariana Trifonova por estar siempre a mi lado tanto a nivel profesional como personal.

UNIVERSITAT ROVIRA I VIRGILI
GAS SENSOR MICROSYSTEMS BASED ON NANOSTRUCTURED LAYERS VIA ANODIC OXIDATION
Raúl Calavia Boldú
Dipòsit Legal: T. 1428-2012

Por otro lado este trabajo no se podría haber realizado sin la incalculable ayuda de los técnicos del departamento de electrónica Jordi Maré, Josep Maria Badia, Jordi Deosdad, Jaume Pros y Carmelo Fuentes que además de compañeros de trabajo son muy buenos amigos.

A Álvaro Morato me gustaría agradecerle esos ratos en los que hacíamos esas interesantísimas discusiones científicas sobre química y que tanto me han ayudado en el desarrollo de este trabajo.

Dicho esto me gustaría agradecer a mis amigos Albert Mota y David Castellví su incondicional amistad demostrada infinidad de veces.

Finalmente me gustaría agradecer a mis padres Alfredo y Maria Dolors, y a mi hermano Francisco Javier su apoyo durante el desarrollo del presente trabajo.

Por último me gustaría agradecer a Mercè Priego su inestimable apoyo que tanto me ha ayudado a hacer realidad esta tesis doctoral, gracias por ser como eres.

Muchas gracias a todos

UNIVERSITAT ROVIRA I VIRGILI
GAS SENSOR MICROSYSTEMS BASED ON NANOSTRUCTURED LAYERS VIA ANODIC OXIDATION
Raúl Calavia Boldú
Dipòsit Legal: T. 1428-2012

Thesis publications

Full journal papers

Calavia, R.; Mozalev, A.; Vazquez, R.; Gracia, I.; Cane, C.; Ionescu, R.; Llobet, E., Fabrication of WO3 nanodot-based microsensors highly sensitive to hydrogen, *Sens. Actuator B-Chem.*, (2010) 149, 352.

Calavia, R., Annanouch, F., Correig, X., Yanes, O.,Nanostructure Initiator Mass Spectrometry for tissue imaging in metabolomics: Future prospects and perspectives, *J Prot*, (2012) 75, 5061.

Vergara A., Calavia R., Vázquez R., Mozalev A., Abdelghani A., Huerta R., Hines E., Llobet E., Multi-Frequency Interrogation of Nanostructured Gas-Sensor Arrays: A Tool for Analyzing Response Kinetics, *Analytical Chemistry*, (2012) 84, 7502.

Mozalev A., Calavia R., Vazquez R., Gracia I., Cané C., Guirado F., Correig X., Vilanova X., Llobet E., Micro-hotplate hydrogen sensor with the porous-alumina-supported nanostructured tungsten-oxide active layer, *In preparation*

International conference contributions

Calavia, R.; Vazquez, R. M.; Llobet, E.; Vergara, A., Multi-Frequency Interrogation of Nanostructured Gas Sensor Arrays, *In 2010 IEEE Sensors*, Kona, HI, USA (2010); pp 1083.

Calavia, R.; Mozalev, A.; Kahtko, V.; Gorokh, G.; Vilanova, X.; Correig, X.; Gràcia, I.; Cané, C.; Llobet, E., A H2 microsensor based on nanocolumnar tungsten oxide grown by template-assisted anodization, *IEEE Transducers*, Denver, CO, USA (2009); pp 1313.

UNIVERSITAT ROVIRA I VIRGILI
GAS SENSOR MICROSYSTEMS BASED ON NANOSTRUCTURED LAYERS VIA ANODIC OXIDATION
Raúl Calavia Boldú
Dipòsit Legal: T. 1428-2012

National conference contributions

Calavia, R.; Mozalev, A.; Vilanova, X.; Correig, X.; Llobet, E., WO(3) nanorods on Si by anodising Al/W/Ti layers, *In Proceedings of the 2009 Spanish Conference on Electron Devices*, Santiago de Compostela, (2009); pp 327.

Other journal publications

Calavia, R.; Brezmes, J.; Ionescu, R.; Llobet, E., Regression using fuzzy adaptive resonant theory neural network, *Electron. Lett.*, (2006) 42, 1415.

UNIVERSITAT ROVIRA I VIRGILI
GAS SENSOR MICROSYSTEMS BASED ON NANOSTRUCTURED LAYERS VIA ANODIC OXIDATION
Raúl Calavia Boldú
Dipòsit Legal: T. 1428-2012

Table of contents

1. Introduction 1

1.1 Motivation 4
1.2 Objectives 5
1.3 Structure of the thesis 9

2. State of the art 11

2.1 Metal oxide gas sensors 13
2.1.1 Micromachined gas sensors 25
2.1.2 Active layer deposition techniques 30
2.1.2.1 Thick film techniques 31
2.1.2.1.1 Screen printing 31
2.1.2.1.2 Sol-gel 31
2.1.2.1.3 Drop-coating 32
2.1.2.2 Thin film techniques 32
2.1.2.2.1 Chemical vapour deposition 32
2.1.2.2.2 Atomic layer deposition 33
2.1.2.2.3 Sputtering 34
2.1.3 Hydrogen detection 35
2.1.4 WO_3 as sensing material 36
2.1.5 Nanostructured gas sensors 40
2.2 Anodising of valve metals 43
2.2.1 Porous anodic alumina formation 46
2.2.2 Pore morphology control 53
2.3 Anodising of aluminium/valve-metal bilayer 56
2.4 Summary 58

UNIVERSITAT ROVIRA I VIRGILI
GAS SENSOR MICROSYSTEMS BASED ON NANOSTRUCTURED LAYERS VIA ANODIC OXIDATION
Raúl Calavia Boldú
Dipòsit Legal: T. 1428-2012

2.5 Bibliography 58

3. Sample fabrication 71

3.1 Experimental set-up 74
3.2 Anodising thin film aluminium on an oxide-coated silicon wafer 86
3.2.1 Preparation of porous alumina supported WO_3 layers 90
3.2.1.1 The formation of porous alumina templates 90
3.2.1.2 Deposition of the sensing material on the alumina templates 93
3.2.1.2.1 WO_3 films sputter-deposited by a magnetron method 93
3.2.1.2.2 ZnO film preparated by atomic layer deposition 97
3.2.2 WO_3 nanodot film grown by self-organised anodising 98
3.3 The technological approaches 102
3.3.1 Combining the anodising with a lift-off process 104
3.3.2 The anodising combined with etch-back photolithography 108
3.3.3 Opening the contact windows to micro-heaters before anodising 112
3.3.4 Bulk micromachining 116
3.3.5 The outcomes of the different approaches 117

UNIVERSITAT ROVIRA I VIRGILI
GAS SENSOR MICROSYSTEMS BASED ON NANOSTRUCTURED LAYERS VIA ANODIC OXIDATION
Raúl Calavia Boldú
Dipòsit Legal: T. 1428-2012

3.3.6 WO_3 nanodot film as active layer for the micro-machined gas sensors 119

3.4 Summary 122

3.5 Bibliography 123

4. Morphological, compositional and crystallographic analysis 125

4.1 Morphological analysis 128

4.1.1 SEM observation 128

4.1.1.1 Porous alumina supported WO_3 layers 129

4.1.1.2 WO_3 nanodots derived from the anodised Al/Ti layers 134

4.2 Elemental and crystallographic analysis 139

4.2.1 Porous alumina supported WO_3 layers 139

4.2.2 WO_3 nanodot film derived from anodised Al/W bilayer 143

4.3 Summary 146

4.4 Bibliography 148

5. Gas sensing characterisation 149

5.1 Gas sensing set-up 151

5.2 Sensor employing porous alumina supported WO_3 active layer 157

5.3 Sensor with WO_3 nanodot active layer 161

5.4 Comparison between the planar and nanostructured WO_3 layers 169

5.5 Gas sensing mechanism 171

UNIVERSITAT ROVIRA I VIRGILI
GAS SENSOR MICROSYSTEMS BASED ON NANOSTRUCTURED LAYERS VIA ANODIC OXIDATION
Raúl Calavia Boldú
Dipòsit Legal: T. 1428-2012

5.6 Summary 173

5.7 Bibliography 174

6. Conclusions and future work 175

6.1 Conclusions 177

6.2 Future work 181

6.2.1 Effect of surface roughness of sputter-deposited aluminium 181

6.2.2 Effect of the aspect ratio of porous-alumina-assisted tungsten oxide nano-structures on their gas sensing properties 187

6.2.3 Employing other read-out techniques like pseudorandom sequences for temperature modulation 187

Appendix 189

Calculation of image corrections for FIB 191

Bibliography 194

Chapter 1

Introduction

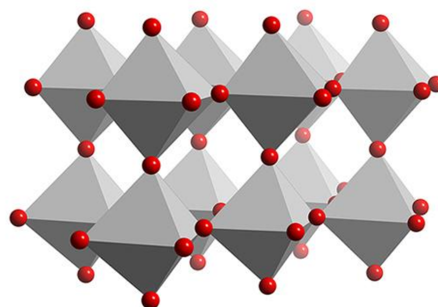

UNIVERSITAT ROVIRA I VIRGILI
GAS SENSOR MICROSYSTEMS BASED ON NANOSTRUCTURED LAYERS VIA ANODIC OXIDATION
Raúl Calavia Boldú
Dipòsit Legal: T. 1428-2012

UNIVERSITAT ROVIRA I VIRGILI
GAS SENSOR MICROSYSTEMS BASED ON NANOSTRUCTURED LAYERS VIA ANODIC OXIDATION
Raúl Calavia Boldú
Dipòsit Legal: T. 1428-2012

1. Introduction

The need for monitoring airborne pollutants, the protection of workers in the petrochemical industry or even the detection of natural gas leaks or carbon monoxide from incomplete combustion in boilers in domestic environments has been driving the development of gas analysing systems.

Gas sensors have experienced a revolution similar to electronics, i.e., a decrease in size and power consumption. While at the beginning, resistive gas sensors were bulky and power consumption of a single device was typically a few hundred milliwatts, nowadays micromachined silicon technology has brought a dramatic decrease in size together with milliwatt power consumption. This has opened the possibility of developing portable analysers for many different applications such as alcoholmeters, fire detection units, carbon monoxide alarm monitors or analyzers for contamination within a fire, only to mention a few. The world market for resistive metal oxide gas sensors only was worth over 300 M € in 2011 with over 200 M units sold.

The technology favours the development of sensors with ever-decreasing size and power consumption. However, decreasing the size of the active area may lead to a decrease in sensitivity. Therefore, nanostructuring of the active layers has been the active and competitive area of research over the last few years. In particular, nanoscience and nanotechnology are enabling the

UNIVERSITAT ROVIRA I VIRGILI
GAS SENSOR MICROSYSTEMS BASED ON NANOSTRUCTURED LAYERS VIA ANODIC OXIDATION
Raúl Calavia Boldú
Dipòsit Legal: T. 1428-2012

growth of well-known gas-sensitive materials with better controlled morphology, crystalline size and chemical composition. Such materials (e.g. nanowires, nanotubes, nanorods) offer not only substantially enlarged surface to volume ratio and, therefore, better sensitivity, but also many new and unusual properties.

This rise in the need for nanostructuring gas-sensitive materials has given a second youth to some well-known techniques, like the anodisation of aluminium, which up to now has been used mainly for electrical isolation, wear and corrosion protection.

1.1 Motivation

Metal-oxide-based gas sensors have been studied over the last few decades because they are rather sensitive, easy to be included in a measuring system, cost-effective and respond to a wide spectrum of oxidising and reducing gases. This is why they are used in both consumer electronic appliances and special-purpose electronics, such as gas alarms, medical diagnostics, leak detection and many more.

Unfortunately, these sensors show some limitations like their poor selectivity (they cannot be made specific for the detection of a given target species) and long-time stability (they generally show some baseline and response drift associated with poisoning and high-temperature rearrangement of their structure during normal operation). However, modern nanotechnologies give rise to new and useful properties of these materials and there has been an

UNIVERSITAT ROVIRA I VIRGILI
GAS SENSOR MICROSYSTEMS BASED ON NANOSTRUCTURED LAYERS VIA ANODIC OXIDATION
Raúl Calavia Boldú
Dipòsit Legal: T. 1428-2012

explosion in the number of studies striving to overcome their drawbacks.

This thesis shows the possibility to form nanostructured metal oxide layers on silicon-based micromachined hotplates using anodising technologies and, specifically, the methods for forming porous alumina as templates and the field-directing systems.

We have focused on tungsten oxide because this is one of the most studied metal oxides for gas sensing applications. However, the results of this work could be extrapolated to other metal oxides, especially those grown on valve metals (e.g., Ti, Zr, Nb) because they can be obtained by similar anodisation techniques.

In this work, the sensors have been characterised mostly in the presence of hydrogen gas. Hydrogen has been in the focus of numerous studies because of a lot of applications related to renewable energy and the green economy that use it, for example, fuel cells or electric vehicles. Since hydrogen is a flammable gas, it must be extensively controlled in order to prevent accidents or to monitor the correct function of industrial processes.

1.2 Objectives

The goal of the present work is to develop integral technologies for tungsten oxide gas sensors on silicon-based micro-hotplates, having a substantially increased sensitivity, due to nanostructuring the sensing layers. To this end, porous anodic alumina films (layers) are to be synthesised and employed as templates and parts of

UNIVERSITAT ROVIRA I VIRGILI
GAS SENSOR MICROSYSTEMS BASED ON NANOSTRUCTURED LAYERS VIA ANODIC OXIDATION
Raúl Calavia Boldú
Dipòsit Legal: T. 1428-2012

electrochemical systems for growing porous-anodic-alumina-supported and self-organized nanostructured tungsten oxide layers.

To achieve the goal, the following objectives are to be met.

1. *Optimization of anodising processes to grow porous alumina layers from sputter-deposited aluminium onto oxide-coated silicon wafers*

The substrate of the metal oxide gas sensors must be an insulator material because the electrodes must measure the conductivity of the sensing layer only. Therefore, the first work is done to improve the anodisation of a thin aluminium layer sputter-deposited onto an insulating substrate (SiO_2). The anodising of such layers differs from that for bulk aluminium because here, the aluminium thickness becomes comparable with the cell and pore size and there is no chance to employ electropolishing. As a result, the voltage and current behaviour becomes increasingly specific because the aluminium layer is consumed very fast. Moreover, all these peculiarities must be considered in relationship with a particular design of gas sensing device to be fabricated and tested, including, for instance, anodisation of aluminium sputtered over a photoresist mask or superimposed on another valve metal for improving the adhesion and providing effective current distribution during the anodising.

UNIVERSITAT ROVIRA I VIRGILI
GAS SENSOR MICROSYSTEMS BASED ON NANOSTRUCTURED LAYERS VIA ANODIC OXIDATION
Raúl Calavia Boldú
Dipòsit Legal: T. 1428-2012

2. *Development of anodising and post-anodising processes to achieve porous-alumina-assisted growth of a tungsten oxide nanodot array on a dielectric substrate.*

Anodising of aluminium superimposed on a different valve metal layer may result in the formation of quasi-one dimensional metal oxide nanostructures, like columns or wires. This behaviour has been known for tungsten oxide grown under the porous alumina film. By this work we extend the possibility of the process striving to fabricate anodic films consisting of tungsten oxide nanodots, not nanocolumns, which are considered more advantageous for the purpose of the present study. To this end, anodising behaviour, cooperative ionic transport and structural evolution of the relevant interfaces is to be studied.

3. *Optimization of technological, electrical and electrolytic conditions for the synthesis of porous-anodic-alumina-supported tungsten trioxide layers.*

The two-step anodizing process for forming porous anodic alumina as a supporting template for sputter-deposition of WO_3 sensing layers has been proved to be promising approach towards increasing the sensitivity of the metal oxide sensors. However, the anodising processes need to be modified in order to simplify the initial stages of film formation and cut down the number of treatments and anodising steps, in order to reduce the number of physical defects in these complex multi-layered structures and substantially increase the average yield of the sensor devices.

UNIVERSITAT ROVIRA I VIRGILI
GAS SENSOR MICROSYSTEMS BASED ON NANOSTRUCTURED LAYERS VIA ANODIC OXIDATION
Raúl Calavia Boldú
Dipòsit Legal: T. 1428-2012

4. *Investigation of surface morphology, chemical composition and crystallographic structure of the porous-alumina-supported WO_3 layers and WO_3 nanodot films synthesised via porous-alumina-assisted anodising.*

Field emission scanning electron microscopy, X-ray diffraction, energy dispersive X-ray analysis, high resolution transmission electron microscopy, sectioning with focused ion beam have been employed in this work to gain insight into the formation-structure-properties relationship of the complex thin film nanostructures in order to clarify their formation mechanism and extend their functionality to new applications.

5. Making the anodizing processes for forming nanoporous alumina templates and porous-alumina-assisted tungsten oxide nanodots compatible with standard silicon-based microtechnology by fabricating practical gas sensors.

The micromachined device that has been selected for the purpose of this study is the micro-hotplate developed at the Centro Nacional de Microelectronica in Barcelona (CNM-IMB). So the above-mentioned compatibility must be provided between the electrochemical processes and relevant materials and the standard techniques utilized in CNM for fabricating the micro-hotplate transducers. As a result, practical gas microsensors will be fabricated on 100-mm silicon wafer, diced and packaged.

UNIVERSITAT ROVIRA I VIRGILI
GAS SENSOR MICROSYSTEMS BASED ON NANOSTRUCTURED LAYERS VIA ANODIC OXIDATION
Raúl Calavia Boldú
Dipòsit Legal: T. 1428-2012

6. *Determining the gas sensing properties of the nanostructured tungsten oxide films prepared on the micro-hotplate transducers.*

Gas sensing studies have been performed for the sensors based on micro-hotplate transducers, prepared in accord with various approaches developed in this thesis for nanostructuring tungsten oxide films with the purpose of their utilisation as active layers for gas detection. A fully automated experimental set-up and relevant methodology has been developed for this purpose. The gas sensing mechanism in the new metal oxide nanostructures has been established and justified experimentally.

1.3 Structure of the thesis

Chapter 2 presents the state of the art in two fields directly related to the present work. The first field is the metal oxide gas sensors, where the basic sensing mechanisms are reviewed. This is followed by a description of the micro-hotplate transducers used as sensor platforms and finally, the influence of nanostructuring the sensing layers on their sensitivity and selectivity is discussed. The second field is the anodising of valve metals, with the focus on aluminium and tungsten, and a review is given of the basics of electrochemical oxidation with comprehensive description of porous anodic films on aluminium and the possibilities to alter the film structure and morphology.

In order to obtain a nanostructured tungsten trioxide gas sensor, various paths have been explored. In the first approach, a porous alumina film was grown and then coated with sputter-deposited

UNIVERSITAT ROVIRA I VIRGILI
GAS SENSOR MICROSYSTEMS BASED ON NANOSTRUCTURED LAYERS VIA ANODIC OXIDATION
Raúl Calavia Boldú
Dipòsit Legal: T. 1428-2012

tungsten oxide to form nanoporous or nanotubular tungsten oxide film. In the second approach, the anodisation of an Al/W bilayer was conducted to obtain self-organised tungsten oxide nanodot film, and to this end, the porous alumina film was selectively etched away. Thus, Chapter 3 shows how to make compatible the above-mentioned anodisation technologies with standard silicon micromachining technology. In this chapter, the different ways are developed and realised to obtain nanostructured tungsten oxide on the membrane of a micro hotplate transduce, and the advantages and disadvantages of each approach are discussed.

Chapter 4 presents the morphological, compositional and crystallographic characterisation of the sensor chips and their parts developed in this work. In case of the morphological analysis, electron microscopy was used, and for crystallographic study, X-ray diffraction was employed. The compositional studies included energy-dispersive X-ray spectroscopy.

The results of gas sensing characterisation of the new sensor chips is shown in Chapter 5, where the response to hydrogen was systematically studied and the results are compared with those obtained with a planar (i.e. unstructured) tungsten oxide active layer prepared on an identical micro-hotplate.

Chapter 6 gives general conclusions derived from the findings of the present work and gives an outlook into future challenges associated with the work done.

UNIVERSITAT ROVIRA I VIRGILI
GAS SENSOR MICROSYSTEMS BASED ON NANOSTRUCTURED LAYERS VIA ANODIC OXIDATION
Raúl Calavia Boldú
Dipòsit Legal: T. 1428-2012

Chapter 2

State of the art

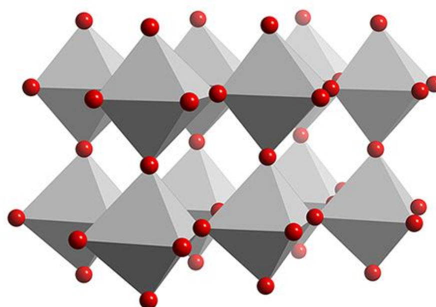

UNIVERSITAT ROVIRA I VIRGILI
GAS SENSOR MICROSYSTEMS BASED ON NANOSTRUCTURED LAYERS VIA ANODIC OXIDATION
Raúl Calavia Boldú
Dipòsit Legal: T. 1428-2012

UNIVERSITAT ROVIRA I VIRGILI
GAS SENSOR MICROSYSTEMS BASED ON NANOSTRUCTURED LAYERS VIA ANODIC OXIDATION
Raúl Calavia Boldú
Dipòsit Legal: T. 1428-2012

2. State of the art

In this chapter we review the state of the art of metal oxide (MOX) gas sensors and show how it is possible to improve their sensitivity and selectivity via nanostructuring the sensing material.

There is a number of techniques for nanostructuring sensing layers but in this chapter anodisation techniques are mostly reviewed because anodisation-related technologies have been developed and utilised in this work.

2.1 Metal oxide gas sensors

A generic chemical sensor is based on a sensitive layer that interacts with chemical or biological substances which are in contact with this layer and a transducer that converts the change in a chemical parameter into an electrical or optical signal, which can be measured.

Gas sensors are a family within chemical sensors, where the chemical substance to be detected is present in the gaseous phase. There are different types of gas sensors depending of the sensing and transduction principles, e.g. semiconductor [1, 2], electrochemical [3], catalytic [4], etc.

MOX based gas sensors are semiconductor type and they are among the most studied. These sensors transduce a chemical signal into an easy-to-measure change in electrical resistance. The MOX sensors have been the subject of research for a few decades.

UNIVERSITAT ROVIRA I VIRGILI
GAS SENSOR MICROSYSTEMS BASED ON NANOSTRUCTURED LAYERS VIA ANODIC OXIDATION
Raúl Calavia Boldú
Dipòsit Legal: T. 1428-2012

For resistive gas sensors, there are different parameters that can be monitored because they qualify the sensor performance. Some of these parameters are as follows:

- Conductance/Resistance: the most important parameter because this is associated with the primary electrical property measured in order to analyse gases.
- Base line: the conductance/resistance of the sensor in the reference or carrier gas, typically dry air.
- Sensor response: the ratio between the change in the sensor resistance and the change in the gas concentration. The response may also be defined as $(S\ in\ gas)/(S\ in\ air)$ where S is the conductance [5].
- Sensitivity: the partial derivative of sensor response to gas concentration.
- Response time: the time taken to achieve 90 % of the final change in conductance. This parameter is used to determine practical applicability of a given sensor.
- Selectivity: the ratio between the response to a target gas and the response to interfering species [6].
- Stability: the chemical reaction at the surface of the sensor generates a long-term drift problem (poisoning) [7]. This problem can be minimised by a periodical calibration [6].

The sensing properties of MOX layers were discovered several decades ago (the 50's of the previous century) and such materials are still being studied in order to improve their sensitivity, selectivity and stability in detection of different gases. In the last

UNIVERSITAT ROVIRA I VIRGILI
GAS SENSOR MICROSYSTEMS BASED ON NANOSTRUCTURED LAYERS VIA ANODIC OXIDATION
Raúl Calavia Boldú
Dipòsit Legal: T. 1428-2012

years, one of the most studied problems in this technology has been the reduction in the power consumption of gas sensitive devices. MOX sensing layers often need temperatures that range from 20 ºC to 500 ºC to work properly. Therefore, a significant amount of energy is required to put the sensing layer to these operating temperatures. Nowadays, the technology is evolving towards a reduction in the dimensions and power consumption of gas sensitive devices in such a way that they become suitable for hand-held or portable detectors. Therefore, much research has been centred in the reduction of power consumption together with an improvement of the mechanical stability and reliability of micromachined transducers, while keeping a high performance in gas detection (sensitivity, selectivity and stability).

Like general semiconductors, MOX layers can be *n* or *p* type if their main charge carriers are electrons or holes, respectively. There are different *p*-type metal oxide materials applied for gas sensing such as CuO [8], Co_3O_4 [9] and TeO_2 [10], but the most common are *n*-type like SnO_2, WO_3 and TiO_2. We will focus on WO_3 semiconductor as the most promising material among the thin film metal oxides.

MOX semiconductor layers work because of oxidation and reduction reactions on their surfaces. Let us assume that we have an *n*-type MOX polycrystalline layer. When an oxidising gas, such as molecular oxygen, reaches the surface of the semiconductor, it chemisorbs and takes electrons from the conduction band of the semiconductor. These negatively charged oxygen ions adsorbed at

the surface of the semiconductor (or oxygen adsorbates) generate a depletion layer that results in free electrons being confined in the centre of MOX grains. As a result, the resistance of the MOX layer increases in the presence of oxygen. The reduction process for the same type of MOX layer is due to the presence of a gas, hydrogen for example, that reacts with oxygen species adsorbed at the surface of the MOX. Since the concentration of oxygen adsorbates is reduced, the depletion layer width is reduced accordingly and this results in a drop in the resistance of the MOX layer.

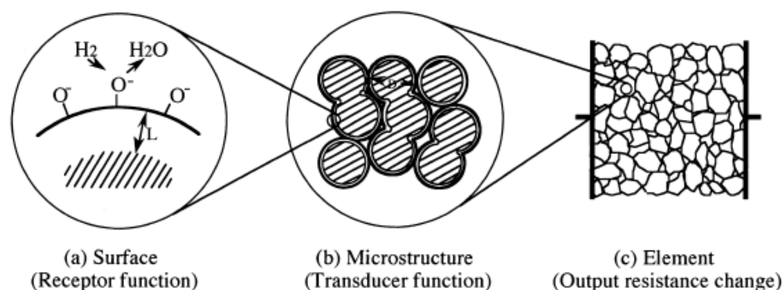

Figure 2-1 Interaction between oxygen molecules and polycrystalline metal oxide surface [11]

In other words, if we consider the grains that are in contact with the polycrystalline MOX film, a Shottky barrier develops between them upon oxygen adsorption. The height of this Shottky barrier can increase or decrease depending on the number of oxygen adsorbates (Figure 2-2), because both the width of the depletion layer and the number of free charge carriers depend on the equilibrium concentration of oxygen ions [12], [13].

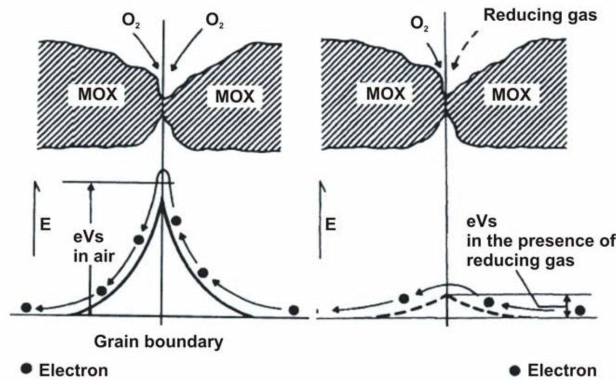

Figure 2-2 Schottky barrier between two nanocrystalls under an oxidising and reducing gas

In a polycrystalline metal oxide layer, every grain works as a simple detector [14], where the conductance of the layer is described by the following equation [15]:

$$G = [n]qu\ \frac{ld}{L} \tag{2-1}$$

where G is the conductance of the MOX crystal, $[n]$ is the free carrier density (electrons or holes), q is the elemental charge unit, u is the mobility of the free carriers and l, L and d are the dimensions of the crystal, i.e. width, length and thickness, respectively. The equation that describes the variation in conductivity is

$$\Delta G = \Delta[ns]qu\ \frac{l}{L} \tag{2-2}$$

where ΔG is the variation of the conductivity and $\Delta[ns]$ is the variation of the free carrier density by surface unit.

The oxygen ions in contact with the MOX crystal surface generate a variation in the free carriers, and finally the conductance changes.

UNIVERSITAT ROVIRA I VIRGILI
GAS SENSOR MICROSYSTEMS BASED ON NANOSTRUCTURED LAYERS VIA ANODIC OXIDATION
Raúl Calavia Boldú
Dipòsit Legal: T. 1428-2012

The normalised response of the gas sensor is shown as the following equation indicates:

$$\Delta G / G = \frac{\Delta[ns]}{[n]d} \qquad (2\text{-}3)$$

In accord with Equation 2-3, the response does not show a dependency with the size of the grain (length and width), but has an inversely proportional dependency with the grain diameter. It can be derived that the MOX layer will show increased response if its thickness is low and the diameter of grains is as small as possible. However, a large surface area should improve the interaction of gas with the sensitive layer and, therefore, the concentration of free carriers will increase.

Equation 2-3 is somewhat simplistic if we consider that the sensing mechanism in MOX gas sensors is rather complex. There are different factors that affect response and the three most important ones are the reception, the transducer and the utility factors (Figure 2-3) [16].

The reception is the chemical interaction between the metal oxide monocrystal grain surface and the oxygen ions and it depends on the oxidation and reduction reactions that may occur on the surface in the presence of a gas.

The transducer factor is the conversion from the chemical reaction of every monocrystal grain to the electrical resistivity. It depends on grain size because, as explained previously, the size of the grains does not directly affect the gas detection properties of a

metal oxide film, but, since every grain works as an individual detector, if the grains are smaller, the number of detectors increases (provided that the gas is able to reach and interact with all grains within a film). If the number of detectors increases, the final sensitivity will also increase [17].

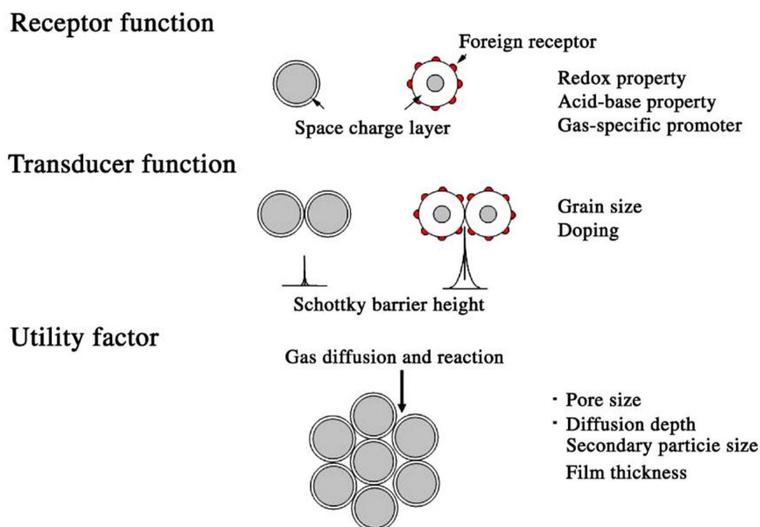

Figure 2-3 Factors that affect the sensitivity of a gas sensor

The third most important parameter to influence the sensitivity of a gas sensor is the utility factor, which indicates the real area of the active layer in contact with the gas, because depending of the gas properties and the morphology of the surface, some areas may not be accessible by the gas.

The porosity is one more important morphological parameter for the sensitivity, because if the material has a high porosity, the gas can enter into the material, and this results in an increase in the effective sensing area. The physical and chemical properties of the

UNIVERSITAT ROVIRA I VIRGILI
GAS SENSOR MICROSYSTEMS BASED ON NANOSTRUCTURED LAYERS VIA ANODIC OXIDATION
Raúl Calavia Boldú
Dipòsit Legal: T. 1428-2012

gas that has to diffuse within the pores of the sensing layer are of importance too and these parameters differ from gas to gas.

The thickness of the sensing layer is another important parameter, in particular, if the sensing layer obtained is compact. Under these conditions it is possible to model the sensor resistance as two resistances in parallel, one in contact with the environment and another without the contact with the gas (Figure 2-4). Only the first resistance is a sensing resistance because it accounts for the sensor area that chemically interacts with the environment. On the other hand, the second resistance can be considered as a fixed resistance. The final variation of the resistance depends on the ratio between the fixed resistance and the sensing resistance, and the maximum sensitivity is obtained when the thickness of the fixed resistance tends to 0 (the value tends to ∞). Therefore, typical methods to increase the sensitivity of a metal oxide gas sensor are based on the reduction of the thickness of the layer with fixed resistance [18] or the increase in film porosity.

The deposition technique can affect the different factors that determine the final sensitivity of the sensor because it determines the crystal phase, porosity, grain size and thickness of the layer. Therefore the deposition technique used is very important for determining the final gas sensing properties.

UNIVERSITAT ROVIRA I VIRGILI
GAS SENSOR MICROSYSTEMS BASED ON NANOSTRUCTURED LAYERS VIA ANODIC OXIDATION
Raúl Calavia Boldú
Dipòsit Legal: T. 1428-2012

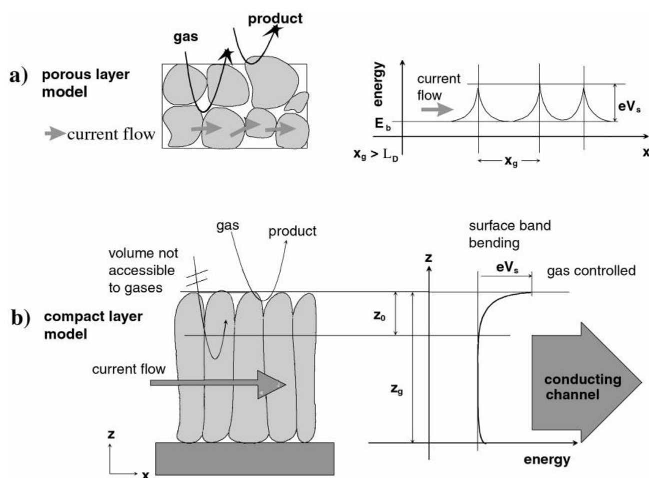

Figure 2-4 Influence of the sensing layer thickness on gas sensitivity.

Considering the different parameters that influence the sensitivity, the most used approach for increasing the sensitivity consists of reducing the size of grains of the metal oxide sensing layer. This can be achieved by using special processes like different calcinations, modified sputtering depositions [19, 20] and others [15]. Additionally, a very often employed strategy both to increase sensitivity and to tune selectivity of MOX films is the addition of small amounts of nanosized grains of noble metal materials. The presence of such surface modifiers increases sensitivity via catalytic effects (chemical sensitization or spill-over effects) [21, 22].

As explained above, the thickness of the sensing layer has a large influence on the sensitivity, and nowadays it is possible to obtain very thin gas sensitive layers with very large area to volume ratio [23].

UNIVERSITAT ROVIRA I VIRGILI
GAS SENSOR MICROSYSTEMS BASED ON NANOSTRUCTURED LAYERS VIA ANODIC OXIDATION
Raúl Calavia Boldú
Dipòsit Legal: T. 1428-2012

Not every substrate offers the best properties for obtaining sensors with a good performance. The good candidate substrates should have the following physical properties:

- Good insulating properties, so that the charge carriers may move between the electrodes across the sensing layer only.
- Thermal and chemical stability of the substrate because, generally, MOX sensors are operated at temperatures that are well above room temperature (e.g. up to 600ºC).
- Provide good adhesion to the gas sensitive layer. Bad adhesion may result in some areas of the layer to peel off and eventually in sensor failure.

Alumina is one of the most suitable substrate materials [11, 24-26] because it has all the physical properties that are needed and is easy to work with. Alumina is compatible with many different deposition techniques (see an example in Figure 2-5) and has become the most used substrate for gas sensors. However, in recent years, other substrate materials such as monocrystalline silicon have been investigated.

Silicon is a promising material because the fabrication of the gas sensor can be made compatible with standard silicon technology. Figure 2-6 shows a gas sensor on a silicon substrate [27]. Standard silicon technology at large scales of production offers an important decrease in the cost of individual gas sensors. Additionally, the gas sensor can be integrated in a chip with advanced electronics in

order to obtain a single device with signal processing and communication capabilities, for example.

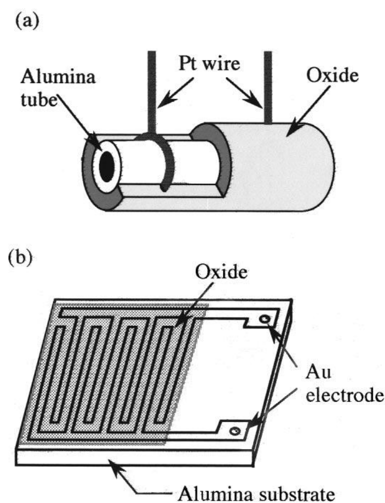

Figure 2-5 Schematic drawing of sensor devices. a) Sintered block type. b) Thick or thin film type

Figure 2-5 shows two typical configurations for a metal oxide gas sensor on alumina substrates, where Figure 2-5.a uses a tube of alumina with a heater coil (not shown) inside the tube and the metal oxide layer deposited in the external part of the alumina tube. Figure 2-5.b shows a planar configuration where one side of the alumina plate comprises the electrodes with the sensing layer on top and the heater is formed on the other side.

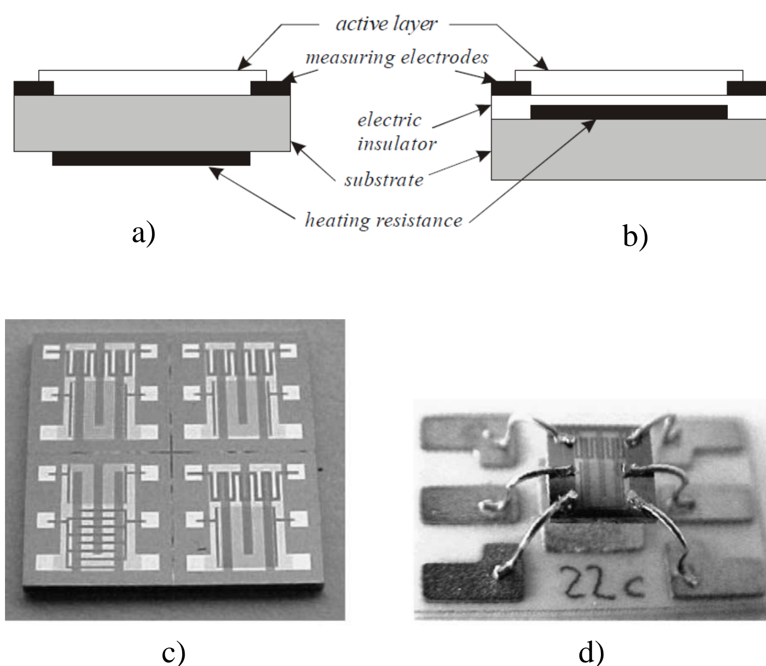

Figure 2-6 Variants of the sensor substrates. Up. Typical configuration of gas sensors. (a) Heater in the bottom. (b) Inner heater with higher power consumption efficiency. Down. (c) Four substrates with the inner heater (before dicing); (d) A mounted sensor

Figure 2-6 shows gas sensors fabricated on silicon substrates. Device architecture can be very similar to the case of planar sensors on alumina substrates (on one side of the silicon chip there are the electrodes and the active film, while on the other side the heater is located, see Figure 2-6.a). A different option is to use only one side of the silicon chip. In this case the heating element is buried to be electrically insulated from the electrodes, which increases the energetic efficiency and reduces the final cost of the device (Figure 2-6.b). Figure 2-6.c and Figure 2-6.d show gas

UNIVERSITAT ROVIRA I VIRGILI
GAS SENSOR MICROSYSTEMS BASED ON NANOSTRUCTURED LAYERS VIA ANODIC OXIDATION
Raúl Calavia Boldú
Dipòsit Legal: T. 1428-2012

sensors on silicon substrates with the configuration shown in Figure 2-6.b.

2.1.1 Micromachined gas sensors

Traditional gas sensors, and especially commercially available sensors [28], are generally based on alumina substrates and characterised by power consumptions that range from 0.1 to about 1 W in order to rise the sensing layer to the working temperature [28, 29]. This power consumption is too high for portable applications that require the use of battery-driven elements.

The easiest way to reduce power consumption is reducing the area of the sensing layer to be heated and, if this reduced size is followed by a high thermal efficiency from the heater and a high thermal isolation of the sensing area from the bulk, the reduction in power consumption may be excellent. A good thermal isolation is recommended not only for minimization of the overall power consumption but also for the integration of signal processing electronics and different sensors in the same chip [30]. It is possible to increase the selectivity and/or the quantification of the sensing by using different mathematical models for multivariable analysis [31-34].

Table 2-1 shows the thermal isolation properties of different materials where it is possible to see that silicon is a very good thermal conductor and it is not the right material for providing a good thermal isolation. But other materials, like silicon nitride and silicon dioxide, have much lower thermal conductivities than the

UNIVERSITAT ROVIRA I VIRGILI
GAS SENSOR MICROSYSTEMS BASED ON NANOSTRUCTURED LAYERS VIA ANODIC OXIDATION
Raúl Calavia Boldú
Dipòsit Legal: T. 1428-2012

pure silicon and are compatible with the standard microelectronics and micromechanical processes.

Material	T(K)	Thermal conductivity ($Wm^{-1}K^{-1}$) [18]
Silicon	300	150
Silicon nitride	300	9-30
Silicon oxide	300	1.4
Aluminium oxide	300	28-35 [35]
Air	293	0.026

Table 2-1 Thermal isolation properties of different materials

If the sensing material is deposited on a very thin membrane with a buried heater, the efficiency of the heater will be very high because the distance from the heater to the sensing material is very short and the thermal isolation of the heated area from the bulk will be very high (e.g. the thin membrane is made of highly thermally insulating materials, so the thermal resistance of this layer will be very high). These membrane structures are common in silicon technology and they are called micro-hotplates. Their use enables the development of portable applications and has been extensively studied during the last few years.

The isolation between the active layer and the substrate is an important parameter because it helps to reduce the power consumption. The sensitivity of the active layer in MOX gas sensors heavily depends on the operating temperature. Therefore, it is important to obtain a well-controlled temperature distribution across the membrane. In the micro-hotplate, the heated area is very

UNIVERSITAT ROVIRA I VIRGILI
GAS SENSOR MICROSYSTEMS BASED ON NANOSTRUCTURED LAYERS VIA ANODIC OXIDATION
Raúl Calavia Boldú
Dipòsit Legal: T. 1428-2012

low and the temperature distribution is quite even, but developing new heater geometries can further enhance the homogeneity of the temperature distribution within the active area [36].

Figure 2-7 shows the standard steps needed to obtain a micro hotplate substrate. The initial structure is a double-side polished silicon wafer where a silicon nitride layer is deposited on both sides. Silicon nitride will be used as a bulk micromachining mask. A heater is formed on the silicon nitride layer of the face side and is then covered by a silicon dioxide layer that is going to prevent the electric contact between the heater and the electrodes that are deposited on top of this silicon dioxide layer. The last layer to be formed is the gas sensing layer. Finally, the silicon bulk under the membrane is etched away using an anisotropic etching technique [37-39]. After these steps, the micromachined sensor is ready to be packaged and used.

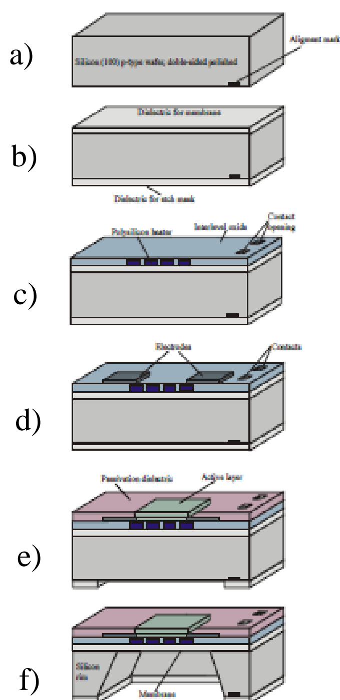

Figure 2-7 Standard steps for micromachined gas sensor fabrication. a) Double polished silicon wafer. b) Silicon nitride deposited onto both wafer sides. c) Polysilicon heater prepared and insulated by SiO_2. d) Electrode deposition and patterning on the SiO_2 layer. e) Sensing layer deposition and bottom silicon nitride patterning. f) Bulk micromachining using silicon nitride bottom as mask

The thermal and electrical isolation within the micro-hotplate membranes can be exploited to design integrated arrays of independent, different sensors in the same silicon chip. Using different sensing materials within an integrated sensor array is advantageous as it helps to increase the overall selectivity (e.g. by using the responses of different sensors with overlapping sensitivities coupled to a mathematical data analysis process).

Micro-hotplates have a fast thermal response due to the high efficiency in the transferring of temperature changes from the heater to the sensing layer, so the temperature modulated operation of such devices has become a largely used technique to improve selectivity [40], sensitivity [41] and reduce heating power [42, 43].

The idea behind temperature modulation is to alter the temperature-dependent conductance of metal oxide gas sensors and the temperature dependent kinetics for adsorption and desorption of gas molecules at the sensor surface. At the receptor, the gas-sensitive surface, temperature modulated operation leads to a modulation of the concentration of the adsorbed oxygen species and thus influences the reaction schemes and absorption rates of incoming gas species. It is then possible to obtain time-dependent gas-specific signal patterns such as the ones shown in Figure 2-8 [44].

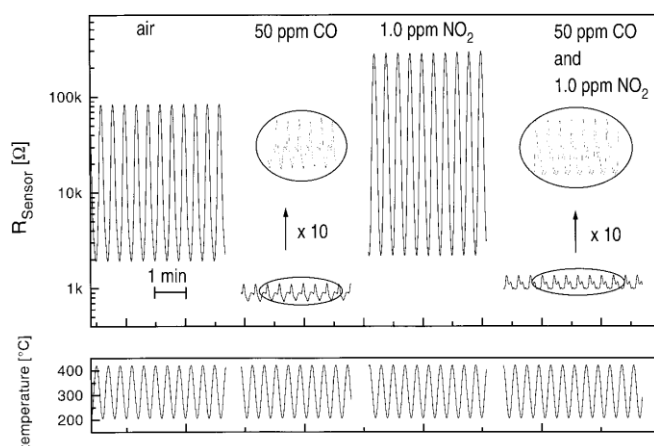

Figure 2-8 Sinusoidal temperature modulations of a micromachined thick film sensor in synthetic air (50% RH) and during exposure to 50 ppm CO, 1.0 ppm NO_2 and mixture of 50 ppm CO and 1.0 ppm NO_2

UNIVERSITAT ROVIRA I VIRGILI
GAS SENSOR MICROSYSTEMS BASED ON NANOSTRUCTURED LAYERS VIA ANODIC OXIDATION
Raúl Calavia Boldú
Dipòsit Legal: T. 1428-2012

Different optimisation techniques can be employed to tune the temperature modulation strategy to solve a given gas analysis problem. For example, multilevel pseudo random sequences (see Figure 2-9) [45], have been used to select, in a systematic way, the modulating frequencies.

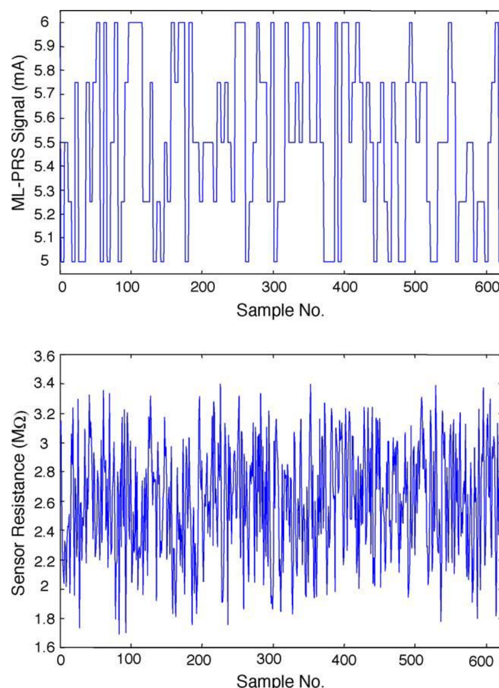

Figure 2-9 Multilevel pseudo random temperature sequence and sensor resistance

2.1.2 Active layer deposition techniques

The gas sensor active layers can be classified in two general types, thick and thin films.

UNIVERSITAT ROVIRA I VIRGILI
GAS SENSOR MICROSYSTEMS BASED ON NANOSTRUCTURED LAYERS VIA ANODIC OXIDATION
Raúl Calavia Boldú
Dipòsit Legal: T. 1428-2012

2.1.2.1 Thick film techniques

In general, the layers with a thickness higher than several micrometers are called thick films and can be deposited by different techniques.

2.1.2.1.1 Screen printing

The screen printing is one of the most used techniques for the deposition of thick active layers [46]. Screen printing is an easy, scalable and flexible technique that can be used for the deposition of active layers on different types of substrates, such as alumina or silicon [30, 47, 48]. This technique is based on using a finely milled metal oxide paste, which includes metal oxide powders mixed to organic vehicles to form a printable paste. Using a mask, the paste is deposited and patterned onto the substrate. It must be then dried and fired at suitable temperatures depending of the deposited material.

2.1.2.1.2 Sol-gel

Sol-gel is a technique that is a versatile solution process for making ceramic and glass materials. The sol-gel process involves the transition of a system from a liquid (sol) into a solid (gel) phase. This technique leads to obtaining ultra-fine or spherical powders, thin films coating, ceramic fibres, etc. In general, the initial material is an inorganic metal salt or an organic compound. In a typical sol-gel process, the precursor is subjected to a series of hydrolysis and polymerisation reactions to form a colloidal

UNIVERSITAT ROVIRA I VIRGILI
GAS SENSOR MICROSYSTEMS BASED ON NANOSTRUCTURED LAYERS VIA ANODIC OXIDATION
Raúl Calavia Boldú
Dipòsit Legal: T. 1428-2012

suspension, or a "sol". Thick films can be produced on a piece of substrate by spin-coating or dip-coating. When the sol is cast into a mould, a wet "gel" will form. With further drying and heat-treatment, the gel is converted into dense ceramic or glass.

2.1.2.1.3 Drop-coating

This technique is based on the deposition of several drops in a substrate. The thickness obtained can be controlled by the number of drops deposited, the viscosity and density of the liquid in which the active material is solved, and also by controlling the pressure applied, which influences drop formation. Once the solution is deposited, the solvent evaporates by itself or with a firing step.

This deposition technique is easy and a physical contact between the injection probe and the sample is not necessary. Therefore, the method can be used for the deposition of active materials onto fragile substrates like membranes or cantilevers for example.

2.1.2.2 Thin film techniques

As explained previously the thickness of the sensing layer is an important factor for the sensitivity of the final gas sensor obtained. In that sense, thin film techniques have been intensively studied in the last years.

2.1.2.2.1 Chemical vapour deposition

Chemical vapour deposition (CVD) is a chemical based deposition technique where the initial compound is a molecule that contains

UNIVERSITAT ROVIRA I VIRGILI
GAS SENSOR MICROSYSTEMS BASED ON NANOSTRUCTURED LAYERS VIA ANODIC OXIDATION
Raúl Calavia Boldú
Dipòsit Legal: T. 1428-2012

the material to be deposited, called precursor. This molecule, which must be in the vapour phase, reacts due to the energy supplied (e.g., temperature, plasma, ion beam or other) and the material is deposited on the substrate in the solid phase. Reaction by-products remain in the vapour phase and are evacuated from the deposition chamber.

Since this technique is based on a chemical reaction of a vapour phase precursor on a substrate, the conformal coverage obtained by this technique is better than in other techniques such as physical vapour deposition. However, sometimes it is difficult to obtain a layer with high purity.

Depending of the precursor used and the deposition conditions there are different CVD types.

The CVD deposition techniques have been very studied in the last years because by controlling the deposition conditions it is possible to obtain metal oxide nanostructures like tungsten oxide nanoneedles [26, 49].

2.1.2.2.2 Atomic layer deposition

Atomic layer deposition (ALD) is a CVD deposition technique. Therefore, ALD is based in a chemical reaction in the sample surface of a precursor, which is generated in vacuum at ranges from 100 to 400 ºC.

ALD is characterised by the deposition of one atomic layer in every deposition step, so the surface coating is conformal.

UNIVERSITAT ROVIRA I VIRGILI
GAS SENSOR MICROSYSTEMS BASED ON NANOSTRUCTURED LAYERS VIA ANODIC OXIDATION
Raúl Calavia Boldú
Dipòsit Legal: T. 1428-2012

Every monoatomic layer deposition is divided in the following steps:

- Cleaning phase: flowing nitrogen into the deposition chamber to be cleaned from impurities.
- Precursor injection: low quantity of evaporated precursor is diluted in nitrogen, which reacts with the heated surface and the material is adhered to the sample surface. This precursor does not react with the material deposited, so only one atomic layer is deposited.
- Excess precursor removal: closing the injection of the precursor in the nitrogen flow and waiting some time for removing the precursor from the chamber.
- Ozone: by injecting a high oxidising gas, such as pure oxygen or ozone, the surface of the deposited material is oxidised and a monoatomic metal oxide layer is deposited.

Since following these steps a monoatomic layer is deposited, by iterating the process it is easy to control the thickness obtained and the coating remains very conformal.

2.1.2.2.3 Sputtering

Sputtering is a physical vapour deposition (PVD) technique based on plasma, argon generally, that physically etches a target and some nanoparticles that are pulled away from it eventually get deposited on the sample.

UNIVERSITAT ROVIRA I VIRGILI
GAS SENSOR MICROSYSTEMS BASED ON NANOSTRUCTURED LAYERS VIA ANODIC OXIDATION
Raúl Calavia Boldú
Dipòsit Legal: T. 1428-2012

This technique has been widely used in gas sensor applications because it is possible to deposit very thin metal oxide layers using a pure metal target and an argon and oxygen reactive plasma [50].

2.1.3 Hydrogen detection

Hydrogen is one the most studied gases because it has been used, from decades ago, in a lot of chemical processes. It is now a species related to the green economy (e.g. fuel cells, electric vehicles, etc.) but also a residue, like in nuclear reactors where hydrogen can be formed in radioactive waste tanks.

Hydrogen, a flammable gas, has been implied in some of the most remembered accidents in history, like LZ 129 Hindenburg Zeppelin in New Jersey in 1937 with 36 people dead.

Since hydrogen is a rather dangerous gas, it is important to control the occurrence of leaks. This explains why in the last two decades different sensors have been developed to measure hydrogen on site, avoiding the use of slow and expensive instrumental analytical techniques.

There are different sensing techniques to detect hydrogen gas such as catalytic, thermal conductivity, electrochemical, optical, semiconductor metal oxide, etc. The following describes the hydrogen sensing mechanism for metal oxides.

UNIVERSITAT ROVIRA I VIRGILI
GAS SENSOR MICROSYSTEMS BASED ON NANOSTRUCTURED LAYERS VIA ANODIC OXIDATION
Raúl Calavia Boldú
Dipòsit Legal: T. 1428-2012

In metal oxide gas sensors the adsorbed oxygen takes electrons from the semiconductor material as the following equation indicates:

$$O_2 + 2e^- \rightarrow 2O_{ads}^- \quad (2\text{-}4)$$

Hydrogen molecules react with the oxygen adsorbates generating a water molecule and releasing electrons:

$$H_2 + O_{ads}^- \rightarrow H_2O + e^- \quad (2\text{-}5)$$

So the number of free electrons in the metal oxide layer increases in the presence of hydrogen and in *n*-type semiconductors; this results in a decrease in the resistance.

Hydrogen can be detected by different metal oxides such as SnO_2, Fe_2O_3, TiO_2, ZnO [51] and WO_3 [52].

In order to increase the sensitivity and selectivity of MOX gas sensors to hydrogen, different authors have reported the doping of active layers with catalytically active metals like palladium, platinum, gold, silver or copper [53-55] or by mixing oxide materials [56].

2.1.4 WO_3 as sensing material

Tungsten trioxide is a wide band gap (E_g≈2.6-2.8 eV), *n*-type semiconductor that encloses interesting physical and chemical properties. This is why it is useful for a wide spectrum of technology applications. For instance, tungsten trioxide is an

UNIVERSITAT ROVIRA I VIRGILI
GAS SENSOR MICROSYSTEMS BASED ON NANOSTRUCTURED LAYERS VIA ANODIC OXIDATION
Raúl Calavia Boldú
Dipòsit Legal: T. 1428-2012

important material for electrochromic and photoelectrochemical devices, catalysts and gas sensors.

The gas sensing properties of WO_3 with or without catalytic particles were discovered several decades ago [57] and nowadays it is one of the most interesting and researched sensing materials [58]. A number of different types of sensors have been demonstrated, including resistive [59], optical [60-62], SAW [63] and capacitive [64] devices for a large variety of different gas analytes such as NOx [20, 65-67], NH_3 [68, 69], CO [70, 71], H_2 [60, 72, 73], O_3 [74, 75], ethanol [76] and H_2S [77-79]. The high response towards NOx (down to 10 ppb [80, 81]) makes WO_3 particularly relevant from the commercial point of view, because of the demand to monitor process or flow gases and to detect leakage/pollution in industrial and automotive applications [82, 83]. Double layers of WO_3 with Pd [73, 79] or Pt [68] nanoparticles have been reported earlier as a feasible method to significantly enhance the selectivity towards H_2 [68, 73, 79], while carbon nanotubes and Au were utilized to improve NOx [70, 80, 84] and CO [81, 85] detection, respectively. This material is more and more studied every day for gas sensing applications as demonstrates the steady growth in the number of published papers (see Figure 2-10).

UNIVERSITAT ROVIRA I VIRGILI
GAS SENSOR MICROSYSTEMS BASED ON NANOSTRUCTURED LAYERS VIA ANODIC OXIDATION
Raúl Calavia Boldú
Dipòsit Legal: T. 1428-2012

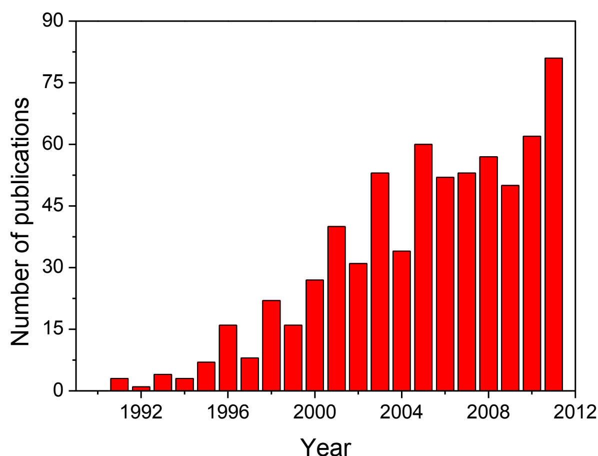

Figure 2-10 Growth in tungsten oxide gas sensor publications since 1990 to 2011 in ISI Web of Knowledge

Tungsten oxide films of various crystal phases, grain sizes, thickness and porosity are synthesized mainly by reactive evaporation [59], sputtering [86] and pulse laser deposition [87] from pure tungsten target in O_2/Ar atmosphere; by CVD and vacuum sublimation methods [73], by wet-chemical processes [85, 88] as well as by thermal [66] and electrochemical oxidation (anodising) [89] of tungsten films. The optimum operating temperature and response of WO_3 sensors strongly depends on the synthesis and deposition method and post-annealing procedure.

Kuzmin proposed a structural model of the WO_3 grain surface [90], where two different situations may be present in the surface of an idealised WO_3 film due to the electrical neutrality condition considering a surface along the (100) crystallographic plane (Figure 2-11). At first, half of W atoms remain in the valence state W^{6+} and

are connected to the terminal oxygen ions, which give one of their electrons to the nearest W ion, leading to a formation of a W^{5+} state. This situation occurs at the free surface of WO_3 single crystal and was directly observed by scanning tunnelling microscopy (STM) technique [91].

In the second situation, all tungsten atoms at the surface change their valence state to W^{5+}, and the surface is represented by $W^{5+}O_2$ terminal layer. In both cases, the surface W^{5+} sites react with the oxidising atmosphere of air, leading presumably to the formation of the W^{6+}-OH bonds in a humid ambient.

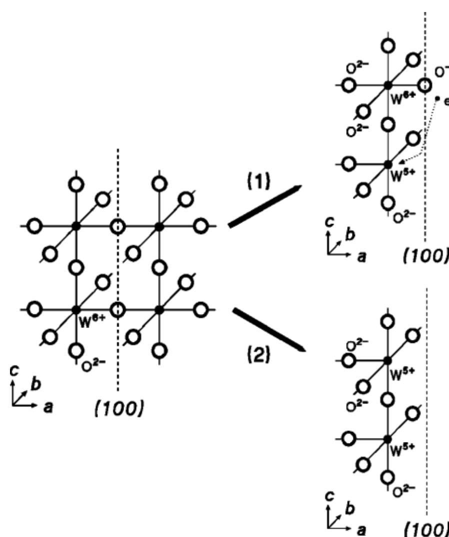

Figure 2-11 Structural model of the WO_3 grain surface. In the left, WO_3 block with the (100) fracture plane is shown. In the right, two possible states of the grain surface are demonstrated.

The different crystallography phases for the WO_3 are shown in the following table [92]; it is called polymorphism.

Structure	Space group	Angstroms			Stability
		a	b	C	Temp (ºC)
Triclinic	P1-C[1]	7.31	7.52	7.69	<17
Monoclinic	$P2_1/n$	7.30	7.54	7.69	17-330
Orthorombic	Pmnb-D[16]	7.34	7.57	7.75	330-740
Tetragonal	P4/nmm-D[7]	5.25	5.25	3.92	>740

Table 2-2 Tungsten oxide crystal phases (polymorphism)

The formation of tungsten states on the film surface plays a significant role in the gas-solid interactions and the most typical crystallographic structure is the monoclinic because it is the most stable at room temperature and in the most typical operating temperature range for gas sensors (near 200 ºC).

2.1.5 Nanostructured gas sensors

In a solid, the chemical environment of surface atoms is very different from that of bulk atoms. This is especially true in materials that are designed for gas sensing purposes.

The gas sensing properties of metal oxides are dominated by surface reactions (Figure 2-3) and, therefore, by surface chemistry (Figure 2-11).

In nanostructured MOX materials, the surface to volume ratio is very high. Therefore, most of the metal oxide atoms are exposed to the environment and the material dimensions are close to the Debye length of the semiconductor.

Therefore, many authors have reported the use of nanostructuring techniques as a way to increase the specific surface area and achieve increased sensitivity (e.g. in biological, electrochemical, gas, optical, pH, humidity sensors etc [93, 94]). Also improvements in sensor response and recovery times have been reported [95].

The most common nanostructured surfaces are the structures called quasi-one dimensional (Q1D) such as nanowires, nanoneedles, nanofibers, nanorods, nanobelts and nanotubes.

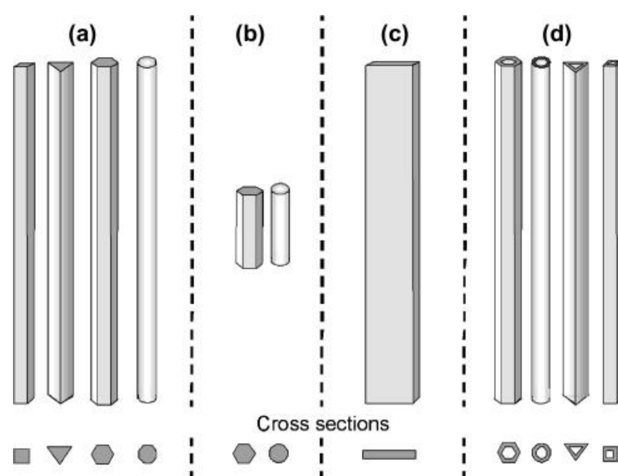

Figure 2-12 Schematic illustration of different quasi-one dimensional nanostructure morphologies and the terms typically used to describe: (a) nanowires, nanoneedles, nanofibers or whiskers; (b) nanorods; (c) nanoberlts or nanoribons and (d) nanotubes [96]

According to a literature review [97], since 2002 the most studied Q1D metal oxide nanostructured materials for gas sensor applications are: tin dioxide (SnO_2) and Zinc oxide (ZnO), but titanium oxide (TiO_2) and tungsten oxide (WO_3) are good

UNIVERSITAT ROVIRA I VIRGILI
GAS SENSOR MICROSYSTEMS BASED ON NANOSTRUCTURED LAYERS VIA ANODIC OXIDATION
Raúl Calavia Boldú
Dipòsit Legal: T. 1428-2012

candidates too and they are becoming more and more studied every year.

These Q1D structures can be obtained from different techniques. For example WO_3 nanoneedles can be obtained by aerosol assisted chemical vapour deposition (AACVD) for gas sensing applications [26].

There are some metals that can be nanostructured by a direct anodizing process [98, 99] where the oxide layer obtained can be used for gas sensing applications. This is, for example, the case of WO_3 [100, 101]. Another approach consists of depositing a sensing layer by PVD or CVD techniques on a nanostructured layer obtained by anodisation.

The latter approach has been implemented in our lab. Mozalev and co-workers studied the coating, with sputtered tungsten oxide films, of a two-step porous alumina grown directly on silicon substrates [102]. It was found that after a suitable pore opening technique, it was possible to obtain a tungsten oxide film that continuously coated the alumina pores. The gas sensing properties of these nanostructured tungsten oxide films supported on porous alumina were investigated [103, 104]. These preliminary results demonstrated that the response of the film can be enhanced by employing this nanostructuring approach. However, the difficulties owing to application of two-step anodizing approach and the specific electrochemical processes that occur at the Al/Si interface [103, 104] require to find the ways for making the anodising

UNIVERSITAT ROVIRA I VIRGILI
GAS SENSOR MICROSYSTEMS BASED ON NANOSTRUCTURED LAYERS VIA ANODIC OXIDATION
Raúl Calavia Boldú
Dipòsit Legal: T. 1428-2012

technique better compatible with the standard silicon-based microfabrication technologies. So far, no practical gas sensors have yet been fabricated by the approaches described in [102-104].

2.2 Anodising of valve metals

The anodisation process has been known and used in the industry for many decades, especially for surface treatment and corrosion protection among many other applications.

One of the most used metals in the world is aluminium because it has some very useful properties like low cost, lightness, easy to work with, and it does not suffer much from corrosion under ambient conditions. Aluminium is a valve metal, such as titanium, tantalum, niobium, hafnium, tungsten and zirconium. When a valve metal is exposed to ambient conditions, a very thin oxide layer grows, the so-called barrier oxide, which immediately prevents the progress of unwanted oxidation. In other words, the oxidation process is stopped and corrosion is mainly avoided.

The thickness of oxide on a valve metal can be increased by an electrochemical anodising process. To do so, the valve metal is polarised positively and immersed in a solution. A counter electrode (cathode), e.g. platinum or stainless steel, has to be added to the electrolyte to complete the electrochemical system (Figure 2-13).

UNIVERSITAT ROVIRA I VIRGILI
GAS SENSOR MICROSYSTEMS BASED ON NANOSTRUCTURED LAYERS VIA ANODIC OXIDATION
Raúl Calavia Boldú
Dipòsit Legal: T. 1428-2012

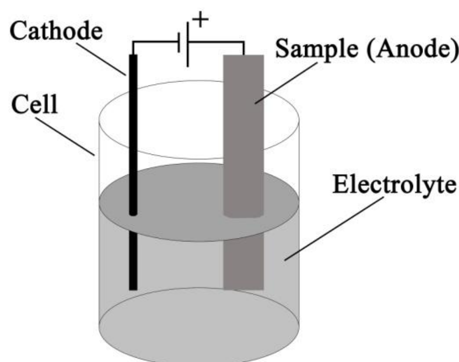

Figure 2-13 Schematic of an electrochemical system for anodising

In order to understand the behaviour of the electrochemical oxidation process in the configuration shown in Figure 2-13, the case of titanium is discussed in details.

When being positively polarised, titanium is oxidised as follows:

$$Ti \rightarrow Ti^{4+} + 4e^{-} \quad (2\text{-}6)$$

Since the anode collects the electrons in the oxidation of titanium, the cathode must inject them. The cathode is the electron donor to the hydrogen ions present in the electrolyte.

$$2H^{+} + 2e^{-} \rightarrow H_2 \quad (2\text{-}7)$$

So during the anodising, molecular hydrogen is generated at the cathode.

Taking into account the oxidation state of titanium considered in this example (Ti^{4+}), for every oxidised Ti atom the anode collects 4 electrons and the cathode injects 4 electrons, which results in the

UNIVERSITAT ROVIRA I VIRGILI
GAS SENSOR MICROSYSTEMS BASED ON NANOSTRUCTURED LAYERS VIA ANODIC OXIDATION
Raúl Calavia Boldú
Dipòsit Legal: T. 1428-2012

formation of 2 hydrogen molecules. Therefore, the final concurrent reactions are as follows:

$$Ti \rightarrow Ti^{4+} + 4e^{-} \quad (2\text{-}8)$$

$$4H^{+} + 4e^{-} \rightarrow 2H_2 \quad (2\text{-}9)$$

Titanium cations react with the oxygen anions, derived from water in the electrolyte, and the metal oxide is formed:

$$Ti^{4+} + 2O^{2-} \rightarrow TiO_2 \quad (2\text{-}10)$$

In the beginning of the electrochemical process, the chemical reaction occurs on the surface of the titanium sample. However, when the surface is oxidised, the electric field drives oxygen ions through the titanium oxide barrier, and the thickness of the oxide increases. When a particular thickness, which depends on the voltage applied, is reached, oxygen ions are no longer able to migrate across the oxide layer, and the oxide formation process stops. Therefore, the anodisation process is associated with a specific oxide thickness that depends on the nature of metal, the electrolyte and the voltage applied.

For some electrolytes and metals, the electrochemical process starts as explained above. In other cases, when the anodic film reaches a determined thickness, the surface starts dissolving more actively and the oxidation continues. Since the oxidation and dissolution rates may become the same, the metal can be consumed completely but the anodic film thickness remains rather constant throughout the process. Such a process can be potentially used for obtaining

UNIVERSITAT ROVIRA I VIRGILI
GAS SENSOR MICROSYSTEMS BASED ON NANOSTRUCTURED LAYERS VIA ANODIC OXIDATION
Raúl Calavia Boldú
Dipòsit Legal: T. 1428-2012

gas sensors with platinum electrodes under the valve metal layer. Upon completing the anodisation, the valve metal is fully consumed (only the anodic film remains), but the platinum electrodes are not affected [67].

Under optimised conditions, anodisation results in the formation of mesoporous films on the surface of the substrate as it has been demonstrated for several metals [89, 105-107] and semiconductors [108-111]. Anodisation can be a particularly useful method to prepare sensor materials and devices, since it helps greatly increase the specific surface area and may lead to anodic films having semiconductor behaviour, for example, in the case of Si, W, Nb or Ti as starting materials [89, 108, 112].

2.2.1 Porous anodic alumina formation

The chemical and thermodynamic equations that describe the growth of aluminium oxide (alumina) are the following [113]:

$$2Al(s) + \frac{3}{2}O_2(g) \rightarrow Al_2O_3(s) \qquad \Delta G^0 = -1582 K_j \cdot mol^{-1} \quad (2\text{-}11)$$

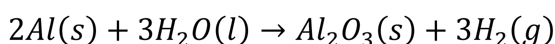

$$2Al(s) + 3H_2O(l) \rightarrow Al_2O_3(s) + 3H_2(g)$$

$$\Delta G^0 = -871 K_j\ mol^{-1} \quad (2\text{-}12)$$

Since the Gibb's energy in the previous chemical reaction is lower than 0, this reaction is spontaneous. This spontaneous chemical reaction creates a thin alumina layer that isolates the pure aluminium metal that lies underneath and prevents its further oxidation. Aluminium can be oxidised employing thermal

UNIVERSITAT ROVIRA I VIRGILI
GAS SENSOR MICROSYSTEMS BASED ON NANOSTRUCTURED LAYERS VIA ANODIC OXIDATION
Raúl Calavia Boldú
Dipòsit Legal: T. 1428-2012

processes, but since aluminium is a valve metal, it can be oxidized much easier and in a better controlled way via an electrochemical process. The anodising of aluminium has some particularities, and it is possible to grow various oxide surfaces depending on the nature, pH and concentration of anodising electrolyte.

If the electrolyte used is neutral, for example, a boric acid or a borate buffer, the resulting oxide layer is a compact, non-porous anodic oxide. Such electrolytes are called barrier-type electrolytes [114].

Using acidic aqueous electrolytes with pH<5 such as sulphuric, oxalic, tartaric, malonic or chromic acids, the oxide layer obtained may be a porous layer [114].

Figure 2-14 shows the aluminium corrosion diagram. For electrolytes with a close to neutral pH (6-7), a passivation layer composed by compact Al_2O_3 grows. For particular acid electrolytes and positive voltages applied, the aluminium oxide is dissolved at a constant rate and the barrier layer thickness is self-maintained constant, too.

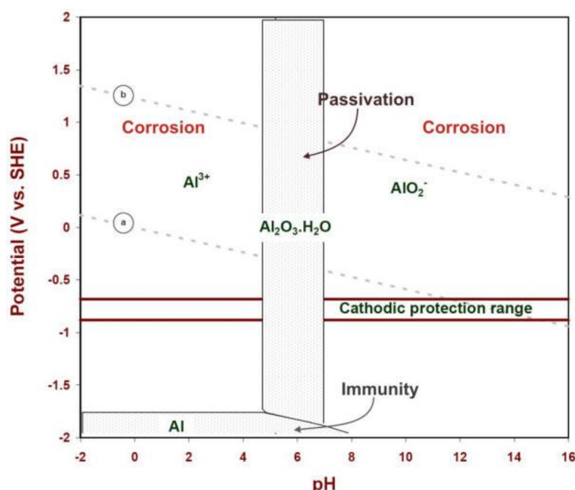

Figure 2-14 Aluminium corrosion diagram

In the electrochemical process, the generation of alumina is as follows [115]:

On the anode:

$$2Al(s) + 3H_2O(l) \rightarrow Al_2O_3(s) + 6H^+(aq) + 6e^- \qquad (2\text{-}13)$$

On the cathode:

$$6H^+(aq) + 6e^- \rightarrow 3H_2(g) \qquad (2\text{-}14)$$

In the anodising process, the aluminium is oxidized generating porous alumina and, for the growth of pores, the alumina must dissolve, so the electrolyte pH must be lower than 5, like is indicated in Figure 2-14. The relevant electrochemical reactions are the following [116]:

On the anode:

$$Al_2O_3(s) + 6H^+(aq) \rightarrow 2Al^{3+}(aq) + 3H_2O(l) \quad (2\text{-}15)$$

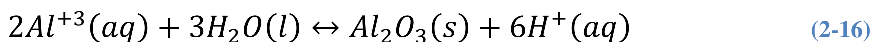

$$2Al^{+3}(aq) + 3H_2O(l) \leftrightarrow Al_2O_3(s) + 6H^+(aq) \quad (2\text{-}16)$$

On the cathode:

$$6H^+(aq) + 6e^- \rightarrow 3H_2(g) \quad (2\text{-}17)$$

The dissolution of alumina is faster in spots where the electric field is more intense. It is in these spots where pores start to grow.

In order to better understand the process of pore formation and growth, the electrochemical process can be divided in three characteristic stages, which are sketched in Figure 2-15.

At the first stage, a uniform (compact) aluminium oxide grows at the surface of the aluminium (Figure 2-15.1). In the local minimums, where the electric field is higher (Figure 2-15.2), the dissolution of the alumina surface starts and the oxidation of aluminium continues. This results in the beginning of pore growth (Figure 2-15.3).

Finally, the alumina dissolution rate and the aluminium oxidation rate arrive to a stabilised ratio and pore growth is sustained at a constant rate, keeping the barrier layer thickness constant.

UNIVERSITAT ROVIRA I VIRGILI
GAS SENSOR MICROSYSTEMS BASED ON NANOSTRUCTURED LAYERS VIA ANODIC OXIDATION
Raúl Calavia Boldú
Dipòsit Legal: T. 1428-2012

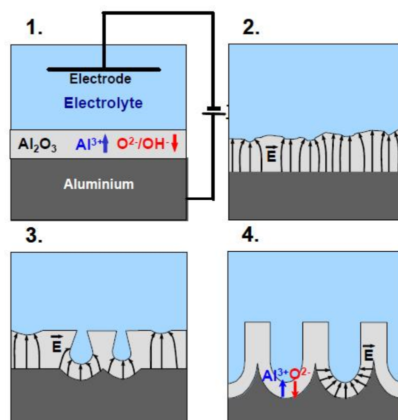

Figure 2-15 Porous anodic alumina formation process. a) Aluminium oxide growth. b) Electric field distribution in the barrier layer gown. c) Pores nucleation. d) Steady-state pore growth [117]

The mechanism of porous anodic alumina growth is a complex electrochemical process and its detailed description can be found in the following articles and electrochemistry books [118-120].

As anodising is an electrochemical process, there are a current and a voltage implied in it. As it has been explained in the text and in Figure 2-15, pore growth is divided in 3 steps, and these steps can easily be identified in the voltage and current behaviour recorded during the anodising process.

The anodising process can be conducted under potentiostatic or galvanostatic modes, where the system must control the voltage or the current, respectively. If the control used is the galvanostatic mode, the free parameter is the voltage and the typical voltage behaviour is shown in Figure 2-16.

UNIVERSITAT ROVIRA I VIRGILI
GAS SENSOR MICROSYSTEMS BASED ON NANOSTRUCTURED LAYERS VIA ANODIC OXIDATION
Raúl Calavia Boldú
Dipòsit Legal: T. 1428-2012

Every step in the growth of alumina pores shown in Figure 2-16 is identified with a different colour. In the beginning, the alumina thickness is very small, so the voltage required to maintain the fixed current is low and the electrochemical oxidation of the aluminium surface starts. While the oxide thickness increases, the pore nucleation begins, although it is not yet seen through the voltage behaviour, and the voltage increases almost linearly if the current is kept constant (Figure 2-16 green). Usually, the pore nucleation already occurs when the voltage attains about 2/3 of its maximum value.

As a result of combination of the alumina growth, alumina dissolution and pore generation, the voltage arrives to its maximum value and then decreases a little because of the competition between the pores, which results in termination of some of the pores and in a continuous growth of the dominant pores (Figure 2-16 orange). Since the nucleation of pores starts at convexities of the surface, the porous layer obtained at the second stage is unorganised.

Finally, when the dissolution and oxidation process are well ballanced, the voltage remains constant and the pore growing rate becomes constant as well (Figure 2-16 blue). In this third step, actually there are two different parts. In the beginning the voltage is not yet completely constant because the pores are growing and rearranging themselves step by step, looking for minimising stress, and once they are stabilised, the voltage finally becomes constant, which is called steady-state anodising.

Stress is lowered when the pores are better organised, so at the surface the pores are unorganised but, as they progress into the bulk, the pores arrive to a self organised arrangement.

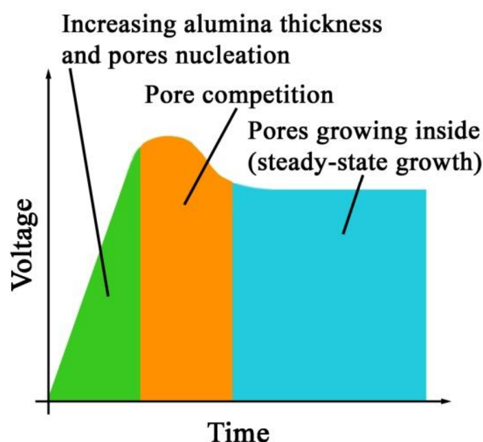

Figure 2-16 Characteristic steps in the formation of pores in anodic aluminaduring galvanostatic anodising of aluminium in a pore-giving electrolyte

As mentioned above, the pores in anodic alumina are poorly organized at the film surface because the pore nucleation starts at random convexities present at the surface of aluminium. However, a better organised surface layer can be formed with the help of additional techniques such as nanoimprinting [121] or two-step anodising process [122].

The above consideration is well related to the case when the thickness of the aluminium layer is enough for the voltage to take up a steady-state value. The situation, however, may drastically change if the aluminium film is thinner than what is needed for the pores to complete the competition process. In such a case, for the

UNIVERSITAT ROVIRA I VIRGILI
GAS SENSOR MICROSYSTEMS BASED ON NANOSTRUCTURED LAYERS VIA ANODIC OXIDATION
Raúl Calavia Boldú
Dipòsit Legal: T. 1428-2012

submicron aluminium thicknesses, a special approach should be developed to grow the pores in inadequately thin alumina layers.

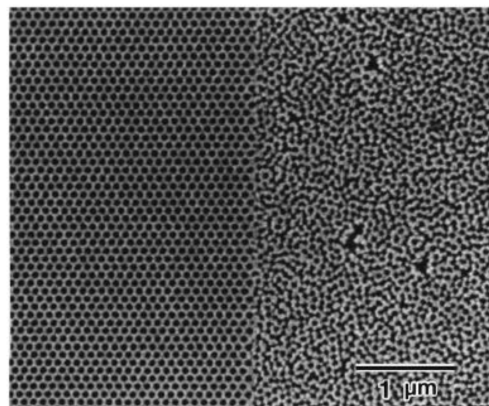

Figure 2-17 Porous alumina layer. a) Organised. b) Unorganised

2.2.2 Pore morphology control

Every acid has a specific ionic conductivity, so the voltage needed for maintaining the current constant changes for every different electrolyte. The electric field makes oxygen ions migrate through the barrier layer. The higher the voltage, the thicker the barrier layer through which the oxygen ions can migrate. Thicker oxide barrier layers result in bigger pore diameters and longer interpore distances. A variety of electrolytes and anodisation potentials can be used to generate desired pore sizes and interpore distances.

UNIVERSITAT ROVIRA I VIRGILI
GAS SENSOR MICROSYSTEMS BASED ON NANOSTRUCTURED LAYERS VIA ANODIC OXIDATION
Raúl Calavia Boldú
Dipòsit Legal: T. 1428-2012

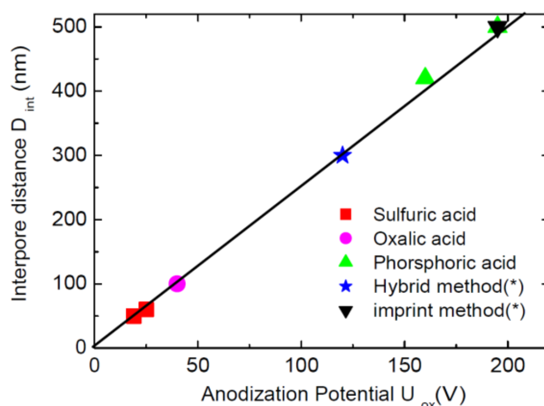

Figure 2-18 Interpore distance versus anodising voltage [117]

Diameters of the pores may be calculated [118], and a linear relationship has been reported between the pore radius and the applied voltage:

$$Rm = -\frac{U_0}{E_{e0}(1-K)}\ln(1-K) \qquad (2\text{-}18)$$

where Rm is the pore radius, Uo is the applied voltage, K is a function of oxide formation and oxide dissolutions constants.

According to Equation 2-18, the pore size and interpore distance may be controlled by controlling the voltage value during the film growth. The application of Equation 2-18 to practical processes should be limited by the range of moderate current densities, beyond which the charge transfer through the alumina barrier layer may become sharply enhanced and thus uncontrolled. Too high a current can interrupt the normal film growth. Since the pore diameter is not directly influenced by the current employed, different acids may be used as the electrolytes to adjust the voltage

UNIVERSITAT ROVIRA I VIRGILI
GAS SENSOR MICROSYSTEMS BASED ON NANOSTRUCTURED LAYERS VIA ANODIC OXIDATION
Raúl Calavia Boldú
Dipòsit Legal: T. 1428-2012

to desired values when keeping the current density within the safe range.

As explained previously, the porous alumina layer can be coated by employing different deposition techniques. For example, magnetron sputtering-deposition was the coating method employed in [103, 104]. The low pore aspect ratio is extremely important in order to obtain a continuous coating over the pores. Pore diameter can be further increased while keeping unchanged the inter-pore distance if the sample is introduced in an etching solution for a while (e.g. a mixture of chromium and phosphoric acids).

Figure 2-19 and Figure 2-20 show a scheme of sputter-deposited tungsten oxide films onto porous alumina obtained by two-step anodising of aluminium in 0.4 M malonic acid at 90 V and 0.4 M tartaric acid at 210 V, respectively. In these figures, *a* sub-plots show the tungsten oxide only covering the film tops because of the relatively bigger pore aspect ratios while the penetration of the tungsten oxide into the pores becomes much more effective when the pore aspect ratio falls to about 1 due to an additional, pore-widening treatment, as indicated in *b* sub-plots of Figure 2-19 and Figure 2-20 .

In the case of the malonic acid electrolyte, the sputtered WO_3 cannot properly coat the pores at any of the conditions employed. However, when the tartaric acid is used, since the interpore distance is relatively bigger, the pores can be widened during a longer etching time and their lower aspect ratio allows for

UNIVERSITAT ROVIRA I VIRGILI
GAS SENSOR MICROSYSTEMS BASED ON NANOSTRUCTURED LAYERS VIA ANODIC OXIDATION
Raúl Calavia Boldú
Dipòsit Legal: T. 1428-2012

continuously coating them by the tungsten trioxide deposit [102]. Further challenge associated with this technique is the preparation and covering with a continuous WO_3 layer of a porous alumina grown in a shorter, one-step anodizing process, on conducting layers between the alumina and the substrate.

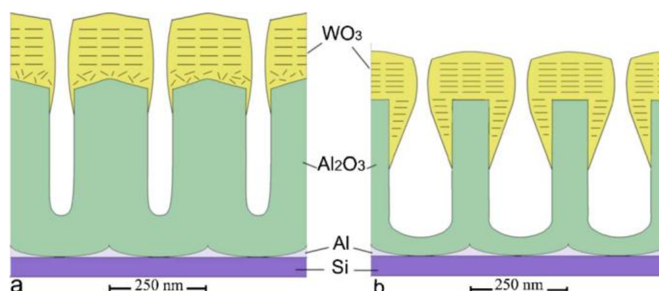

Figure 2-19 Distribution of sputtered WO_3 on porous alumina obtained by anodising in 0.4 M malonic acid at 90 V. a) As anodised. b) After pore widening step

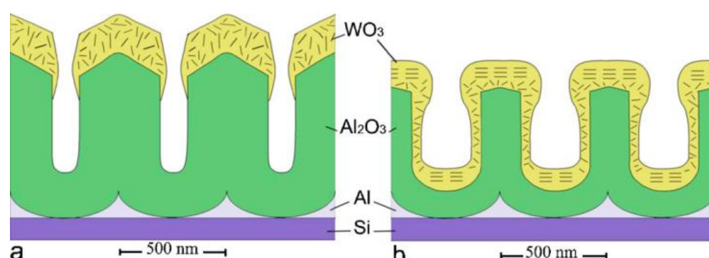

Figure 2-20 Distribution of sputtered WO_3 on porous alumina obtained by anodising in 0.4 M tartaric acid at 210 V. a) As anodised. b) After pore widening step

2.3 Anodising of aluminium/valve-metal bilayer

At it has already been mentioned Al, Ti, Ta, Nb, Hf, W and Zr are classified as valve metals [123, 124]. They can be anodised to obtain, depending on the electrolyte used and the conditions of the anodising process, a continuous oxide layer or structured layers of nanotubes or nanopores [67, 100, 125, 126]. This is illustrated in Figure 2-21 [127] with an example of titanium oxide.

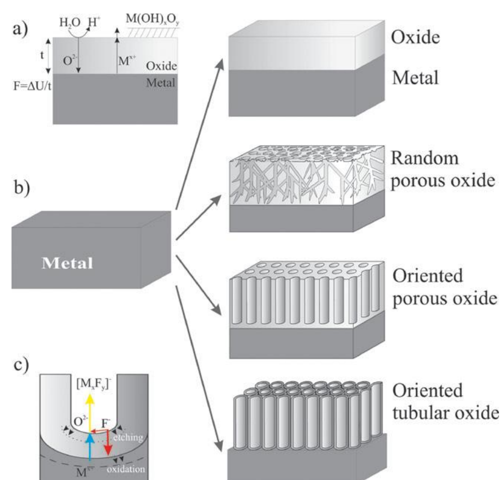

Figure 2-21 a) Oxide formation mechanism on a valve metal. b) Morphologies which can be obtained by electrochemical anodization of metallic titanium -a compact oxide film, a disordered nanoporous layer, a self-ordered nanoporous or self-ordered nanotube layer. c) Nanotube formation mechanism [127]

A bilayer consisted of an aluminium layer on top of another valve metal can be employed to obtain a nanostructured metal oxide. In this case the aluminium layer develops into porous alumina, which acts as a pattern template for the growth of a nanostructured valve-metal oxide [128].

The use a two-step or even a multi-step anodisation technique allows one to obtain relatively better ordered nanoporous alumina, in the pores of which metal oxide nanocolums, mainly composed of tantalum oxide or tungsten oxide, may be grown [129]. Although the above-mentioned techniques look very promising for developing nanostructured gas sensors, efforts are needed to reduce the number of anodising steps, optimise the film morphology and make the materials and processes compatible with existing Si-based microfabrication technologies.

UNIVERSITAT ROVIRA I VIRGILI
GAS SENSOR MICROSYSTEMS BASED ON NANOSTRUCTURED LAYERS VIA ANODIC OXIDATION
Raúl Calavia Boldú
Dipòsit Legal: T. 1428-2012

Some metals may work as valve metals under specific conditions. This is, for example, the case of tin [130], which increases the usefulness of the anodising electrochemical process to obtain nanostructured metal oxides.

2.4 Summary

We have reviewed the state of the art in the metal oxide gas sensors in general and in the tungsten oxide sensors in particular. We have also discussed the improvements derived from the nanostructuring of the sensing layers and the basics of the anodisation of valve metals with the focus on sensor-related technologies. Finally we have discussed how anodisation techniques can be used to obtain nanostructured metal oxide layers, which can be of interest for developing a new generation of more sensitive gas sensors, and what drawbacks must be overcome in order to make the anodising techniques compatible with standard microelectronic technologies.

The main revelation from the critical review done is that a lot of improvements of the existing approaches and development of new, original techniques, first of all, electrochemistry-based technologies, are needed to successfully reach the goal and meet the objectives set for the present study.

2.5 Bibliography

[1] Stoycheva, T. T.; Vallejos, S.; Pavelko, R. G.; Popov, V. S.; Sevastyanov, V. G.; Correig, X., Aerosol-Assisted CVD of SnO(2) Thin Films for Gas-Sensor Applications, *Chem. Vapor Depos.*, (2011) **17**, 247.

UNIVERSITAT ROVIRA I VIRGILI
GAS SENSOR MICROSYSTEMS BASED ON NANOSTRUCTURED LAYERS VIA ANODIC OXIDATION
Raúl Calavia Boldú
Dipòsit Legal: T. 1428-2012

[2] Yamazoe, N.; Suematsu, K.; Shimanoe, K., Extension of receptor function theory to include two types of adsorbed oxygen for oxide semiconductor gas sensors, *Sens. Actuator B-Chem.*, (2012) **163**, 128.
[3] Dossi, N.; Toniolo, R.; Pizzariello, A.; Carrilho, E.; Piccin, E.; Battiston, S.; Bontempelli, G., An electrochemical gas sensor based on paper supported room temperature ionic liquids, *Lab Chip*, (2012) **12**, 153.
[4] Xu, L.; Li, T.; Gao, X. L.; Wang, Y. L., A High-Performance Three-Dimensional Microheater-Based Catalytic Gas Sensor, *IEEE Electron Device Lett.*, (2012) **33**, 284.
[5] Jones, T. A., Characterization of semiconductor gas sensors, In *Solid state gas sensors*, Tofield, P. T. M. a. B. C. Ed. IOP Publishing Ltd.: Bristol, (1987); pp 51.
[6] X. Vilanova, X. C., E. Llobet, J. Brezmes, R. Calavia and X. Sanchez, Analyzing system for the detection of reducing and oxiding gases in a carrier gas with a metal oxide-semiconductor sensor arrangement, US Patent 2006/0052953 A1, (2006).
[7] Morrison, S. R., Chemical sensors, In *Semiconductor sensors*, S. M. SZE, J. W. S., Inc. Ed. (1994); pp 383.
[8] Hennemann, J.; Sauerwald, T.; Kohl, C. D.; Wagner, T.; Bognitzki, M.; Greiner, A., Electrospun copper oxide nanofibers for H2S dosimetry, *Phys. Status Solidi A-Appl. Mat.*, (2012) **209**, 911.
[9] Yoon, J. W.; Choi, J. K.; Lee, J. H., Design of a highly sensitive and selective C2H5OH sensor using p-type Co3O4 nanofibers, *Sens. Actuator B-Chem.*, (2012) **161**, 570.
[10] Kim, H.; Park, S.; Jin, C.; Lee, C., ENHANCED GAS SENSING PROPERTIES OF p-TYPE TeO2 NANORODS FUNCTIONALIZED WITH Pd, *Nano*, (2011) **6**, 455.
[11] Yamazoe, N.; Sakai, G.; Shimanoe, K., Oxide semiconductor gas sensors, *Catalysis Surveys from Asia*, (2003) **-7**,
[12] Morrison, S. R., Semiconductor Gas Sensors, *Sensors and Actuators*, (1982) **2**, 329.
[13] Martinelli, G.; Carotta, M. C., Thick-Film Gas Sensors, *Sens. Actuator B-Chem.*, (1995) **23**, 157.
[14] Rantala, T.; Lantto, V., Computational approaches to the chemical sensitivity of semiconducting tin dioxide, *Sens. Actuator B-Chem.*, (1998) **47**, 59.

UNIVERSITAT ROVIRA I VIRGILI
GAS SENSOR MICROSYSTEMS BASED ON NANOSTRUCTURED LAYERS VIA ANODIC OXIDATION
Raúl Calavia Boldú
Dipòsit Legal: T. 1428-2012

[15] Ménil, F., *Microcapteurs de gaz*, Hermes Science: Paris, (2008); p 450.
[16] Yamazoe, N.; Shimanoe, K.; Sawada, C., Contribution of electron tunneling transport in semiconductor gas sensor, *Thin Solid Films*, (2007) **515**, 8302.
[17] Matsushima, S.; Teraoka, Y.; Miura, N.; Yamazoe, N., Electronic Interaction between Metal Additives and Tin Dioxide in Tin Dioxide-Based Gas Sensors, *Jpn. J. Appl. Phys. Part 1 - Regul. Pap. Short Notes Rev. Pap.*, (1988) **27**, 1798.
[18] Simon, T.; Barsan, N.; Bauer, M.; Weimar, U., Micromachined metal oxide gas sensors: opportunities to improve sensor performance, *Sens. Actuator B-Chem.*, (2001) **73**, 1.
[19] Khatko, V.; Calderer, J.; Vallejos, S.; Llobet, E.; Correig, X., Technology of metal oxide thin film deposition with interruptions, *Surf. Coat. Technol.*, (2007) **202**, 453.
[20] Khatko, V.; Vallejos, S.; Calderer, J.; Gracia, I.; Cane, C.; Llobet, E.; Correig, X., Micro-machined WO3-based sensors with improved characteristics, *Sens. Actuator B-Chem.*, (2009) **140**, 356.
[21] Kohl, D., The Role of Noble-Metals in the Chemistry of Solid-State Gas Sensors, *Sens. Actuator B-Chem.*, (1990) **1**, 158.
[22] Cabot, A.; Arbiol, J.; Morante, J. R.; Weimar, U.; Barsan, N.; Gopel, W., Analysis of the noble metal catalytic additives introduced by impregnation of as obtained SnO2 sol-gel nanocrystals for gas sensors, *Sens. Actuator B-Chem.*, (2000) **70**, 87.
[23] Korotcenkov, G.; Brinzari, V.; Cerneavschi, A.; Ivanov, M.; Golovanov, V.; Cornet, A.; Morante, J.; Cabot, A.; Arbiol, J., The influence of film structure on In2O3 gas response, *Thin Solid Films*, (2004) **460**, 315.
[24] Kida, T.; Nishiyama, A.; Yuasa, M.; Shimanoe, K.; Yamazoe, N., Highly sensitive NO2 sensors using lamellar-structured WO3 particles prepared by an acidification method, *Sens. Actuator B-Chem.*, (2009) **135**, 568.
[25] Sotter, E.; Vilanova, X.; Llobet, E.; Vasiliev, A.; Correig, X., Thick film titania sensors for detecting traces of oxygen, *Sens. Actuator B-Chem.*, (2007) **127**, 567.
[26] Vallejos, S.; Stoycheva, T.; Umek, P.; Navio, C.; Snyders, R.; Bittencourt, C.; Llobet, E.; Blackman, C.; Moniz, S.; Correig, X., Au nanoparticle-functionalised WO3 nanoneedles and their application in high sensitivity gas sensor devices, *Chem. Commun.*, (2011) **47**, 565.

UNIVERSITAT ROVIRA I VIRGILI
GAS SENSOR MICROSYSTEMS BASED ON NANOSTRUCTURED LAYERS VIA ANODIC OXIDATION
Raúl Calavia Boldú
Dipòsit Legal: T. 1428-2012

[27] Stankova, A.; Vilanova, X.; Llobet, E.; Calderer, J.; Bittencourt, C.; Pireaux, J. J.; Coffeig, X., Influence of the annealing and operating temperatures on the gas-sensing properties of rf sputtered WO3 thin-film sensors, *Sens. Actuator B-Chem.*, (2005) **105**, 271.
[28] Inc., F. E., http://www.figarosensor.com/, In JAPAN, (2005).
[29] FIS, www.fisinc.co.jp/, In Kitazono, Itami, Hyogo 664-0891, JAPAN, (2010).
[30] Stankova, M.; Ivanov, P.; Llobet, E.; Brezmes, J.; Vilanova, X.; Gracia, I.; Cane, C.; Hubalek, J.; Malysz, K.; Correig, X., Sputtered and screen-printed metal oxide-based integrated microsensor arrays for the quantitative analysis of gas mixtures, *Sens. Actuator B-Chem.*, (2004) **103**, 23.
[31] Calavia, R.; Brezmes, J.; Ionescu, R.; Llobet, E., Regression using fuzzy adaptive resonant theory neural network, *Electron. Lett.*, (2006) **42**, 1415.
[32] Llobet, E.; Brezmes, J.; Ionescu, R.; Vilanova, X.; Al-Khalifa, S.; Gardner, J. W.; Barsan, N.; Correig, X., Wavelet transform and fuzzy ARTMAP-based pattern recognition for fast gas identification using a micro-hotplate gas sensor, *Sens. Actuator B-Chem.*, (2002) **83**, 238.
[33] Schierbaum, K. D.; Weimar, U.; Gopel, W., Multicomponent Gas-Analysis - an Analytical-Chemistry Approach Applied to Modified Sno2 Sensors, *Sens. Actuator B-Chem.*, (1990) **2**, 71.
[34] Vinaixa, M.; Vergara, A.; Duran, C.; Llobet, E.; Badia, C.; Brezmes, J.; Vilanova, X.; Correig, X., Fast detection of rancidity in potato crisps using e-noses based on mass spectrometry or gas sensors, *Sens. Actuator B-Chem.*, (2005) **106**, 67.
[35] Metals, alloys, compounds, polymers, composites, In *Goodfellow Cambridge Ltd.*, (1994).
[36] Ingles, R.; Pallares, J.; Gracia, I.; Gue, A. M.; Ramirez, J. L., Electro-thermal simulation and characterization of preconcentration membranes, In *Eurosensor Xxiv Conference*, Jakoby, B.; Vellekoop, M. J. Eds.; Elsevier Science Bv: Amsterdam, (2010); Vol. 5, pp 1264.
[37] Horrillo, M. C.; Sayago, I.; Ares, L.; Rodrigo, J.; Gutierrez, J.; Gotz, A.; Gracia, I.; Fonseca, L.; Cane, C.; Lora-Tamayo, E., Detection of low NO2 concentrations with low power

UNIVERSITAT ROVIRA I VIRGILI
GAS SENSOR MICROSYSTEMS BASED ON NANOSTRUCTURED LAYERS VIA ANODIC OXIDATION
Raúl Calavia Boldú
Dipòsit Legal: T. 1428-2012

micromachined tin oxide gas sensors, *Sens. Actuator B-Chem.*, (1999) **58**, 325.
[38] Rickerby, D. G.; Wachter, N.; Horrillo, M. C.; Gutierrez, J.; Gracia, I.; Cane, C., Structural and dimensional control in micromachined integrated solid state gas sensors, *Sens. Actuator B-Chem.*, (2000) **69**, 314.
[39] Gracia, I.; Santander, J.; Cane, C.; Horrillo, M. C.; Sayago, I.; Gutierrez, J., Results on the reliability of silicon micromachined structures for semiconductor gas sensors, *Sens. Actuator B-Chem.*, (2001) **77**, 409.
[40] R. Cavicchi, J. S., P. Chaparada, K. Kreider, M. Gaitan, S. Semancik, Micro-hotplate gas sensor, In *Solid State and Actuator Workshop*, Hilton Head, SC, USA, (1994); pp 53.
[41] Oyabu, T.; Matuura, Y.; Murai, R., Carbon-Monoxide Gas Detector with Shortened Detecting Cycle, *Sens. Actuator B-Chem.*, (1990) **1**, 218.
[42] Sears, W. M.; Colbow, K.; Consadori, F., Algorithms to Improve the Selectivity of Thermally-Cycled Tin Oxide Gas Sensors, *Sensors and Actuators*, (1989) **19**, 333.
[43] R. Cavicchi, J. S., P. Chaparada, G. Poirier, K. Kreider, M. Gaitan, S. Semancik, Micro-hotplate temperature control for sensor fabrication, study, and operation, In *Fifth International Meeting on Cheical Sensors*, (1994); pp 1136.
[44] Heilig, A.; Barsan, N.; Weimar, U.; Schweizer-Berberich, M.; Gardner, J. W.; Gopel, W., Gas identification by modulating temperatures of SnO2-based thick film sensors, *Sens. Actuator B-Chem.*, (1997) **43**, 45.
[45] Vergara, A.; Llobet, E.; Brezmes, J.; Ivanov, P.; Vilanova, X.; Gracia, I.; Cane, C.; Correig, X., Optimised temperature modulation of metal oxide micro-hotplate gas sensors through multilevel pseudo random sequences, *Sens. Actuator B-Chem.*, (2005) **111**, 271.
[46] White, N. M.; Turner, J. D., Thick-film sensors: Past, present and future, *Meas. Sci. Technol.*, (1997) **8**, 1.
[47] Binions, R.; Afonja, A.; Dungey, S.; Lewis, D. W.; Parkin, I. P.; Williams, D. E., Discrimination Effects in Zeolite Modified Metal Oxide Semiconductor Gas Sensors, *IEEE Sens. J.*, (2011) **11**, 1145.
[48] Khadayate, R. S.; Patil, P. P., CO gas sensing properties of screen printed SnO2 thick films, *J. Optoelectron. Adv. Mater.*, (2010) **12**, 1338.

UNIVERSITAT ROVIRA I VIRGILI
GAS SENSOR MICROSYSTEMS BASED ON NANOSTRUCTURED LAYERS VIA ANODIC OXIDATION
Raúl Calavia Boldú
Dipòsit Legal: T. 1428-2012

[49] Qadri, M. U.; Stoycheva, T.; Pujol, M. C.; Llobet, E.; Correig, X.; Borull, J. F.; Aguilo, M.; Diaz, F., WO3 nano-needles by Aerosol Assisted CVD for optical sensing, In *Eurosensors Xxv*, Elsevier Science Bv: Amsterdam, (2011); Vol. 25.
[50] Stankova, M.; Vilanova, X.; Calderer, J.; Llobet, E.; Brezmes, J.; Gracia, I.; Cane, C.; Correig, X., Sensitivity and selectivity improvement of rf sputtered WO3 microhotplate gas sensors, *Sens. Actuator B-Chem.*, (2006) **113**, 241.
[51] Aroutiounian, V., Metal oxide hydrogen, oxygen, and carbon monoxide sensors for hydrogen setups and cells, *Int. J. Hydrog. Energy*, (2007) **32**, 1145.
[52] Kukkola, J.; Maklin, J.; Halonen, N.; Kyllonen, T.; Toth, G.; Szabo, M.; Shchukarev, A.; Mikkola, J. P.; Jantunen, H.; Kordas, K., Gas sensors based on anodic tungsten oxide, *Sens. Actuator B-Chem.*, (2011) **153**, 293.
[53] Ippolito, S. J.; Kandasamy, S.; Kalantar-zadeh, K.; Wlodarski, W., Hydrogen sensing characteristics of WO3 thin film conductometric sensors activated by Pt and Au catalysts, *Sens. Actuator B-Chem.*, (2005) **108**, 154.
[54] Matushko, I. P.; Yatsimirskii, V. K.; Maksimovich, N. P.; Nikitina, N. V.; Silenko, P. M.; Ruchko, V. P.; Ishchenko, V. B., Sensitivity to hydrogen of sensor materials based on SnO(2) promoted with 3d metals, *Theor. Exp. Chem.*, (2008) **44**, 128.
[55] Zhang, C.; Boudiba, A.; Olivier, M. G.; Snyders, R.; Debliquy, M., Magnetron sputtered tungsten oxide films activated by dip-coated platinum for ppm-level hydrogen detection, *Thin Solid Films*, (2012) **520**, 3679.
[56] Choi, U. S.; Sakai, G.; Shimanoe, K.; Yamazoe, N., Sensing properties of SnO2-Co3O4 composites to CO and H-2, *Sens. Actuator B-Chem.*, (2004) **98**, 166.
[57] Shaver, P. J., Activated Tungsten Oxide Gas Detectors, *Appl. Phys. Lett.*, (1967) **11**, 255.
[58] Akiyama, M.; Tamaki, J.; Miura, N.; Yamazoe, N., Tungsten Oxide-Based Semiconductor Sensor Highly Sensitive to No and No2, *Chem. Lett.*, (1991), 1611.
[59] Meng, D.; Yamazaki, T.; Shen, Y. B.; Liu, Z. F.; Kikuta, T., Preparation of WO3 nanoparticles and application to NO2 sensor, *Appl. Surf. Sci.*, (2009) **256**, 1050.
[60] Hsu, W. C.; Chan, C. C.; Peng, C. H.; Chang, C. C., Hydrogen sensing characteristics of an electrodeposited WO3 thin

UNIVERSITAT ROVIRA I VIRGILI
GAS SENSOR MICROSYSTEMS BASED ON NANOSTRUCTURED LAYERS VIA ANODIC OXIDATION
Raúl Calavia Boldú
Dipòsit Legal: T. 1428-2012

film gasochromic sensor activated by Pt catalyst, *Thin Solid Films*, (2007) **516**, 407.
[61] Matsuyama, N.; Okazaki, S.; Nakagawa, H.; Sone, H.; Fukuda, K., Response kinetics of a fiber-optic gas sensor using Pt/WO3 thin film to hydrogen, *Thin Solid Films*, (2009) **517**, 4650.
[62] Yoshimura, K.; Hakoda, T.; Yamamoto, S.; Yoshikawa, M., Optical detection of organic hydrides with platinum-loaded tungsten trioxide, *J. Phys. Chem. Solids*, (2012) **73**, 696.
[63] Hejczyk, T.; Urbanczyk, M., WO3-Pd Structure in SAW Sensor for Hydrogen Detection, *Acta Phys. Pol. A*, (2011) **120**, 616.
[64] Tutov, E. A., MOS structures with amorphous tungsten trioxide for capacitive humidity sensors, *Semiconductors*, (2008) **42**, 1561.
[65] Liu, Z. F.; Yamazaki, T.; Shen, Y.; Kikuta, T.; Nakatani, N., Influence of annealing on microstructure and NO2-sensing properties of sputtered WO3 thin films, *Sens. Actuator B-Chem.*, (2007) **128**, 173.
[66] Siciliano, T.; Tepore, A.; Micocci, G.; Serra, A.; Manno, D.; Filippo, E., WO3 gas sensors prepared by thermal oxidization of tungsten, *Sens. Actuator B-Chem.*, (2008) **133**, 321.
[67] Zeng, J.; Hu, M.; Wang, W. D.; Chen, H. D.; Qin, Y. X., NO2-sensing properties of porous WO3 gas sensor based on anodized sputtered tungsten thin film, *Sens. Actuator B-Chem.*, (2012) **161**, 447.
[68] Srivastava, V.; Jain, K., Highly sensitive NH3 sensor using Pt catalyzed silica coating over WO3 thick films, *Sens. Actuator B-Chem.*, (2008) **133**, 46.
[69] Szilagyi, I. M.; Wang, L. S.; Gouma, P. I.; Balaszsi, C.; Madarasz, J.; Pokol, G., Preparation of hexagonal WO3 from hexagonal ammonium tungsten bronze for sensing NH3, *Mater. Res. Bull.*, (2009) **44**, 505.
[70] Ionescu, R.; Espinosa, E.; Bittencourt, C.; Felten, A.; Pireaux, J. J.; Llobet, E., Gas sensing using CNT-doped WO3, In *2005 Spanish Conference on Electron Devices, Proceedings*, Ieee: New York, (2005); pp 615.
[71] Khatko, V.; Ionescu, R.; Llobet, E.; Vilanova, X.; Brezmes, J.; Hubalek, J.; Malysz, K.; Correig, X., Gas sensors based on nanoparticle WO3 thick films, In *Proceedings of the Ieee Sensors 2004, Vols 1-3*, Rocha, D.; Sarro, P. M.; Vellekoop, M. J. Eds.; Ieee: New York, (2004); pp 188.

UNIVERSITAT ROVIRA I VIRGILI
GAS SENSOR MICROSYSTEMS BASED ON NANOSTRUCTURED LAYERS VIA ANODIC OXIDATION
Raúl Calavia Boldú
Dipòsit Legal: T. 1428-2012

[72] Fominski, V. Y.; Grigoriev, S. N.; Romanov, R. I.; Zuev, V. V.; Grigoriev, V. V., Properties of tungsten oxide thin films formed by ion-plasma and laser deposition methods for MOSiC-based hydrogen sensors, *Semiconductors*, (2012) **46**, 401.
[73] Jakubik, W. P., Hydrogen gas-sensing with bilayer structures of WO3 and Pd in SAW and electric systems, *Thin Solid Films*, (2009) **517**, 6188.
[74] Bendahan, M.; Guerin, J.; Boulmani, R.; Aguir, K., WO3 sensor response according to operating temperature: Experiment and modeling, *Sens. Actuator B-Chem.*, (2007) **124**, 24.
[75] Labidi, A.; Gaidi, M.; Guerin, J.; Bejaoui, A.; Maaref, M.; Aguir, K., Alternating current investigation and modeling of the temperature and ozone effects on the grains and the grain boundary contributions to the WO3 sensor responses, *Thin Solid Films*, (2009) **518**, 355.
[76] Labidi, A.; Lambert-Mauriat, C.; Jacolin, C.; Bendahan, M.; Maaref, M.; Aguir, K., dc and ac characterizations of WO3 sensors under ethanol vapors, *Sens. Actuator B-Chem.*, (2006) **119**, 374.
[77] Ghimbeu, C. M.; Lumbreras, M.; Siadat, M.; Schoonman, J., Detection of H2S, SO2, and NO2 using electrostatic sprayed tungsten oxide films, *Mater. Sci. Semicond. Process*, (2010) **13**, 1.
[78] Solis, J. L.; Saukko, S.; Kish, L.; Granqvist, C. G.; Lantto, V., Semiconductor gas sensors based on nanostructured tungsten oxide, *Thin Solid Films*, (2001) **391**, 255.
[79] Solntsev, V. S.; Gorbanyuk, T. I.; Litovchenko, V. G.; Evtukh, A. A., MIS gas sensors based on porous silicon with Pd and WO3/Pd electrodes, *Thin Solid Films*, (2009) **517**, 6202.
[80] Balazsi, C.; Sedlackova, K.; Llobet, E.; Ionescu, R., Novel hexagonal WO3 nanopowder with metal decorated carbon nanotubes as NO2 gas sensor, *Sens. Actuator B-Chem.*, (2008) **133**, 151.
[81] Tamaki, J.; Hashishin, T.; Uno, Y.; Dao, D. V.; Sugiyama, S., Ultrahigh-sensitive WO3 nanosensor with interdigitated Au nano-electrode for NO2 detection, *Sens. Actuator B-Chem.*, (2008) **132**, 234.
[82] Cantalini, C.; Sun, H. T.; Faccio, M.; Pelino, M.; Santucci, S.; Lozzi, L.; Passacantando, M., NO2 sensitivity of WO3 thin film obtained by high vacuum thermal evaporation, *Sens. Actuator B-Chem.*, (1996) **31**, 81.

UNIVERSITAT ROVIRA I VIRGILI
GAS SENSOR MICROSYSTEMS BASED ON NANOSTRUCTURED LAYERS VIA ANODIC OXIDATION
Raúl Calavia Boldú
Dipòsit Legal: T. 1428-2012

[83] Liu, Z. F.; Miyauchi, M.; Yamazaki, T.; Shen, Y. B., Facile synthesis and NO2 gas sensing of tungsten oxide nanorods assembled microspheres, *Sens. Actuator B-Chem.*, (2009) **140**, 514.
[84] Hashishin, T.; Tamaki, J., Conductivity-type sensor based on CNT-WO3 composite for NO2 detection, *J. Nanomater.*, (2008),
[85] Xia, H. J.; Wang, Y.; Kong, F. H.; Wang, S. R.; Zhu, B. L.; Guo, X. Z.; Zhang, J.; Wang, Y. M.; Wu, S. H., Au-doped WO3-based sensor for NO2 detection at low operating temperature, *Sens. Actuator B-Chem.*, (2008) **134**, 133.
[86] Kim, T. S.; Kim, Y. B.; Yoo, K. S.; Sung, G. S.; Jung, H. J., Sensing characteristics of dc reactive sputtered WO3 thin films as an NOx gas sensor, *Sens. Actuator B-Chem.*, (2000) **62**, 102.
[87] Di Fonzo, F.; Bailini, A.; Russo, V.; Baserga, A.; Cattaneo, D.; Beghi, M. G.; Ossi, P. M.; Casari, C. S.; Bassi, A. L.; Bottani, C. E., Synthesis and characterization of tungsten and tungsten oxide nanostructured films, *Catal. Today*, (2006) **116**, 69.
[88] Artzi-Gerlitz, R.; Benkstein, K. D.; Lahr, D. L.; Hertz, J. L.; Montgomery, C. B.; Bonevich, J. E.; Semancik, S.; Tarlov, M. J., Fabrication and gas sensing performance of parallel assemblies of metal oxide nanotubes supported by porous aluminum oxide membranes, *Sens. Actuator B-Chem.*, (2009) **136**, 257.
[89] Watcharenwong, A.; Chanmanee, W.; de Tacconi, N. R.; Chenthamarakshan, C. R.; Kajitvichyanukul, P.; Rajeshwar, K., Anodic growth of nanoporous WO3 films: Morphology, photoelectrochemical response and photocatalytic activity for methylene blue and hexavalent chrome conversion, *J. Electroanal. Chem.*, (2008) **612**, 112.
[90] Kuzmin, A.; Purans, J.; Cazzanelli, E.; Vinegoni, C.; Mariotto, G., X-ray diffraction, extended x-ray absorption fine structure and Raman spectroscopy studies of WO3 powders and, (1-x)WO3-y center dot xReO(2) mixtures, *J. Appl. Phys.*, (1998) **84**, 5515.
[91] Li, M.; Altman, E. I.; Posadas, A.; Ahn, C. H., Surface phase transitions upon reduction of epitaxial WO3 (100) thin films, *Thin Solid Films*, (2004) **446**, 238.
[92] LeGore, L. J.; Lad, R. J.; Moulzolf, S. C.; Vetelino, J. F.; Frederick, B. G.; Kenik, E. A., Defects and morphology of tungsten trioxide thin films, *Thin Solid Films*, (2002) **406**, 79.
[93] Huang, X. J.; Choi, Y. K., Chemical sensors based on nanostructured materials, *Sens. Actuator B-Chem.*, (2007) **122**, 659.

UNIVERSITAT ROVIRA I VIRGILI
GAS SENSOR MICROSYSTEMS BASED ON NANOSTRUCTURED LAYERS VIA ANODIC OXIDATION
Raúl Calavia Boldú
Dipòsit Legal: T. 1428-2012

[94] Liu, A. H., Towards development of chemosensors and biosensors with metal-oxide-based nanowires or nanotubes, *Biosens. Bioelectron.*, (2008) **24**, 167.
[95] Blaser, G.; Ruhl, T.; Diehl, C.; Ulrich, M.; Kohl, D., Nanostructured semiconductor gas sensors to overcome sensitivity limitations due to percolation effects, *Physica A*, (1999) **266**, 218.
[96] Barth, S.; Hernandez-Ramirez, F.; Holmes, J. D.; Romano-Rodriguez, A., Synthesis and applications of one-dimensional semiconductors, *Prog. Mater. Sci.*, (2010) **55**, 563.
[97] Choi, K. J.; Jang, H. W., One-Dimensional Oxide Nanostructures as Gas-Sensing Materials: Review and Issues, *Sensors*, (2010) **10**, 4083.
[98] Minagar, S.; Berndt, C. C.; Wang, J.; Ivanova, E.; Wen, C., A review of the application of anodization for the fabrication of nanotubes on metal implant surfaces, *Acta biomaterialia*, (2012) **8**, 2875.
[99] Kamalov, S.; Abidov, A.; Allaberganov, B.; Jo, S. J.; Lee, E. Y.; Lee, J. H.; Kim, I.; Park, N. J.; Kim, S., Fabrication and characterization of ordered microsized tubular TiO2 films by using various anodizing conditions, *Res. Chem. Intermed.*, (2012) **38**, 1007.
[100] Kalantar-Zadeh, K.; Sadek, A. Z.; Zheng, H. D.; Bansal, V.; Bhargava, S. K.; Wlodarski, W.; Zhu, J. M.; Yu, L. S.; Hu, Z., Nanostructured WO(3) films using high temperature anodization, *Sens. Actuator B-Chem.*, (2009) **142**, 230.
[101] Ou, J. Z.; Ahmad, M. Z.; Latham, K.; Kalantar-zadeh, K.; Sberveglieri, G.; Wlodarski, W., Synthesis of the nanostructured WO3 via anodization at elevated temperature for H-2 sensing applications, In *Eurosensors Xxv*, Elsevier Science Bv: Amsterdam, (2011); Vol. 25.
[102] Khatko, V.; Mozalev, A.; Gorokh, G.; Solovei, D.; Guirado, F.; Llobet, E.; Correig, X., Evolution of surface morphology, crystallite size, and texture of WO(3) layers sputtered onto Si-supported nanoporous alumina templates, *J. Electrochem. Soc.*, (2008) **155**, K116.
[103] Gorokh, G.; Mozalev, A.; Solovei, D.; Khatko, V.; Llobet, E.; Correig, X., Anodic formation of low-aspect-ratio porous alumina films for metal-oxide sensor application, *Electrochim. Acta*, (2006) **52**, 1771.
[104] Khatko, V.; Gorokh, G.; Mozalev, A.; Solovei, D.; Llobet, E.; Vilanova, X.; Correig, X., Tungsten trioxide sensing layers on

UNIVERSITAT ROVIRA I VIRGILI
GAS SENSOR MICROSYSTEMS BASED ON NANOSTRUCTURED LAYERS VIA ANODIC OXIDATION
Raúl Calavia Boldú
Dipòsit Legal: T. 1428-2012

highly ordered nanoporous alumina template, *Sens. Actuator B-Chem.*, (2006) **118**, 255.
[105] Kordas, K.; Toth, G.; Levoska, J.; Huuhtanen, M.; Keiski, R.; Harkonen, M.; George, T. F.; Vahakangas, J., Room temperature chemical deposition of palladium nanoparticles in anodic aluminium oxide templates, *Nanotechnology*, (2006) **17**, 1459.
[106] Kukkola, J.; Rautio, A.; Sala, G.; Pino, F.; Toth, G.; Leino, A. R.; Maklin, J.; Jantunen, H.; Uusimaki, A.; Kordas, K.; Gracia, E.; Terrones, M.; Shchukarev, A.; Mikkola, J. P., Electrical transport through single-wall carbon nanotube-anodic aluminum oxide-aluminum heterostructures, *Nanotechnology*, (2010) **21**,
[107] Miao, Z.; Xu, D. S.; Ouyang, J. H.; Guo, G. L.; Zhao, X. S.; Tang, Y. Q., Electrochemically induced sol-gel preparation of single-crystalline TiO2 nanowires, *Nano Lett.*, (2002) **2**, 717.
[108] Kordas, K.; Remes, J.; Beke, S.; Hu, T.; Leppavuori, S., Manufacturing of porous silicon; porosity and thickness dependence on electrolyte composition, *Appl. Surf. Sci.*, (2001) **178**, 190.
[109] Lehmann, V.; Gosele, U., Porous Silicon Formation - a Quantum Wire Effect, *Appl. Phys. Lett.*, (1991) **58**, 856.
[110] Mizsei, J., Gas sensor applications of porous Si layers, *Thin Solid Films*, (2007) **515**, 8310.
[111] Pap, A. E.; Kordas, K.; Toth, G.; Levoska, J.; Uusimaki, A.; Vahakangas, J.; Leppavuori, S.; George, T. F., Thermal oxidation of porous silicon: Study on structure, *Appl. Phys. Lett.*, (2005) **86**,
[112] Zwilling, V.; Darque-Ceretti, E.; Boutry-Forveille, A.; David, D.; Perrin, M. Y.; Aucouturier, M., Structure and physicochemistry of anodic oxide films on titanium and TA6V alloy, *Surf. Interface Anal.*, (1999) **27**, 629.
[113] Li, F., Nanostructure of anodic porous alumina films of interest in magnetic recording, PhD Thesis, University of Alabama (1998).
[114] Diggle, J. W.; Downie, T. C.; Goulding, C. W., Anodic Oxide Films on Aluminum, *Chem. Rev.*, (1969) **69**, 365.
[115] Dekker, M., In *Encyclopedia of electrochemistry of the elements*, J., P. A. M. E. A. Ed. (1973); Vol. 6.
[116] Santos, A., Structural engineering of nanoporous anodic alumina and applications, PhD Thesis, Rovira i Virgili University Tarragona, (2010).

UNIVERSITAT ROVIRA I VIRGILI
GAS SENSOR MICROSYSTEMS BASED ON NANOSTRUCTURED LAYERS VIA ANODIC OXIDATION
Raúl Calavia Boldú
Dipòsit Legal: T. 1428-2012

[117] Choi, J., Fabrication of monodomain porous alumina using nanoimprint lithography and its applications, Martin-Luther University Wittenberg, (2004).
[118] Li, F. Y.; Zhang, L.; Metzger, R. M., On the growth of highly ordered pores in anodized aluminum oxide, *Chemistry of materials*, (1998) **10**, 2470.
[119] Wu, Z.; Richter, C.; Menon, L., A study of anodization process during pore formation in nanoporous alumina templates, *J. Electrochem. Soc.*, (2007) **154**, E8.
[120] Friedman, A. L.; Brittain, D.; Menon, L., Roles of pH and acid type in the anodic growth of porous alumina, *J. Chem. Phys.*, (2007) **127**,
[121] Asoh, H.; Nishio, K.; Nakao, M.; Tamamura, T.; Masuda, H., Conditions for fabrication of ideally ordered anodic porous alumina using pretextured Al, *J. Electrochem. Soc.*, (2001) **148**, B152.
[122] Masuda, H.; Fukuda, K., Ordered Metal Nanohole Arrays Made by a 2-Step Replication of Honeycomb Structures of Anodic Alumina, *Science*, (1995) **268**, 1466.
[123] Aladjem, A., Review - Anodic-Oxidation of Titanium and Its Alloys, *J. Mater. Sci.*, (1973) **8**, 688.
[124] Schultze, J. W.; Lohrengel, M. M., Stability, reactivity and breakdown of passive films. Problems of recent and future research, *Electrochim. Acta*, (2000) **45**, 2499.
[125] Hu, M.; Zeng, J.; Wang, W. D.; Chen, H. Q.; Qin, Y. X., Porous WO3 from anodized sputtered tungsten thin films for NO2 detection, *Appl. Surf. Sci.*, (2011) **258**, 1062.
[126] Zhang, J.; Wang, X. L.; Xia, X. H.; Gu, C. D.; Zhao, Z. J.; Tu, J. P., Enhanced electrochromic performance of macroporous WO3 films formed by anodic oxidation of DC-sputtered tungsten layers, *Electrochim. Acta*, (2010) **55**, 6953.
[127] Ghicov, A.; Schmuki, P., Self-ordering electrochemistry: a review on growth and functionality of TiO2 nanotubes and other self-aligned MOx structures, *Chem. Commun.*, (2009), 2791.
[128] Mozalev, A.; Sakairi, M.; Takahashi, H., Structure, morphology, and dielectric properties of nanocomposite oxide films formed by anodizing of sputter-deposited Ta-Al bilayers, *J. Electrochem. Soc.*, (2004) **151**, F257.
[129] Mozalev, A.; Smith, A. J.; Borodin, S.; Plihauka, A.; Hassel, A. W.; Sakairi, M.; Takahashi, H., Growth of multioxide

UNIVERSITAT ROVIRA I VIRGILI
GAS SENSOR MICROSYSTEMS BASED ON NANOSTRUCTURED LAYERS VIA ANODIC OXIDATION
Raúl Calavia Boldú
Dipòsit Legal: T. 1428-2012

planar film with the nanoscale inner structure via anodizing Al/Ta layers on Si, *Electrochim. Acta*, (2009) **54**, 935.
[130] Metikoshukovic, M.; Resetic, A.; Gvozdic, V., Behavior of Tin as a Valve Metal, *Electrochim. Acta*, (1995) **40**, 1777.

UNIVERSITAT ROVIRA I VIRGILI
GAS SENSOR MICROSYSTEMS BASED ON NANOSTRUCTURED LAYERS VIA ANODIC OXIDATION
Raúl Calavia Boldú
Dipòsit Legal: T. 1428-2012

Chapter 3

Sample fabrication

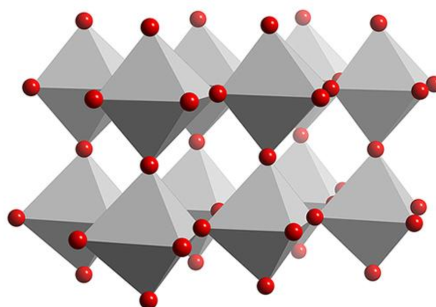

UNIVERSITAT ROVIRA I VIRGILI
GAS SENSOR MICROSYSTEMS BASED ON NANOSTRUCTURED LAYERS VIA ANODIC OXIDATION
Raúl Calavia Boldú
Dipòsit Legal: T. 1428-2012

UNIVERSITAT ROVIRA I VIRGILI
GAS SENSOR MICROSYSTEMS BASED ON NANOSTRUCTURED LAYERS VIA ANODIC OXIDATION
Raúl Calavia Boldú
Dipòsit Legal: T. 1428-2012

3. Sample fabrication

As explained in the previous chapter, the gas sensing properties of metal oxides are based on chemical reactions that occur, generally, at high temperatures. One important problem of traditional gas sensors is the high power consumption needed to keep the sensor at the working temperature. Micromachined gas sensors reach their operating temperatures using very low power because they employ a miniaturised silicon micro-hotplate membrane. The area left on the membrane for the sensing material is very low (i.e., the area of the membrane that is evenly heated).

One of the main objectives of this thesis is to increase the area of the sensing material that is in contact with the environment without increasing the area to be heated in the micro-hotplate. This would enable to keep low power consumption and, at the same time, increase sensor response.

One of the approaches to meet this objective implemented in this work includes the coating of nanoporous alumina layers by the sensing material. A porous alumina layer sits on the heated area of the micro-hotplate and the surface and pore walls of this layer are coated with tungsten oxide. As a result, the tungsten oxide film has an increased surface area (e.g. compared with a standard film deposited directly on the heated area of the micro-hotplate).

The second approach developed consists of a nanodot based tungsten oxide layer obtained by sputter-deposition and anodising

UNIVERSITAT ROVIRA I VIRGILI
GAS SENSOR MICROSYSTEMS BASED ON NANOSTRUCTURED LAYERS VIA ANODIC OXIDATION
Raúl Calavia Boldú
Dipòsit Legal: T. 1428-2012

of a pure tungsten layer under an aluminium layer (Al/W bilayer). First, the aluminium layer is anodised and when consumed, the tungsten layer is oxidised under the alumina layer. As a result, at the bottom of the alumina pores, a growth of tungsten oxide nanodots is obtained. After the selective removal of the porous alumina, the layer obtained in this approach is a nanodot metal oxide layer. Like it happens in the previous approach, the effective surface area is increased.

The micro-hotplates used in this work were fabricated using standard silicon technology at the Centro Nacional de Microelectrónica in Barcelona (CNM-IMB), so porous anodic alumina must be obtained on an oxide-coated silicon wafer and the process must be compatible with the standard silicon technology employed for micro-hotplate fabrication.

3.1 Experimental set-up

The experimental set-up is divided in two parts: at first the chemical cell is described and, secondly, the control electronics of the electrochemical process are reviewed.

The anodising cells must be fabricated in Teflon in order to not be corroded by the acid electrolytes employed. In this thesis the porous alumina must be obtained employing techniques that are fully compatible with standard silicon technologies and, as already explained in the state of the art Chapter, our micro-hotplates use a silicon dioxide layer to isolate the sensing layer from the heater. Therefore, the anodising cells developed must provide a contact to

UNIVERSITAT ROVIRA I VIRGILI
GAS SENSOR MICROSYSTEMS BASED ON NANOSTRUCTURED LAYERS VIA ANODIC OXIDATION
Raúl Calavia Boldú
Dipòsit Legal: T. 1428-2012

an area of the surface of the sample that will not undergo anodisation in order to guarantee that a good electric contact to the aluminium layer will be maintained during the whole anodising process.

For this thesis, two electrochemical cells with different sizes were designed and fabricated. One was used for processing small samples (wafer pieces), so it was developed for a small anodising area (a circle of 15 mm in diameter and 1.75 cm^2 area). The second one was used for anodising the whole 4” silicon wafer. The latter was designed for proving the compatibility of the anodisation techniques with the standard technology of the CNM-IMB, which is the supplier of micro hotplates on 100-mm wafers. In this case, the anodised area was a circle of 90 mm in diameter and 63.62 cm^2 area.

Figure 3-1.a shows the assembly drawing of the small electrochemical cell, which consists of two parts, the base and the tank. The base is where the silicon wafer is placed for the anodising with the aluminium-covered side facing up and the tank is screwed to the base in such a way that it firmly holds the wafer. The area of the tank progressively decreases down to the final anodizing area. Figure 3-1.b shows a photograph of this cell with the two parts set apart. The base comprises a stainless steel disc where the sample is positioned and a flexible U-shaped stainless steel fastener provides the electric contact to the sample. The junction consists of a polished Teflon ring to prevent the leakage of the electrolyte.

UNIVERSITAT ROVIRA I VIRGILI
GAS SENSOR MICROSYSTEMS BASED ON NANOSTRUCTURED LAYERS VIA ANODIC OXIDATION
Raúl Calavia Boldú
Dipòsit Legal: T. 1428-2012

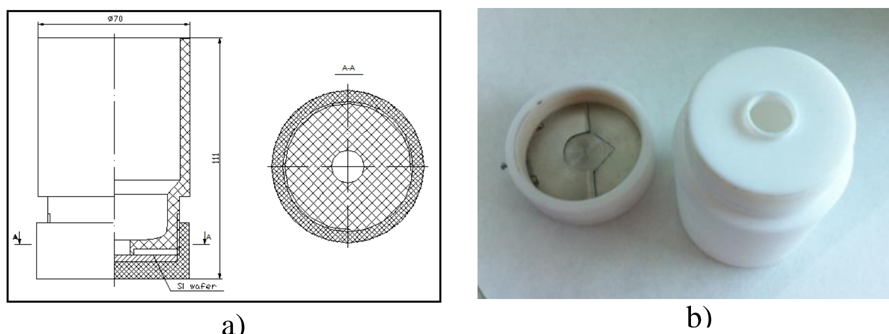

Figure 3-1 Teflon cell to anodise a 15 mm diameter circle on aluminium layers sputter-deposited on insulating substrates a) Assembly drawing of the cell b) Photograph of the cell with the u-shaped stainless steel fastener

Figure 3-2.a shows the schema of the large Teflon cell developed to be compatible with the 4" silicon wafer. Generally, this cell is similar to the small one because, once more, it is composed of two parts, the base, where the silicon wafer is placed, and the electrolyte tank. In this case the electric contact is made by connecting a piece of stainless steel to the external aluminium ring, which is delimited by the Teflon ring. This second electrochemical cell has been developed in order to make the anodising process compatible with integral technologies applied to 100 mm wafers.

Figure 3-2.b shows a photo of the Teflon cell fabricated where the contact to the anode (AEC), the cathode (CEC), the electrolyte tank (ET) and the polished base where the silicon wafer (BW) is placed are clearly indicated. Figure 3-2.c shows a 4" silicon wafer with an anodised aluminium layer on top that has been obtained using the Teflon cell developed.

UNIVERSITAT ROVIRA I VIRGILI
GAS SENSOR MICROSYSTEMS BASED ON NANOSTRUCTURED LAYERS VIA ANODIC OXIDATION
Raúl Calavia Boldú
Dipòsit Legal: T. 1428-2012

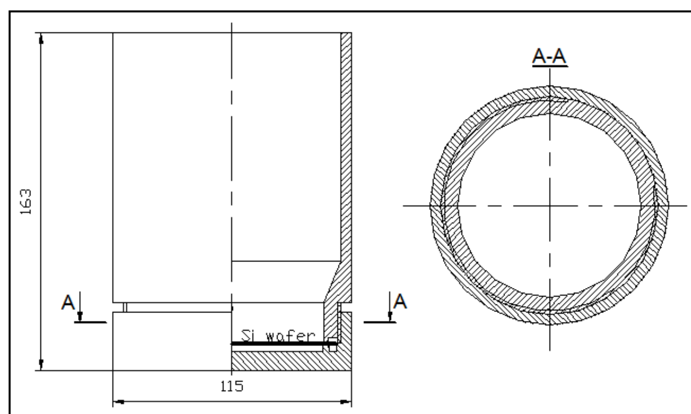

a)

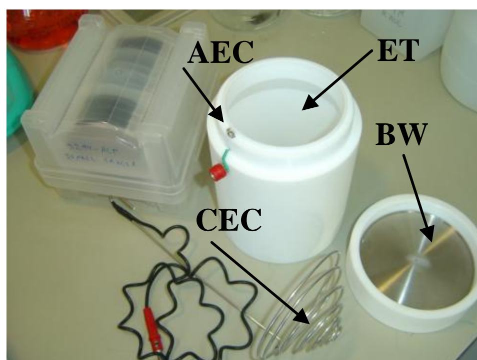

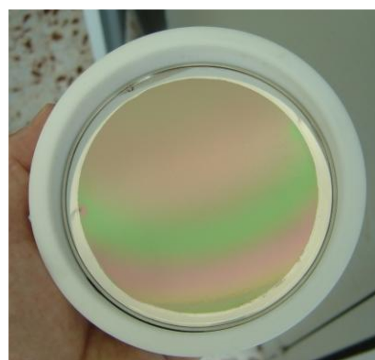

b) c)

Figure 3-2 Teflon cell to anodise 4-inch silicon wafers. a) Assembly drawing. b) Photo of the all parts of the fabricated Teflon cell. c) Base of Teflon cell with a 4-inch silicon wafer after anodising

In both Teflon cells, the cathode is a spiral-shaped, stainless steel wire with the surface area comparable with that of the sample to be anodized.

As explained in the state of the art section, the anodising is an electrochemical process and it can be conducted in a potentiostatic (voltage-stabilising) or galvanostatic (current-stabilising) modes. The parameter that decides the diameters of pores in anodic alumina film is the voltage in both cases, so if this parameter is

UNIVERSITAT ROVIRA I VIRGILI
GAS SENSOR MICROSYSTEMS BASED ON NANOSTRUCTURED LAYERS VIA ANODIC OXIDATION
Raúl Calavia Boldú
Dipòsit Legal: T. 1428-2012

kept the same, the pore would grow of the same size regardless of the anodising mode. On the other hand, the current that flows through the circuit depends on the anodised area and the current density set. Since we developed two anodising cells for processing samples of very different sizes, a system is needed to control, with high precision, the voltage and the current at very different output powers.

For this reason, two set-ups were developed, one for the low anodising area cell and another one for the large anodising area cell. In both cases the power supply can be controlled up to 500 V. However, one set-up is for controlling low currents (10^{-5} – $2 \cdot 10^{-2}$ A) with high precision and accuracy and the second one is for high currents ($2 \cdot 10^{-3}$ - 1.5 A) with an acceptable precision and accuracy.

For the small cell, a Keithley 2410 power supply was selected because it has high accuracy in the entire voltage range, from 0 to 1100 V. This high range in the voltage offers high flexibility for using it with different electrolytes. This requires employing very different working voltages and allows us to obtain a high range of different morphologies for the resulting porous alumina.

This power supply has two maximum current output ranges: 1 A up to 20 V and 20 mA up to 1100 V. Since in the formation of porous alumina it is common to use voltages that are higher than 20 V, this power supply is ideal for small samples because it offers high

UNIVERSITAT ROVIRA I VIRGILI
GAS SENSOR MICROSYSTEMS BASED ON NANOSTRUCTURED LAYERS VIA ANODIC OXIDATION
Raúl Calavia Boldú
Dipòsit Legal: T. 1428-2012

accuracy in a wide voltage range at small and moderate currents (i.e. up to 20 mA).

Table 3-1 shows the voltage ranges, accuracy and noise levels for Keithley 2410. The maximum voltage required for anodising is 1000 V, and for the range of 0-1000 V, the programming resolution is 50 mV with an accuracy of 0.02 % (200 mV in the worst case) plus 100 mV of constant error and 20 mV noise. Therefore, the maximum error at 1000 V is 320 mV. It can be concluded that this power supply has very high precision control in the high voltage range.

Range	Programming Resolution	Accuracy 23 ºC ±5 ºC ±(% rdg. + volts)	Noise (peak to peak) 0.1 Hz to 10 Hz
200 mV	5 µV	0.02% + 600 µV	5 µV
2 V	50 µV	0.02% + 600 µV	50 µV
20 V	500 µV	0.02% + 2.4 mV	5 mV
1000 V	50 mV	0.02% + 100 mV	20 mV

Table 3-1 Voltage accuracy for a 2410 Keithley power supply

Table 3-2 shows the accuracy parameters for the current supply of Keithley 2410. For the small anodizing area cell, the estimated current needed is lower than 20 mA, so the highest current range will be 20 mA. At this working range, the programming resolution is 500 nA with an accuracy error of 9 µA plus 4 µA and 200 nA of noise. Therefore, the maximum current error is 13.2 µA.

Range	Programming Resolution	Accuracy 23 ºC ±5 ºC ±(% rdg. + amps)	Noise (peak to peak) 0.1 Hz to 10 Hz
1 µA	50 pA	0.035% + 600 pA	5 pA
10 µA	500 pA	0.033% + 2 nA	50 pA
100 µA	5 nA	0.031% + 20 nA	500 pA
1 mA	50 nA	0.034% + 200 nA	5 nA
20 mA	500 nA	0.045% + 4 µA	200 nA
100 mA	5 µA	0.066% + 20 µA	1 µA
1 A	50 µA	0.27% + 900 µA	100 µA

Table 3-2 Current accuracy for a 2410 Keithley power supply

In summary, Keithley 2410 power supply has a very good control of the voltage in its full-scale range and also of the current (provided that the current is kept lower or equal to 20 mA) and, therefore, this power supply is ideal for being used with the low anodising area cell.

For the large cell, we have used two Agilent power supplies, the 5751A and 5752A models. These have a maximum voltage range of 300 V and 600 V, respectively and the maximum currents are 2.5 A and 1.3 A, respectively. The technical specifications of these two models are shown in Table 3-3.

UNIVERSITAT ROVIRA I VIRGILI
GAS SENSOR MICROSYSTEMS BASED ON NANOSTRUCTURED LAYERS VIA ANODIC OXIDATION
Raúl Calavia Boldú
Dipòsit Legal: T. 1428-2012

Parameter	N5751A	N5752A
Programming		
Accuracy ±(% rdg + volts)	0.05% + 150 mV	0.05% + 300 mV
Accuracy ±(% rdg + amps)	0.1% + 2.5 mA	0.1% + 1.3 mA
Resolution (volts)	36 mV	72 mV
Resolution (amps)	0.3 mA	0.156 mA
Measurement		
Accuracy ±(% rdg + volts)	0.1% + 300 mV	0.1% + 600 mV
Accuracy ±(% rdg + amps)	0.1% + 7.5 mA	0.1% + 3.9 mA
Resolution (volts)	36 mV	72 mV
Resolution (amps)	0.3 mA	0.156 mA
General		
Noise (peak to peak) 5 Hz to 1 MHz	13 mA	8 mA

Table 3-3 Technical specifications for N5751A and N5752A Agilent power supplies

For 5751A model, the maximum voltage supplied is 300 V and for this voltage range the maximum error is 600 mV. For the maximum current (i.e. 2.5 A) the maximum error is 23 mA.

For the 5752A model, the maximum voltage supplied is 600 V and for this range the maximum error is 1.2 V. For the maximum current (i.e., 1.3 A) the maximum error is 15 mA.

The Agilent power supplies used in the second set-up are not suitable for accurately measuring low currents (i.e. <10 mA). Therefore, when the set-up uses these power supplies, the current read-out is performed by a 3401A Agilent multimeter. The main characteristics of this multimeter are reported in Table 3-4.

UNIVERSITAT ROVIRA I VIRGILI
GAS SENSOR MICROSYSTEMS BASED ON NANOSTRUCTURED LAYERS VIA ANODIC OXIDATION
Raúl Calavia Boldú
Dipòsit Legal: T. 1428-2012

Features	3401A
DC Voltage	
Accuracy	0.02%
Range	500 mV – 1000 V
RMS AC Voltage	
Accuracy	0.35%
Range	500 mV – 750 V
DC Current	
Accuracy	0.05%
Range	500 μA – 10 A
RMS AC Current	
Accuracy	0.5%
Range	500 μA – 10 A
Resistance	
Accuracy	0.1%
Range	500 Ω – 50 MΩ

Table 3-4 Technical specifications for a 3401A Agilent multimeter

Combining the power supplies Keithley 2410, Agilent 5751A and 5752A, it is possible to control with high accuracy the voltage and the current in a wide range of interest. This allows us to obtain porous alumina with different morphologies and this gives us the flexibility in choosing the formation conditions without being confined by the limitations of each device.

In order to get the maximum performance of the power supplies and to enable a post-process analysis (e.g., to analyse the voltage-

UNIVERSITAT ROVIRA I VIRGILI
GAS SENSOR MICROSYSTEMS BASED ON NANOSTRUCTURED LAYERS VIA ANODIC OXIDATION
Raúl Calavia Boldú
Dipòsit Legal: T. 1428-2012

time and current-time behaviour during the anodising) it was necessary to develop a controlling software.

This controlling software was developed in Labview programming language and the GPIB was used for communication between the power supplies and a computer. All power supplies installed in this set-up are compatible with the standard protocol IEEE 488.2, so the control software employs this protocol to communicate with the power supplies.

The software developed allows to configure the following process parameters:

- Step time: Selects the monitoring/control scan time. The minimum step time is 0.1 s.
- Voltage/current control: Selects the operation mode of the power supply, voltage or current control mode. It leads to configure the electrochemical process as potentiostatic or galvanostatic, respectively (Figure 3-3 Tab control 1).
- Voltage/current limit: This value marks the maximum value for the uncontrolled parameter, current in potentiostatic and voltage in galvanostatic mode. If the power supply rises to this protection value, the system changes automatically to the other control mode in order to maintain this value.
- Ramp/constant/file tap: Using this control the user can configure different profiles for the controlled parameter (i.e, voltage or current), see Figure 3-3 Tab control 2.

UNIVERSITAT ROVIRA I VIRGILI
GAS SENSOR MICROSYSTEMS BASED ON NANOSTRUCTURED LAYERS VIA ANODIC OXIDATION
Raúl Calavia Boldú
Dipòsit Legal: T. 1428-2012

  - Ramp: The controlled parameter increases using a constant rate. In this mode the user can control the rate and the initial and final values.
  - Constant: Selects a constant value for the parameter during the time indicated in this tab.
  - File: Selects a text file with the profile of the voltage/current. This option leads to generate an arbitrary behaviour during the anodising process.
- Stop: Stop the control process and shut down the power supply immediately.
- Simulation: When using a file as source for the voltage/current behaviour it is important to simulate the profile loaded in order to check for data errors. If the data is not verified and the profile is not properly loaded, abnormally high voltage or currents levels may occur, which could damage the sample.
- Data storage: This control is employed to save or discard the actual current/voltage curve. The user can select the path for the destination of the data file generated.

The software developed shows in real time the current and voltage employing two graphs. Therefore, it is possible to completely control the anodising process with traditional or new profiles. The software can be used for a wide range of applications such as anodising, other electrochemical processes, auto annealing gas sensors, semiconductor test, etc.

UNIVERSITAT ROVIRA I VIRGILI
GAS SENSOR MICROSYSTEMS BASED ON NANOSTRUCTURED LAYERS VIA ANODIC OXIDATION
Raúl Calavia Boldú
Dipòsit Legal: T. 1428-2012

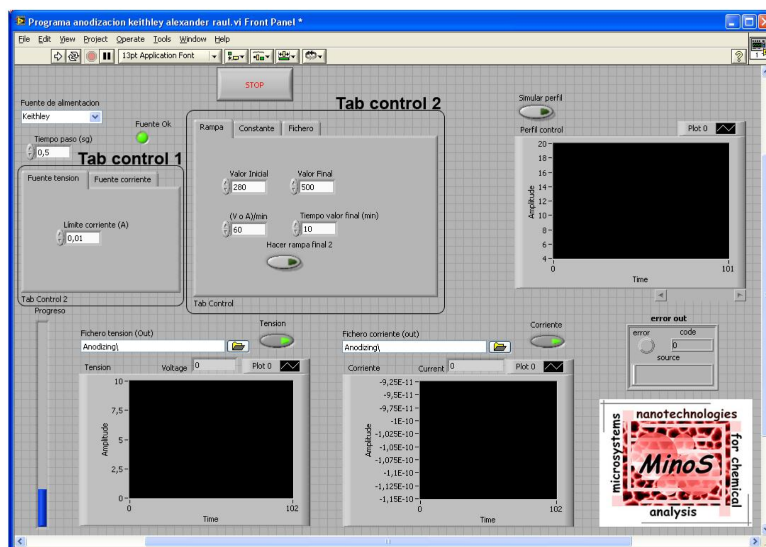

Figure 3-3 Screen capture of the Labview software developed to control the anodising system

In summary, Figure 3-4 shows the complete experimental set-up developed in this work. It is composed of the electrochemical Teflon cell (developed for anodising metals on silicon) and the controlling devices (power supply, multimeter and computer).

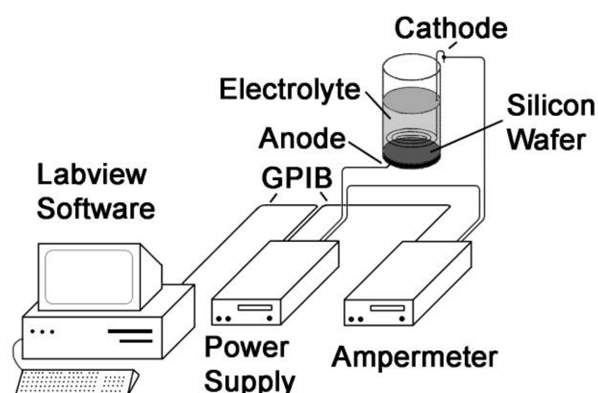

Figure 3-4 Scheme of the anodisation system developed for anodisation purposes

UNIVERSITAT ROVIRA I VIRGILI
GAS SENSOR MICROSYSTEMS BASED ON NANOSTRUCTURED LAYERS VIA ANODIC OXIDATION
Raúl Calavia Boldú
Dipòsit Legal: T. 1428-2012

3.2 Anodising thin film aluminium on an oxide-coated silicon wafer

As already explained in Chapter 2, gas sensitivity of metal oxide based devices is improved by increasing the surface in contact to the environment. Therefore, preparing nanostructured films on oxide-coated silicon wafers is a good strategy to improve sensor response of micromachined gas sensors.

This strategy was first introduced by our group [1] in which a *two-step* anodisation process was implemented to obtain self ordered porous alumina on oxidised silicon wafers subsequently coated by sputtered WO_3. Unlike in [1], the samples developed in this work have been obtained using a simplified, one-step anodisation process in order to be compatible with standard silicon technology (e.g. lift-off process).

During the formation of porous alumina, the growth rate of pores is not completely homogenous and some areas grow faster than others. Since this difference is at the nanoscale range (few nm/min), this is not a problem when an aluminium foil or a thicker sheet is to be anodised. However, in the case of thin film aluminium layers (below 1 μm) sputter-deposited on an insulating substrate, like the samples employed in this work, small differences in growth rate can generates areas in which the aluminium layer is not completely consumed.

The aluminium layers are deposited by sputtering. Typically sputtering does not cover in a completely homogeneous way silicon

UNIVERSITAT ROVIRA I VIRGILI
GAS SENSOR MICROSYSTEMS BASED ON NANOSTRUCTURED LAYERS VIA ANODIC OXIDATION
Raúl Calavia Boldú
Dipòsit Legal: T. 1428-2012

wafers, where the thickness distribution depends on the sputtering machine employed [2].

Since the thickness obtained is not completely homogeneous, during the anodising process the aluminium is consumed earlier in some areas (i.e. thinner areas) than in others.

These two problems may result in islands of non-anodised aluminium, remaining at the film/substrate interface.

This can be improved by using a thin titanium layer under the aluminium. In that way, a metallic titanium layer remains during the whole anodising process, which allows for totally oxidising the aluminium across the whole wafer surface.

Titanium is considered compatible with silicon technology because it is a typical material used in order to improve the adhesion of different metal layers (e.g. Pt) onto silicon or silicon dioxide. However, titanium is a very reactive material. It may react, especially if heated, with silicon or silicon oxide, which makes more difficult the compatibility of anodising with standard silicon technology.

The thickness of the aluminium layers sputtered on silicon wafers ranges from 400 nm to 1 μm, depending on the depth required for the pores of the porous alumina layer obtained. The titanium layer deposited under aluminium is very thin (20 to 40 nm) because it is used only as an adhesion promoter and is thick enough to enable the full anodisation of the aluminium layer.

UNIVERSITAT ROVIRA I VIRGILI
GAS SENSOR MICROSYSTEMS BASED ON NANOSTRUCTURED LAYERS VIA ANODIC OXIDATION
Raúl Calavia Boldú
Dipòsit Legal: T. 1428-2012

As already explained in the state of the art section, the voltages applied during the anodising process decide the pore diameters and interpore distances [3]. Therefore, controlling voltages is a good strategy to control the morphology of the porous alumina. Once porous alumina is grown, its pore diameter can be increased by a pore widening process implying immersing the sample in 20 g/l CrO_3 and 35 ml/l H_3PO_4 at 60 ºC during several minutes. However, the control mode used in this work is galvanostatic because it generates more homogeneous porous alumina films [4]. This means that the current densities used for galvanostatic anodising modes should be set with respect to the value of voltage desired for each particular case.

Figure 3-5 shows SEM images of the surface of a porous alumina film obtained using a water solution of 0.4 M tartaric acid at 180 V before and after pore widening treatments at 60 ºC during 5 and 10 minutes. As a result of this etching process, the pores become wider while the interpore distance remains essentially the same.

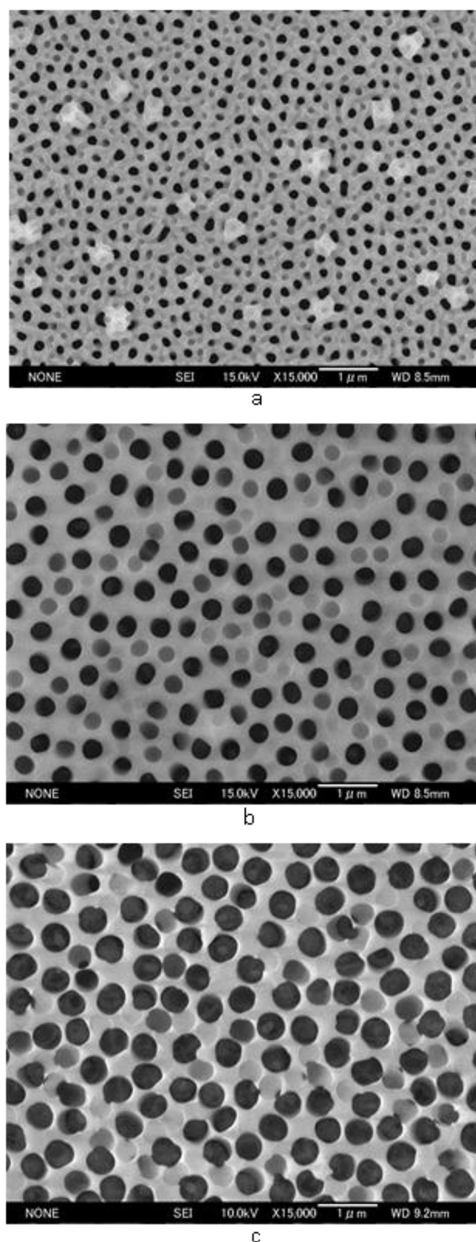

Figure 3-5 The effect of pore widening in 20 g/l CrO_3 and 35 ml/l H_3PO_4 solution. a) Porous alumina as anodised in 0.4 M tartaric acid. b) The same film after 5 min in the pore widening solution. c) The same film after 10 min in the pore widening solution.

3.2.1 Preparation of porous alumina supported WO_3 layers

3.2.1.1 The formation of porous alumina templates

In the state of the art chapter, a process for growing a porous alumina layer was described (the case of a thick aluminium foil). However, here the aluminium layer to be anodised is a thin, submicrometer in thickness layer sputter-deposited onto a silicon dioxide layer, which is an insulator. Such anodising needs special consideration if the purpose is to grow a porous-type anodic film, like in the present study.

A typical voltage-time behaviour for anodising an aluminium foil employing the galvanostatic mode is shown in the literature review. When the voltage becomes stable, the pores grow at a constant rate and, as the aluminium is thick, the pore depth would mainly depend on the anodising time.

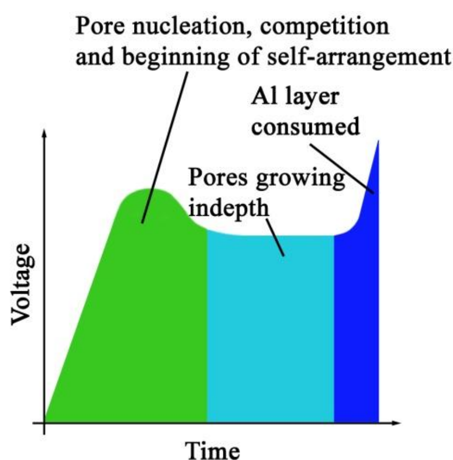

Figure 3-6 Voltage-time behaviour for anodising thin film aluminium on a dielectric substrate using a galvanostatic mode.

UNIVERSITAT ROVIRA I VIRGILI
GAS SENSOR MICROSYSTEMS BASED ON NANOSTRUCTURED LAYERS VIA ANODIC OXIDATION
Raúl Calavia Boldú
Dipòsit Legal: T. 1428-2012

In the case of a sputtered thin aluminium layer, the behaviour is alike the previously explained until the anodising front is approaching the dielectric substrate. Then, the voltage will increase because the substrate surface is insulating (aluminium is deposited on an oxide-coated silicon wafer) or on a metallic layer whose oxide has a substantial ionic resistance (e.g. a titanium underlayer).

The electrolyte used was an aqueous solution of 0.4 M tartaric acid and the electrochemical control used was galvanostatic-potentiostatic configured at 10 mA/cm^2 and a maximum voltage set at 230 V.

Figure 3-7 shows the voltage-time and current-time behaviours during the one-step anodising of a thin aluminium layer superimposed on a titanium layer sputter-deposited on an oxidised silicon wafer. In the curve it is possible to identify three specific stages.

In the first stage (Figure 3-7 I), the current is set to a constant value by the power supply and a compact alumina layer begins to grow. As a result, the resistance increases and so does the voltage. During this growth, the dissolution of alumina at high electric field points starts and so does the nucleation of pores. Before reaching the steady-state film growth (the voltage remains constant during this process), the aluminium layer is consumed and the voltage starts to increase because of the oxidation of the titanium underlayer. When the voltage arrives to the value of 230 V, which had been configured in the power supply, the set-up changes to the

potentiostatic mode and the current begins to decrease (Figure 3-7 stage II). This configuration is maintained during 400 seconds in order to ensure that the entire aluminium layer is anodised across the whole wafer surface. As the pores begin to nucleate already at the stage of the linear voltage growth, a porous film, although having not well organised pores, forms before the voltage begins to increase. Such an extreme regime is expected to give porous film with the minimal possible pore aspect ratio, which are important requirements for the films synthesised in this study for being used as templates for later sputter-deposition of WO_3 sensing layers.

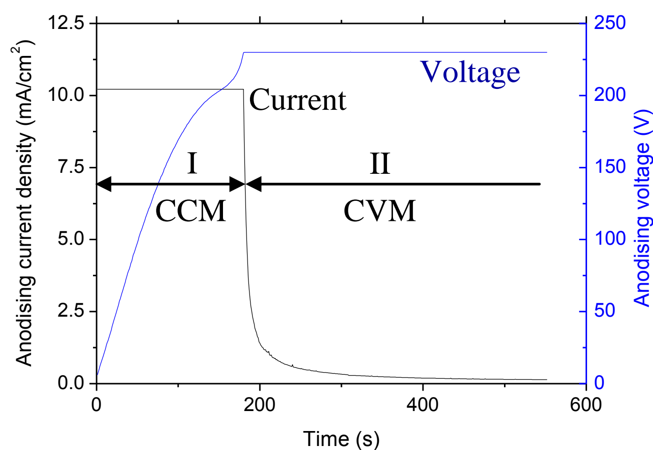

Figure 3-7 Current-time and voltage-time behaviour during *one-step* galvanostatic-potentiostatic anodising in 0.4 M tartaric acid of an aluminium/titanium thin-film bilayer onto silicon dioxide/silicon substrate

A photo of the anodised aluminium/titanium bilayer on an oxidised 100-mm silicon wafer is shown in Figure 3-2.c.

UNIVERSITAT ROVIRA I VIRGILI
GAS SENSOR MICROSYSTEMS BASED ON NANOSTRUCTURED LAYERS VIA ANODIC OXIDATION
Raúl Calavia Boldú
Dipòsit Legal: T. 1428-2012

3.2.1.2 Deposition of the sensing material on the alumina templates

As explained before, the porous alumina layer on the membrane of a micromachined transducer is to be formed in order to increase the surface of the sensing material in contact with a gas without increasing the area to be heated. This helps keeping very low power consumption of the gas sensor chips. To this end, the sensing material is to be deposited over the pores but without clogging their outlets, in order to provide a large surface/volume ratio of the deposited material. Two deposition techniques were implemented: magnetron RF sputter-deposition and atomic layer deposition.

3.2.1.2.1 WO_3 films sputter-deposited by a magnetron method

Sputtering belongs to PVD techniques because the deposition is not based on a chemical reaction on the surface of the sample. This technique has been widely employed and studied in the deposition of metal oxide gas sensing layers.

In this deposition technique, the temperature is an important parameter because the size of the grains in the deposited layer increases with temperature. If a long deposition time is needed, the temperature of the substrate may significantly increase during the process and the surface of the deposited layer becomes rather rough; this is especially the case for some metals such as gold or aluminium.

Sputtering is not an optimal technique when there is a need for coating vertical walls of structural elements on the substrate. For

UNIVERSITAT ROVIRA I VIRGILI
GAS SENSOR MICROSYSTEMS BASED ON NANOSTRUCTURED LAYERS VIA ANODIC OXIDATION
Raúl Calavia Boldú
Dipòsit Legal: T. 1428-2012

example, when the layer deposited is too thin, a discontinuous layer forms (Figure 3-8.b). In some applications, a discontinuous layer is of interest, for example in a lift-off process; the discontinuities favour the removal of the photoresist. But in other applications, like in the deposition of metal layers for a subsequent anodisation, it is very important that a continuous layer is obtained. Therefore, there must be minimum thickness to be deposited in order to ensure that the resulting layer is continuous.

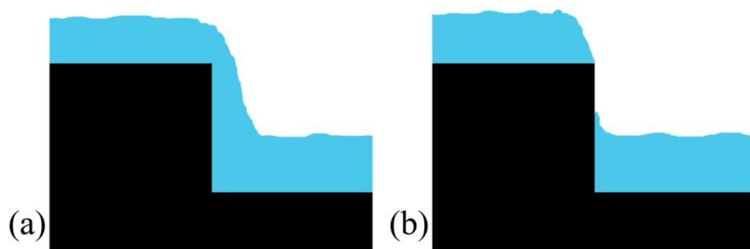

Figure 3-8 Vertical wall coveage by a sputtering deposition technique. a) Continuous layer. b) Discontinuous layer

The sample to be coated by magnetron sputtered WO_3 has a porous alumina layer on top, so in order to prevent clogging the pores by the deposit, it is important to adjust their diameter/depth ratio. The depth of the pores is determined by the aluminium layer thickness, and by using different electrolytes it is possible to obtain different ratios. Figure 3-9 shows schematically the results of the sputter-deposition of a 250-nm thick WO_3 film onto the porous alumina layer, which was grown by one-step anodising of aluminium in 0.4 M tartaric acid (Figure 3-9.a) and 0.4 M malonic acid (Figure 3-9.b). The anodising voltage for malonic acid is lower than that

UNIVERSITAT ROVIRA I VIRGILI
GAS SENSOR MICROSYSTEMS BASED ON NANOSTRUCTURED LAYERS VIA ANODIC OXIDATION
Raúl Calavia Boldú
Dipòsit Legal: T. 1428-2012

for tartaric acid, so the diameter to depth ratio of alumina pores is higher for the second electrolyte and the sputtered layer obtained properly coats the pores in this case. In the case of the malonic acid, sputtered WO_3 does not cover completely the wall of the pores and does not reach the pore bottoms.

Onto these porous alumina layers, tungsten oxide was deposited by reactive RF sputtering using an ESM100 Edwards sputtering system and a tungsten target of 99.95 % purity with a diameter of 4” and a thickness of 0.125”. The distance between the target and the wafers was 70 mm and the pressure in the deposition chamber before starting the sputtering process was $6x10^{-3}$ mbar. The reactive sputtering atmosphere consisted of Ar-O_2 mixed gas and its flow rate was controlled by separated gas flow-meters to provide Ar:O_2 flow ratio of 1:1. The pressure in the deposition chamber during the deposition process was 5x10-3 mbar and the power was set to100 W.

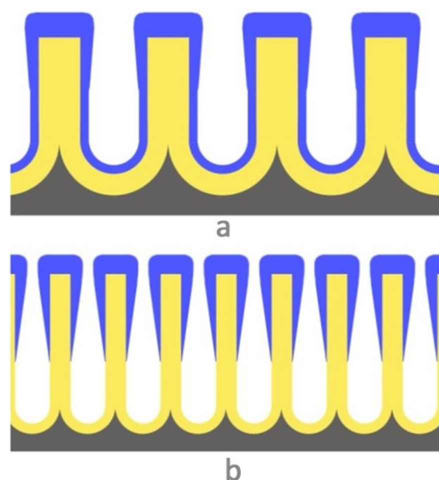

Figure 3-9 Schematic view of tungsten oxide layers sputter-deposited over porous anodic alumina templates with different pore aspect ratios. a) Porous alumina formed in 0.4 M tartaric acid. b) Porous alumina formed in 0.4 M malonic acid. In both cases, the films were grown by ONE-STEP anodizing.

Figure 3-10 shows an SEM image of the porous-alumina-supported tungsten oxide layer. The film was grown by one-step anodising in the tartaric acid electrolyte with a subsequent pore widening at the conditions as in Figure 3-7.

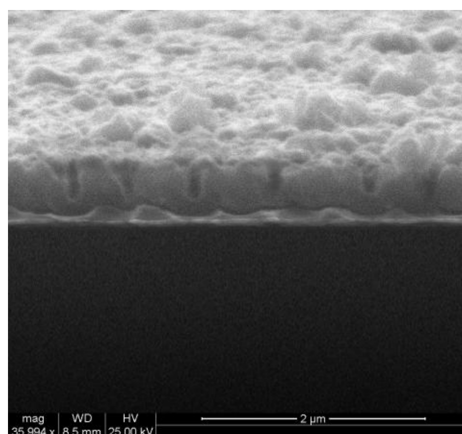

Figure 3-10 SEM image of a porous alumina grown in 0.4 M tartaric acid solution and covered by sputter-deposited WO3 layer

UNIVERSITAT ROVIRA I VIRGILI
GAS SENSOR MICROSYSTEMS BASED ON NANOSTRUCTURED LAYERS VIA ANODIC OXIDATION
Raúl Calavia Boldú
Dipòsit Legal: T. 1428-2012

The findings ultimately show that, despite the one-step anodizing approach developed and employed here, the technique allows for completely covering the pore walls and film surface if the film is formed in 0.4 M tartaric acid and subjected to pore widening in the chromium-containing solution for 5 to 10 min.

3.2.1.2.2 ZnO film prepared by atomic layer deposition

As explained in chapter 2, for gas sensor application, if the sensing layer thickness is reduced, the sensitivity may increase significantly. Therefore, ALD is a very promising technique because it allows for depositing extremely thin layers. The conformal deposition is also important to ensure a proper coating of the whole surface of a porous alumina film.

Figure 3-11 shows an SEM image of an FIB (Focused Ion Beam)-cut sample where it is possible to identify the porous alumina with the barrier layer. This porous alumina was obtained galvanostatically in 0.4 M tartaric acid electrolyte at 4.5 mA/cm^2. The substrate was an oxide-coated silicon wafer. The initial films were 20 nm titanium deposited by RF sputtering and 600 nm aluminium deposited by DC sputtering. The shiny thin layer that uniformly covers the alumina pores is a zinc oxide film deposited by ALD. Its thickness is estimated to be about 10 nm. The upper layer is a platinum stub deposited by the FIB in order to protect the film surface from being etched. From the image, it is clear that the ZnO layer covers the pore walls and pore bottoms extremely uniformly and has unchanged thickness across the whole film section. This confirms that the ALD technique may be a perfect

UNIVERSITAT ROVIRA I VIRGILI
GAS SENSOR MICROSYSTEMS BASED ON NANOSTRUCTURED LAYERS VIA ANODIC OXIDATION
Raúl Calavia Boldú
Dipòsit Legal: T. 1428-2012

alternative to magnetron sputter-deposition and is worth studying in a future work.

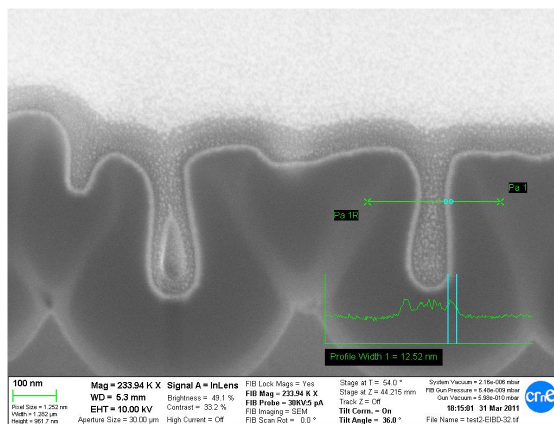

Figure 3-11 SEM image of an FIB prepared section of ALD deposited zinc oxide film over a porous alumina grown in 0.4 M tartaric acid at 200 V.

3.2.2 WO_3 nanodot film grown by self-organised anodising

These samples were developed by anodising Al/W thin film layers sputter-deposited onto oxidised silicon wafers. First, a porous alumina was grown from the aluminium layer and then the tungsten layer was anodized under the alumina film to grow self-organised tungsten oxide nanodots.

Anodising was carried out in an aqueous solution of 0.4 mol dm^{-3} $H_2C_2O_4$ modified by the addition of 2.4 m mol dm^{-3} NH_4F [5]. The anodising mode used was potentiodynamic-potentiostatic realised as follows. At the beginning, the voltage is linearly swept from 0 V to 27 V in 100 seconds. Then, the power supply maintains the voltage constant during 15 minutes (see Figure 3-12). It is possible to identify 3 different regions in this figure.

UNIVERSITAT ROVIRA I VIRGILI
GAS SENSOR MICROSYSTEMS BASED ON NANOSTRUCTURED LAYERS VIA ANODIC OXIDATION
Raúl Calavia Boldú
Dipòsit Legal: T. 1428-2012

The first region (Figure 3-12 I) corresponds to sweeping the voltage and the second (Figure 3-12 II) to its stabilisation. When the voltage is stabilised it is possible to identify the typical behaviour of the current-time curve when the pores are self-organised and start to grow indepth. The gradually increased current at the II stage may be due to an increased dissolution of the alumina owing to the addition of ammonium fluoride in the electrolyte.

In the third anodising region (Figure 3-12 III) the aluminium layer is consumed and the electrochemical process arrives to the tungsten layer. Since tungsten is a valve metal, it starts to be oxidised and the current decreases due to the fact that the ionic resistivity of tungsten oxide is lower than that of alumina. This condition is maintained during several minutes in order to ensure the complete consumption of the aluminium layer and homogeneous oxidation of the tungsten underlayer.

To improve the regularity of the oxide regions protruding from the tungsten layer across the sample surface, and increase the percentage of tungsten oxide in the film composition, a reanodisation process was carried out in the same electrolyte by sweeping the voltage from 27 to 100 V at a constant rate with the final current decay (Figure 3-13).

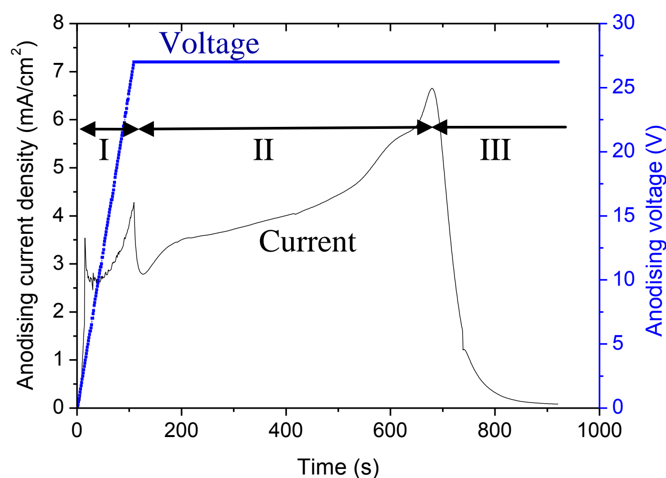

Figure 3-12 Voltage-time and current-time behaviour during anodising Al/W metal layers, which has 3 stages. I) Voltage sweep from 0 to 27 V. II) Potentiostatic anodising of Al at 27 V. III) Constant voltage anodising of the tungsten layer to form tungsten oxide nanodots.

During reanodising in the given electrolyte, columns of anodic tungsten oxide grew in the alumina pores as explained in [6] and simultaneously dissolved at the electrolyte / WO_3 interface due to the aggressiveness of the electrolyte. This is reflected by the current-time behaviour during the voltage sweep (Figure 3-13): the current rises up until the voltage is stopped and then, when the voltage is kept constant, the current does not decay normally and the current-time curve has a number of overshoots, arisen from the enhanced electrochemical dissolution of the material. With an adjusted voltage sweep rate it was possible to reach an equality between the oxide growth and dissolution so that, at the end of the voltage-stabilisation period, arrays of tungsten oxide nanodots, of

UNIVERSITAT ROVIRA I VIRGILI
GAS SENSOR MICROSYSTEMS BASED ON NANOSTRUCTURED LAYERS VIA ANODIC OXIDATION
Raúl Calavia Boldú
Dipòsit Legal: T. 1428-2012

nearly round shape, each surrounded by a very thin ring of tungsten oxide, were obtained.

The conditions applied here have been developed to grow tungsten oxide nanodots, not columns as reported in the previously published paper [6], because the dot-like film is considered advantageous compared with the column-like films. The advantage arises from the improved composition of the dot-like film and better compatibility of the dot-like morphology with the technique for making top sensor electrodes over the film in the practical microsensors by sputter-deposition of Pt and lift-off process; the details are given in the later text.

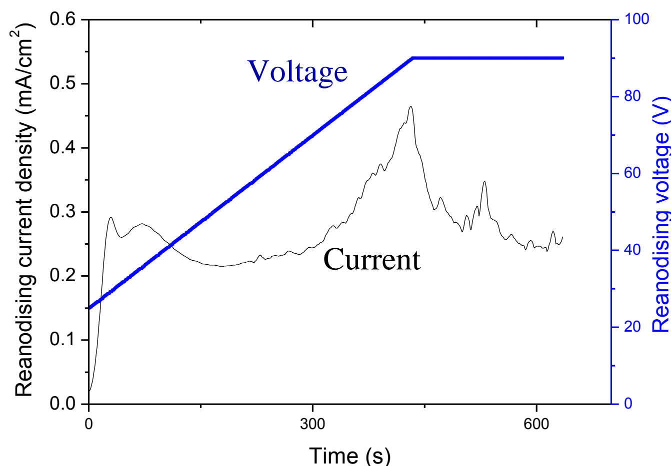

Figure 3-13 Voltage-time and current-time behaviour for reanodizing of the Al/W bilayer which had been anodised as shown in Figure 3-12. During the reanodising, tungsten oxide nanodots grow homogeneously across the whole sample surface.

After the anodising and reanodising processes, the wafer was immersed in a porous alumina selective etching solution consisting

of 20 g l^{-1} CrO_3; 35ml l^{-1} H_3PO_4 kept at 60 ºC for 15 min in order to remove completely the porous alumina. Once the nanostructured tungsten oxide layer was derived, the wafer was heated up to 500 ºC during 2 h in order to crystallise the tungsten oxide.

Figure 3-14 shows an SEM image of the surface and cross section of the WO_3 nanodot film. It is possible to identify the high density of nanodots obtained. This is expected to increase the surface of the sensing material in contact with the environment.

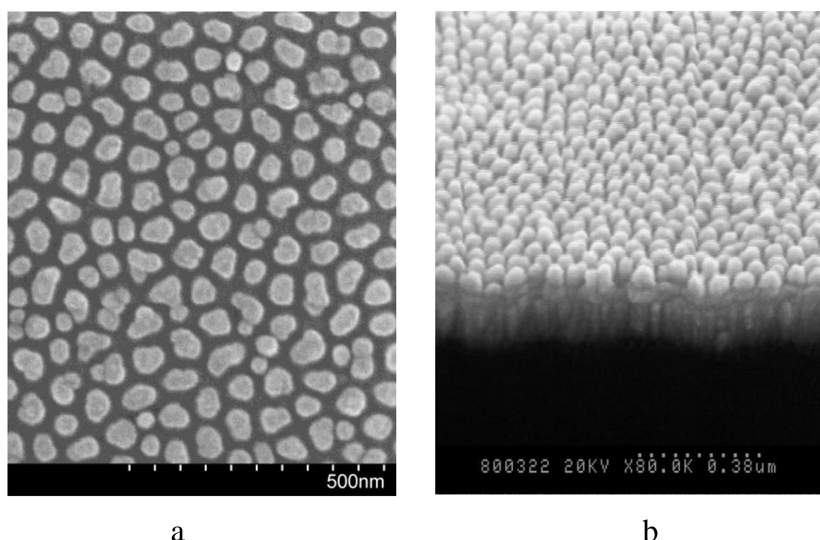

Figure 3-14 SEM images of the WO_3 nanodot film obtained by anodising/reanodising of Al/W metal layers at 27V/100V onto a SiO_2/Si substrate.

3.3 The technological approaches

The methods to grow a porous alumina film and the other valve metal oxides must be compatible with the standard silicon microtechnology and, to this end, two different approaches have been developed in this work and justified experimentally.

UNIVERSITAT ROVIRA I VIRGILI
GAS SENSOR MICROSYSTEMS BASED ON NANOSTRUCTURED LAYERS VIA ANODIC OXIDATION
Raúl Calavia Boldú
Dipòsit Legal: T. 1428-2012

The initial structure of the gas sensor used in this work is the micro-hotplate membrane based on standard Microsystems technology [7]. The initial steps to obtain such structures are as follows (see Figure 3-15):

- Substrate: the substrate used is a 300 µm thick silicon wafer, four inches in diameter, *p*-type (B), 40 $Ohm \cdot cm^{-2}$ of resistivity, double face polished and with (100) orientation (Figure 3-15.a).
- Silicon nitride deposition: a 300 nm silicon nitride (Si_3N_4) is grown by low pressure chemical vapour deposition (LPCVD) on both wafer sides (Figure 3-15.b).
- Heater deposition and patterning: a 480 nm thick micro-heater is formed on the face side of the wafer by LPCVD employing $POCl_3$-doped polysilicon (Figure 3-15.c).
- Silicon dioxide growth: an 800 nm thick silicon dioxide layer is grown by LPCVD over the face of the wafer to electrically isolate the heaters from the active layers and sensor electrodes, which are to be deposited and patterned later (Figure 3-15.d).

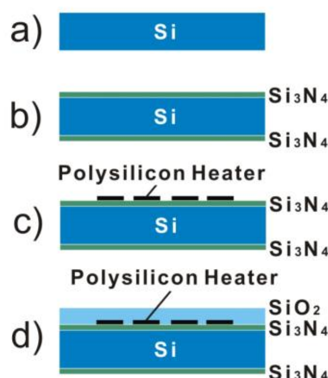

Figure 3-15 Preparation of the silicon wafer for the micromachined membrane for gas sensor applications. a) Silicon wafer, *p*-type, 40 Ohm cm^{-2}, (100) orientation. b) 300nm Si_3N_4 deposition on both sides. c) Deposition and patterning of a 480 nm thick polysilicon for heater. d) Deposition of 800 nm SiO_2 layer to insulate the heater

These steps are within the standard technology process employed to obtain the membranes of micromachined gas sensors at the Centre Nacional de Microelectrònica in Barcelona, Spain.

3.3.1 Combining the anodising with a lift-off process

In order to develop processes compatible with Miscrosystems technology, the most important is the delimitation of the areas on the wafer with porous alumina using compatible solutions and processes.

The first approach developed for this purpose, i.e. for removing the porous alumina from outside the active area, is a lift-off technique. This technique is well known and, generally, it consists of the following steps (the use of a positive photoresist is considered here). Deposition of a photoresist layer on a substrate by spin coating (Figure 3-16.b). By using a photomask (Figure 3-16.c), the

UNIVERSITAT ROVIRA I VIRGILI
GAS SENSOR MICROSYSTEMS BASED ON NANOSTRUCTURED LAYERS VIA ANODIC OXIDATION
Raúl Calavia Boldú
Dipòsit Legal: T. 1428-2012

photoresist is insolated by ultraviolet light (Figure 3-16.d) and is developed (Figure 3-16.e). Then it is necessary to make the deposition of the material to be patterned (Figure 3-16.f). Finally, the photoresist with the material deposited is removed in acetone (Figure 3-16.g). In the end, only the material deposited in the areas that had been insolated from the ultraviolet light (i.e., in which the photoresist had been removed during the development step), remain on the sample.

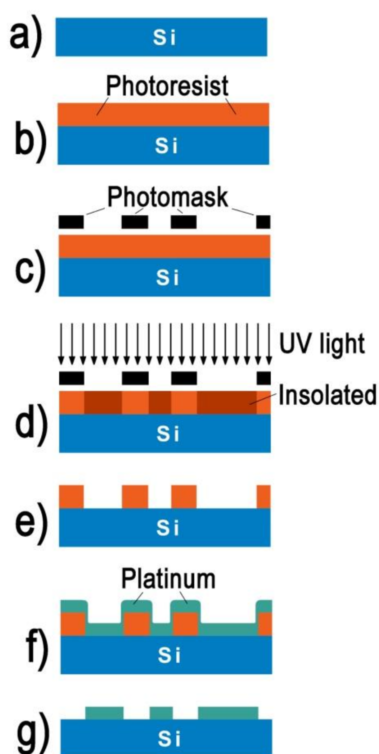

Figure 3-16 Steps for a lift-off process for patterning platinum (for patterning alumina the procedure would be equivalent). a) Silicon wafer. b) Spin-coated photoresist. c) Patterned photmask. d) Insolation of exposed photoresist areas. e) Developing the photoresist. f) Deposition of the material to be patterned (e.g. platinum). g) Material patterned on the silicon wafer after lift-off (e.g. platinum)

UNIVERSITAT ROVIRA I VIRGILI
GAS SENSOR MICROSYSTEMS BASED ON NANOSTRUCTURED LAYERS VIA ANODIC OXIDATION
Raúl Calavia Boldú
Dipòsit Legal: T. 1428-2012

The process for obtaining porous alumina on the micro-hotplate membranes using the lift-off approach (see Figure 3-17) starts with a pre-processed 4 inches silicon wafer having undergone the steps shown in Figure 3-15. Then a photoresist is coated and patterned following the steps described in Figure 3-16.a to Figure 3-16.e. In the third step, a 20 nm thick titanium and 500 nm thick aluminium layers are deposited by RF magnetron sputtering (Figure 3-17.b).

The aluminium layer is anodised in the 4 inch electrochemical cell (Figure 3-17.c) and the remaining photoresist is lifted off together with the alumina on it (Figure 3-17.d). The contact windows to the heater are opened in SiO_2 by reactive ion etching (RIE). Finally the WO_3 active layer (Figure 3-17.e) is formed over the porous alumina layer, and the platinum electrodes and contact pads for the heaters are deposited by sputtering and patterned by the lift-off technique (Figure 3-17.f).

This approach was implemented successfully and the resulting micromachined gas sensors were fabricated and characterised. The morphology, composition and gas sensing characteristics were studied.

UNIVERSITAT ROVIRA I VIRGILI
GAS SENSOR MICROSYSTEMS BASED ON NANOSTRUCTURED LAYERS VIA ANODIC OXIDATION
Raúl Calavia Boldú
Dipòsit Legal: T. 1428-2012

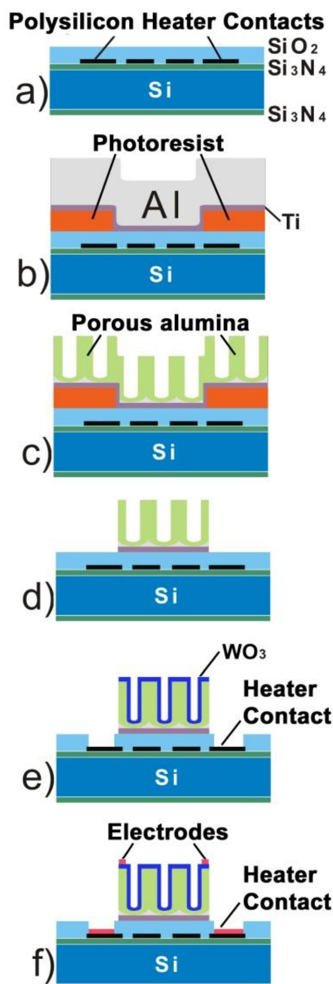

Figure 3-17 Steps to obtain porous alumina supported WO_3 sensing layer by the lift-off approach. a) Silicon wafer ready to be micromachined. b) Deposition of Al/Ti bilayer on patterned photoresist. c) Anodisation of Al/Ti bilayer. d) Lift-off to leave the porous alumina on the membrane area of the micro-hotplate only. e) Opening heater contacts and deposition of WO_3 by RF magnetron sputtering. f) Platinum electrodes and heater contacts made by sputter-deposition and lift-off technique.

3.3.2 The anodising combined with etch-back photolithography

Although the lift-off process has become a common technique in silicon microtechnology, there is an alternative based on chemical etching through a patterned photoresist (so called etch back), which is applied when the smaller sizes and improved quality of the elements must be provided.

This technique starts with a silicon wafer (Figure 3-18.a) and the material to be patterned is deposited on the front side of the wafer (an example with aluminium is illustrated in Figure 3-18.b). A (positive) photoresist is then spin-coated (Figure 3-18.c) and, using a reverse photomask (Figure 3-18.d), the photoresist is insolated (Figure 3-18.e) and developed (Figure 3-18.f). Once the photoresist is developed, the uncovered material is chemically etched away (e.g. by wet etching, RIE) (Figure 3-18.g). Finally, the remaining photoresist is removed in acetone (Figure 3-18.h).

UNIVERSITAT ROVIRA I VIRGILI
GAS SENSOR MICROSYSTEMS BASED ON NANOSTRUCTURED LAYERS VIA ANODIC OXIDATION
Raúl Calavia Boldú
Dipòsit Legal: T. 1428-2012

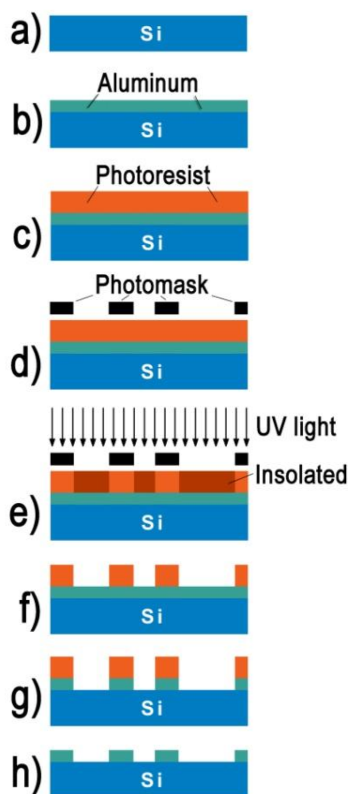

Figure 3-18 Steps to obtain patterned aluminium with help of etch-back photolithography. a) Silicon wafer. b) Deposited material (e.g. aluminium). c) Spin-coated photoresist. d) Use of a photomask. e) Insolation of exposed photoresist areas. f) Developing of the photoresist. g) Removing unprotected material areas by chemical etching. h) The material patterned on the silicon wafer (e.g. aluminium)

For anodising purpose, the etch-back approach seems more advantageous than one based on the lift-off process because in the former the aluminium layer is sputter-deposited directly on the wafer, not on the patterned photoresist, so that the film is smooth and the step-covering problems that are usual for the lift-off photolithography are avoided.

UNIVERSITAT ROVIRA I VIRGILI
GAS SENSOR MICROSYSTEMS BASED ON NANOSTRUCTURED LAYERS VIA ANODIC OXIDATION
Raúl Calavia Boldú
Dipòsit Legal: T. 1428-2012

The initial structure (semi-processed wafer) for the etch-back approach is identical to that employed in the lift-off approach (Figure 3-19.a). An Al (800 nm) / Ti (40 nm) bilayer is deposited by RF magnetron sputtering (Figure 3-19.b). The metals are anodised over the whole wafer surface using the electrochemical cell for 4-inch silicon wafers (Figure 3-19.c) and annealed at 500 ºC to thermally oxidise areas of titanium metal that may remain after the anodising. After the annealing, the windows openings in the SiO_2 layer to the heater contacts are made by etch-back photolithography and wet etching of the anodised metals and silicon dioxide (Figure 3-19.d).

The experience with this technology revealed that, with a standard 1.2-μm thick photoresist and 85 % H_3PO_4 water solution for etching the anodised metals, in order to keep the integrity of the photoresist during the etching step, it is necessary to bake the photoresist mask at 125 ºC and keep the etching time below 7 minutes. If the alumina is not removed completely, more cycles of hard baking and etching should be performed.

Once the contact windows to the heaters in the SiO_2 layer are opened by standard etching technique, the WO_3 sensing layer is formed over the designated areas of the anodised metals by RF magnetron sputtering and lift-off process (Figure 3-19.e). Finally, platinum electrodes and platinum heater contacts are deposited and patterned by lift-off technique in the usual way (Figure 3-19.f).

UNIVERSITAT ROVIRA I VIRGILI
GAS SENSOR MICROSYSTEMS BASED ON NANOSTRUCTURED LAYERS VIA ANODIC OXIDATION
Raúl Calavia Boldú
Dipòsit Legal: T. 1428-2012

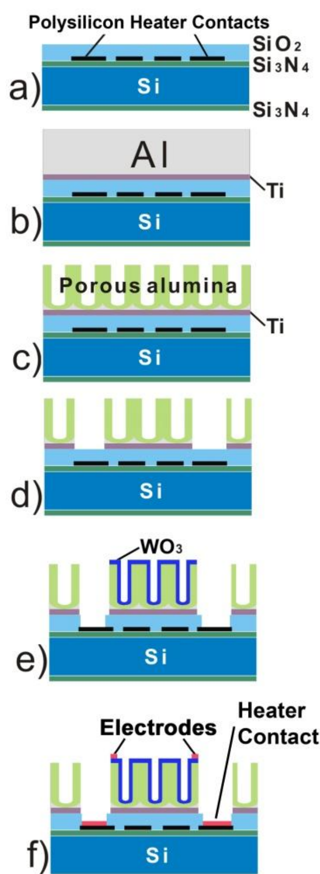

Figure 3-19 Steps to obtain porous alumina supported WO_3 sensing layers via the etch-back approach. a) Silicon wafer ready to be micromachined. b) Deposition of Al/Ti bilayer. c) Anodisation of the Al/Ti bilayer and annealing at 500°C. d) Chemical removing of the porous alumina and titanium layers over the heater contacts. e) Opening the heater contacts in the SiO_2 layer and deposition of WO_3 by reactive sputtering. f) Platinum deposition for electrodes and heater contacts and their patterning by lift-off

The etch-back approach was not fulfilled successfully because it was not possible to completely open the contacts to the polysilicon heater by a selective etching of the silicon dioxide after the removal of the anodised metals. Most likely, this happened because of the

UNIVERSITAT ROVIRA I VIRGILI
GAS SENSOR MICROSYSTEMS BASED ON NANOSTRUCTURED LAYERS VIA ANODIC OXIDATION
Raúl Calavia Boldú
Dipòsit Legal: T. 1428-2012

mixing of Ti with alumina and silicon oxide during the annealing performed before removing the porous alumina/TiO_2 onto the SiO_2 layer. The situation could be the subject for future study, because this approach seems to be clearly advantageous for the quality of the anodisation and the perfectness of the areas of porous alumina that should be formed on the wafer.

3.3.3 Opening the contact windows to micro-heaters before anodising

As it has been discussed above, the most promising approach to make compatible the anodising and silicon microtechnology is based on the process shown in Figure 3-19. However, to avoid the problems encountered during the opening of the heater contact contacts, the SiO_2 layer can be etched before anodising. This would involve the selective etching of aluminium and titanium, not their oxides and before annealing the samples, which is a well-known process in silicon technology and standard solutions are used.

Like in the previously described approaches, the initial structure is the one shown in Figure 3-20.a. A 40 nm thick titanium layer and a 400 nm thick aluminium layer are sputter-deposited on the wafer with preformed layers (Figure 3-20.b). Then the windows are opened in the Al/Ti bilayer on top of the polysilicon heater contact areas (Figure 3-20.c) using a photolithography and a wet selective etching process (Figure 3-18).

Once the windows in the initial metals are opened, the aluminium/titanium bilayer is anodised using the 4-inch cell

UNIVERSITAT ROVIRA I VIRGILI
GAS SENSOR MICROSYSTEMS BASED ON NANOSTRUCTURED LAYERS VIA ANODIC OXIDATION
Raúl Calavia Boldú
Dipòsit Legal: T. 1428-2012

(Figure 3-20.d). After the anodising, the silicon dioxide over the heater contact areas is removed by chemical etching (Figure 3-20.e). The main difference between this approach and the previously described is that here there is no need to remove the alumina from the heater contact areas because the initial Al/Ti metal stack had been selectively etched away from the contact window areas before performing the anodisation step. Also, the mixing of the metals and oxide in the contact windows during the annealing will be avoided.

UNIVERSITAT ROVIRA I VIRGILI
GAS SENSOR MICROSYSTEMS BASED ON NANOSTRUCTURED LAYERS VIA ANODIC OXIDATION
Raúl Calavia Boldú
Dipòsit Legal: T. 1428-2012

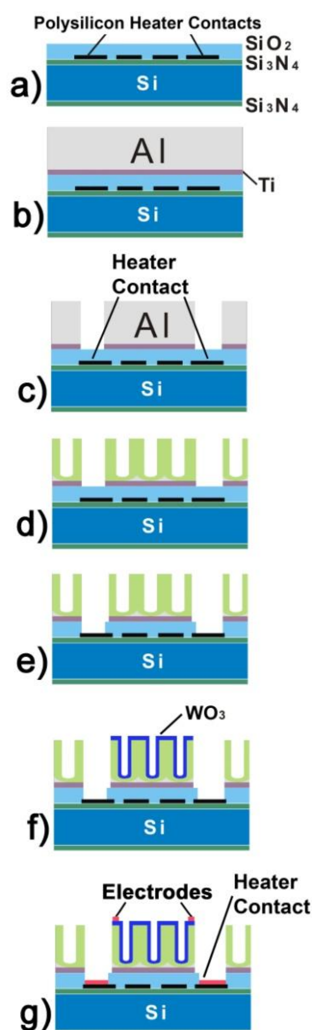

Figure 3-20 Steps to obtain porous alumina supported WO_3 sensing layer using the approach of removing the Al/Ti bilayer from the heater contact areas before anodising. a) Silicon wafer ready to be micromachined. b) Deposition of an Al/Ti bilayer. c) Chemical removing of the aluminium and titanium layers over the heater contact areas. d) Anodisation of the Al/Ti bilayer and annealing for reaching a complete oxidation of the titanium layer. e) Opening of the heater contacts by etching the SiO_2 layer). f) Deposition of WO_3 by reactive sputtering. g) Platinum deposition for electrodes and heater contacts and their pattering by lift-off technique.

UNIVERSITAT ROVIRA I VIRGILI
GAS SENSOR MICROSYSTEMS BASED ON NANOSTRUCTURED LAYERS VIA ANODIC OXIDATION
Raúl Calavia Boldú
Dipòsit Legal: T. 1428-2012

Finally the WO_3 active layer (Figure 3-20.f) and the platinum electrodes (Figure 3-20.g) are deposited over the porous alumina film by sputtering and patterned by lift-off.

This approach was not developed to the end because, in the standard process for obtaining these devices at the CNM-IMB, the etching of the silicon dioxide for opening the window contacts is performed simultaneously with the etching of chip separation lines (Figure 3-21). As this step is performed before the anodisation, the Al/Ti layers appeared to be completely electrically isolated from each other and from the place where the electric contact to the aluminium layer is done, and thus the anodisation was impossible. To solve this problem and correctly implement this approach, a new photomask is required, with help of which the contact windows in the Al/Ti bilayer would be opened only, but not the lines separating the chips. This could be considered in a future work.

UNIVERSITAT ROVIRA I VIRGILI
GAS SENSOR MICROSYSTEMS BASED ON NANOSTRUCTURED LAYERS VIA ANODIC OXIDATION
Raúl Calavia Boldú
Dipòsit Legal: T. 1428-2012

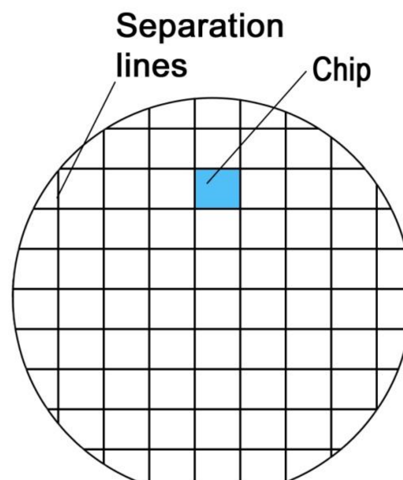

Figure 3-21 Separation lines of the chips in a silicon wafer

3.3.4 Bulk micromachining

All the approaches that have been developed and implemented in this work were expected to result in a semi-processed wafer, the structure of which is ready for the bulk micromachining step to create the membranes (Figure 3-22.a). This bulk micromachining starts with the etching, using RIE, of the silicon nitride deposited on the back side of the semi-processed wafer (Figure 3-22.b). This determines the areas in the silicon to be micromachined by an anisotropic etching using 40 wt % KOH. When the silicon is etched up to the silicon nitride layer that had been grown on the front side of the silicon wafer, the etching process is practically stopped because the etch rate for silicon nitride in this solution is very low (Figure 3-22.c), so that the membranes of the micro hotplates are done.

UNIVERSITAT ROVIRA I VIRGILI
GAS SENSOR MICROSYSTEMS BASED ON NANOSTRUCTURED LAYERS VIA ANODIC OXIDATION
Raúl Calavia Boldú
Dipòsit Legal: T. 1428-2012

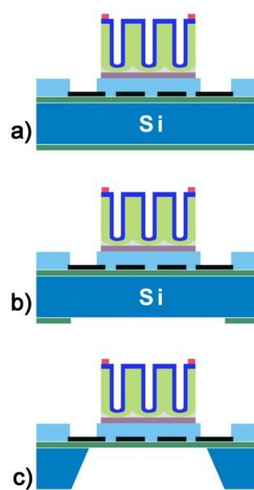

Figure 3-22 Bulk micromachining of a semi-processed silicon wafer. a) Sensor with the sensing material and electrodes ready to be micromachined. b) Si_3N_4 patterning by chemical etching. c) Bulk micromachining by KOH using the patterned Si_3N_4 as etching mask

After the bulk micromachining process, the devices are ready to be diced, mounted and wire-bonded to standard TO8 packages. Ultrasonic wire bonding and Au wires are employed.

3.3.5 The outcomes of the different approaches

As already mentioned, from the different approaches developed, only one was successfully implemented with the end devices fabricated. This was the one based on the lift-off process to pattern the porous alumina areas to create the alumina-supported WO_3 sensing layers, although it was not the ideal option from the anodising point of view.

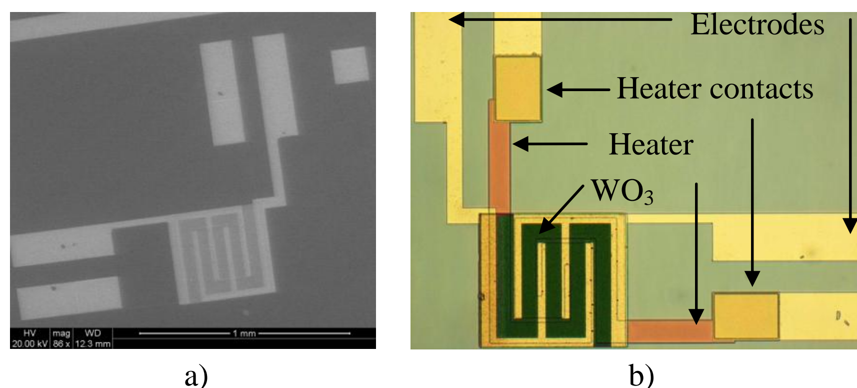

Figure 3-23 Images of the gas sensor obtained. a) SEM image. b) 5x optical image

Figure 3-23.a shows an SEM image of the sensor ready to be packaged and Figure 3-23.b shows a 5-times magnification optical image of the sensor, where it is possible to see the embedded heater with the contact pads, the patterned sensing layer and the platinum electrodes.

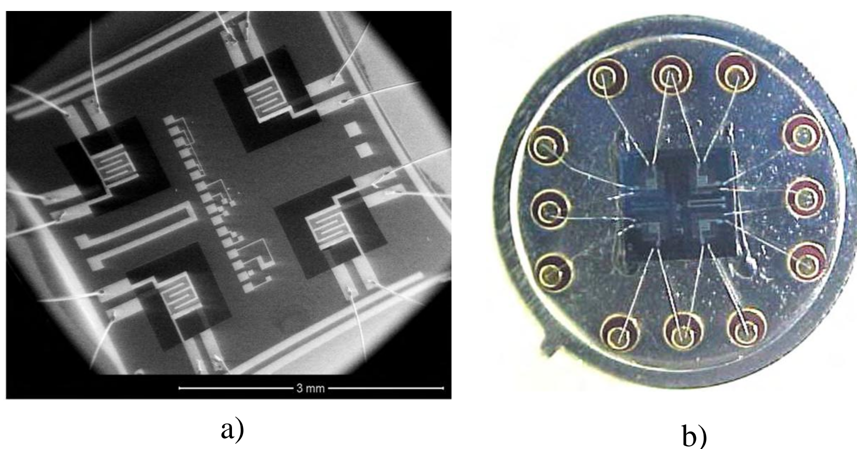

Figure 3-24 Image of a packaged chip. a) SEM view. b) optical view

UNIVERSITAT ROVIRA I VIRGILI
GAS SENSOR MICROSYSTEMS BASED ON NANOSTRUCTURED LAYERS VIA ANODIC OXIDATION
Raúl Calavia Boldú
Dipòsit Legal: T. 1428-2012

Figure 3-24 shows the final TO-8 packaged chip, which contains 4 individual sensors.

3.3.6 WO_3 nanodot film as active layer for the micro-machined gas sensors

As shown before, tungsten is a valve metal and it can be oxidised using anodisation techniques. Additionally, using a porous alumina layer superimposed on the tungsten layer, it is possible to obtain self-organised nanostructured WO_3 that can be used as gas sensing layer.

The process developed in order to obtain a micromachined gas sensor having WO_3 nanodot active layer is based on the anodising of metal layers deposited on a patterned photoresist (Figure 3-17) because this is a technique fully compatible with the standard silicon technology that we have successfully developed and implemented in this work.

The initial structure was the semi-processed silicon wafer (Figure 3-25.a) obtained as described in Figure 3-15. On top of this semi-processed wafer, three metal layers were sputter-deposited (Figure 3-25.b): a 20 nm thick titanium adhesion layer, a 50 nm thick tungsten layer, which will be used for electrochemically growing WO_3 nanodots, and a 500 nm thick aluminium to be converted into porous alumina via anodisation. An aqueous solution of 0.4 mol dm^{-3} $H_2C_2O_4$ modified by the addition of 2.4 m mol^{-3} NH_4F was employed for the anodisation (Figure 3-25.c).

UNIVERSITAT ROVIRA I VIRGILI
GAS SENSOR MICROSYSTEMS BASED ON NANOSTRUCTURED LAYERS VIA ANODIC OXIDATION
Raúl Calavia Boldú
Dipòsit Legal: T. 1428-2012

When the aluminium metal was fully consumed and the alumina barrier layer reached the tungsten film, discrete regions of anodic tungsten oxide, of nanometer sizes, began to form at the Al_2O_3/W interface (Figure 3-25.d) by self-organisation beneath the alumina pores. This was reflected through the voltage increasing in relation with the increment in the thickness of WO_3, which penetrated the inner part of the pores (Figure 3-25.e).

After completing the reanodisation process, the photoresist clad with the anodised Al/W/Ti trilayer was removed by a lift-off process, so that the square areas of the anodised metal stacks remained on the wafer in the centre of each microsensor. Then the nanoporous alumina layer, which cover the tungsten oxide nanodots, was selectively etched away by dipping the wafers in 20 g l^{-1} CrO_3 and 35 ml l^{-1} H_3PO_4 solution kept at 60 ºC for 15 min (Figure 3-25.f). Following etching, the wafers were thoroughly washed in running distilled water and dried in a hot air stream. Then the wafers were subjected to heating in air at 500 ºC during 2 hours in order to crystallize the tungsten oxide nanodots.

After opening contact windows in the SiO_2 layer at the heater ends, pairs of platinum interdigitated electrodes (with 50 µm interline gap), placed over the sensing film (Figure 3-25.g), and pairs of platinum micropads for electrically contacting the heaters, placed beside the sensing film, were prepared by photolithography, sputtering-deposition and a lift-off process. In order to complete the formation of the supporting membranes, micromachining of the back silicon up to the face Si_3N_4 layer was done.

UNIVERSITAT ROVIRA I VIRGILI
GAS SENSOR MICROSYSTEMS BASED ON NANOSTRUCTURED LAYERS VIA ANODIC OXIDATION
Raúl Calavia Boldú
Dipòsit Legal: T. 1428-2012

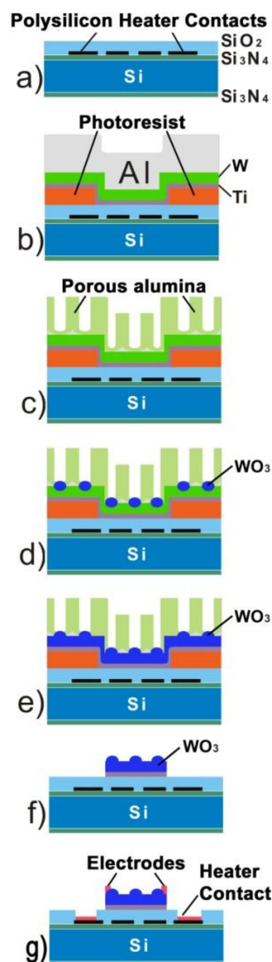

Figure 3-25 Steps to obtain micromachined gas sensors with WO_3 nanodot film as sensing layer. a) Silicon wafer ready to be micromachined. b) Al/W/Ti layers deposited onto patterned photoresist. c) Aluminium anodisation. d) WO_3 nanodots nucleation. e) WO_3 nanodots grown and tungsten layer consumed. f) Nanodot WO_3 film after photoresist and porous alumina removing. g) Opening heater contacts windows and platinum electrodes deposition

Figure 3-26 shows an AFM image of the WO_3 nanodot film prepared as described above on the micromachined hotplate transducer. The closely packed array of the tungsten oxide

UNIVERSITAT ROVIRA I VIRGILI
GAS SENSOR MICROSYSTEMS BASED ON NANOSTRUCTURED LAYERS VIA ANODIC OXIDATION
Raúl Calavia Boldú
Dipòsit Legal: T. 1428-2012

nanodots is clearly seen over a bigger grain morphology, which is due to the polysilicon and silicon dioxide formed under the nanodot film.

The fabrication process ended with wafer dicing and packaging of microchips, each comprising four sensors, assembled on a standard TO-8 (Figure 3-24).

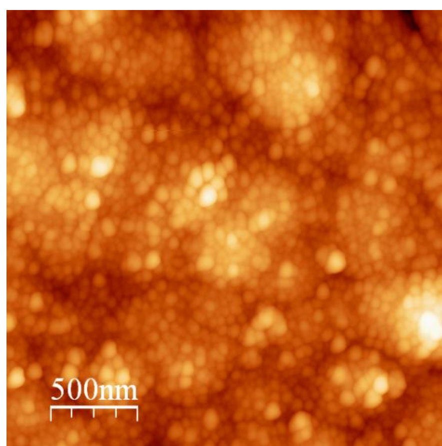

Figure 3-26 AFM image of the WO_3 nanodot film prepared on the micromachined hotplate as sketched in Figure 3-24.

3.4 Summary

In the work described in Chapter 3, experimental setup has been developed and integrated with relevant instrumentation and controlling software for anodising metal layers sputter-deposited onto silicon wafers of various sizes, up to 100 mm in diameter. With the setup developed, experiments on anodising thin layers of aluminium and aluminium superimposed on titanium layer have been performed in order to optimise the formation conditions for

UNIVERSITAT ROVIRA I VIRGILI
GAS SENSOR MICROSYSTEMS BASED ON NANOSTRUCTURED LAYERS VIA ANODIC OXIDATION
Raúl Calavia Boldú
Dipòsit Legal: T. 1428-2012

growing the porous alumina templates and for performing porous-alumina-assisted anodising of the underlying tungsten metal.

The facile, one-step method has been developed and experimentally justified for preparing nanoporous alumina templates suitable for being used as supporting layers for tungsten oxide sputter-deposition. Alternatively, a modified version of anodising the Al/W metal bilayer has been developed to grow an array of tungsten oxide nanodots for being used as gas sensing film having significantly enlarged surface to volume ratio.

Further, the steps have been developed to make compatible the anodising technologies for forming the nanostructured tungsten oxide sensing layers with the standard silicon-based technology for fabricating micro-hotplate transducers as platforms for gas microsensors.

We have been successful in implementing the two original approaches based on a lift-off patterning process, and synthesised two different types of nanostructured tungsten oxide layers using porous alumina as (1) supporting template for magnetron sputter-deposition of WO_3 layers and (2) as part of the electrochemical system that provided the growth of self-organised WO_3 nanodots. Gas sensor chips have been fabricated on 100-mm silicon wafers in accordance with the technologies developed and packaged for being used in gas sensing tests.

3.5 Bibliography

[1] Khatko, V.; Gorokh, G.; Mozalev, A.; Solovei, D.; Llobet, E.; Vilanova, X.; Correig, X., Tungsten trioxide sensing layers on

UNIVERSITAT ROVIRA I VIRGILI
GAS SENSOR MICROSYSTEMS BASED ON NANOSTRUCTURED LAYERS VIA ANODIC OXIDATION
Raúl Calavia Boldú
Dipòsit Legal: T. 1428-2012

highly ordered nanoporous alumina template, *Sens. Actuator B-Chem.*, (2006) **118**, 255.

[2] Kadlec, S.; Musil, J.; Vyskocil, J., Growth and Properties of Hard Coatings Prepared by Physical Vapor-Deposition Methods, *Surf. Coat. Technol.*, (1992) **54**, 287.

[3] Choi, J., Fabrication of monodomain porous alumina using nanoimprint lithography and its applications, Martin-Luther University Wittenberg, (2004).

[4] Gorokh, G.; Mozalev, A.; Solovei, D.; Khatko, V.; Llobet, E.; Correig, X., Anodic formation of low-aspect-ratio porous alumina films for metal-oxide sensor application, *Electrochim. Acta*, (2006) **52**, 1771.

[5] Mozalev, A.; Poznyak, A.; Mozaleva, I.; Hassel, A. W., The voltage-time behaviour for porous anodizing of aluminium in a fluoride-containing oxalic acid electrolyte, *Electrochem. Commun.*, (2001) **3**, 299.

[6] Mozalev, A.; Khatko, V.; Bittencourt, C.; Hassel, A. W.; Gorokh, G.; Llobet, E.; Correig, X., Nanostructured Columnlike Tungsten Oxide Film by Anodizing Al/W/Ti Layers on Si, *Chemistry of materials*, (2008) **20**, 6482.

[7] Puigcorbe, J.; Vogel, D.; Michel, B.; Vila, A.; Gracia, I.; Cane, C.; Morante, J. R., Thermal and mechanical analysis of micromachined gas sensors, *J. Micromech. Microeng.*, (2003) **13**, 548.

Chapter 4

Morphological, compositional and crystallographic analysis

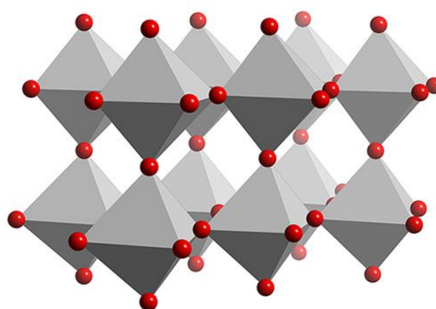

UNIVERSITAT ROVIRA I VIRGILI
GAS SENSOR MICROSYSTEMS BASED ON NANOSTRUCTURED LAYERS VIA ANODIC OXIDATION
Raúl Calavia Boldú
Dipòsit Legal: T. 1428-2012

UNIVERSITAT ROVIRA I VIRGILI
GAS SENSOR MICROSYSTEMS BASED ON NANOSTRUCTURED LAYERS VIA ANODIC OXIDATION
Raúl Calavia Boldú
Dipòsit Legal: T. 1428-2012

4. Morphological, compositional and crystallographic analysis

In the previous chapter, various options to obtain micromachined gas sensors with the nanostructured WO_3 active layers were described. In this chapter we are going to show and discuss in details the morphology, elemental composition and crystalline structure of the sensing layers.

The morphological characterisation of the nanostructured tungsten oxide films was carried out using field-emission scanning electron microscopy (FE-SEM) where the equipment used was a Hitachi S-4800, environmental scanning electron microscopy (ESEM) employing a Quanta 600 microscope from FEI company, focused ion beam (FIB) combined with high resolution scanning electron microscopy (HR-SEM) for sectioning the samples and observing the sections (using a Strata DB235 from FEI Company) and atomic force microscopy (AFM) where the equipment used was an Agilent 5500.

A compositional study was carried out by Energy Dispersive X-ray Spectrometry (EDS) using an X-Ray detector from Oxford instruments installed in the ESEM. The crystalline structure of samples was determined by X-ray diffraction (XRD) using a Bruker D8 Discover equipment.

Using these analysis techniques we will determine if the final devices obtained are ready to work as gas sensors, and if the main

UNIVERSITAT ROVIRA I VIRGILI
GAS SENSOR MICROSYSTEMS BASED ON NANOSTRUCTURED LAYERS VIA ANODIC OXIDATION
Raúl Calavia Boldú
Dipòsit Legal: T. 1428-2012

objectives of this work (namely to increase the sensing surface area without increasing the area to be heated and to make the anodising technique compatible with silicon micromachining) are accomplished.

The devices obtained in this work are gas sensors and the results of as sensing characterisation will be reported and discussed in the next chapter.

4.1 Morphological analysis

The morphological characterisation includes the surface and the inner layers of the samples obtained. This characterisation of the samples is very important for the development of quality gas sensors because, as it was explained in the state of the art section, sensitivity heavily depends on the surface area that is in contact with the gases to be detected and the thickness of the sensing material. All these parameters are analysed and studied in the morphological characterisation section.

4.1.1 SEM observation.

The surface characterisation is the study employing electron microscopy (FIB, ESEM and AFM) of the morphology of the different gas sensitive layers developed. Namely, active layers based either on porous alumina supported RF sputtered WO_3 layers or anodically grown WO_3 nanodots.

UNIVERSITAT ROVIRA I VIRGILI
GAS SENSOR MICROSYSTEMS BASED ON NANOSTRUCTURED LAYERS VIA ANODIC OXIDATION
Raúl Calavia Boldú
Dipòsit Legal: T. 1428-2012

4.1.1.1 Porous alumina supported WO_3 layers

As explained in chapter 3, the sputtering technique is not an optimal technique for covering vertical walls and long deposition times are necessary in order to obtain a continuous layer onto a texturised substrate. In the case of porous alumina it was necessary to obtain wide pores with low aspect ratios and, therefore, a pore widening step was performed after the anodising process. This pore widening was made by immersing the silicon wafers with porous alumina on top in an aqueous solution of 20 g/l CrO_3 and 35 ml/l H_3PO_4 at 60 ºC during the optimal time of 10 minutes for the film grown in 0.4 M tartaric acid at 200 V, as determined in Chapter 3. Figure 4-1 shows an FE-SEM image of a porous film prepared by the one-step anodising of the Al/Ti bilayer on a silicon wafer in the tartaric-acid, this followed by 10-min pore-widening in the chromium-containing solution, where it is possible to see the wide pores obtained after the anodising and pore widening step.

It should be noted that, under the conditions developed (see chapter 3), the titanium underlayer does not yet penetrate in the pores but is incorporated in the alumina barrier layer, so that the results of this work are not affected by the changes at the alumina/titania interface.

The porous alumina obtained on the silicon substrate was then covered by an RF sputtered, 250 nm thick, tungsten oxide film. The experimental conditions have been reported in Chapter 3.

UNIVERSITAT ROVIRA I VIRGILI
GAS SENSOR MICROSYSTEMS BASED ON NANOSTRUCTURED LAYERS VIA ANODIC OXIDATION
Raúl Calavia Boldú
Dipòsit Legal: T. 1428-2012

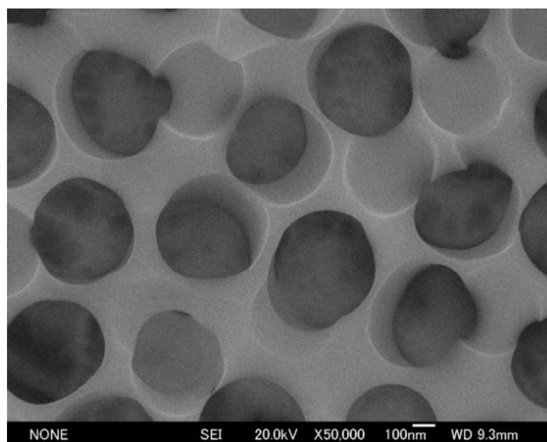

Figure 4-1 Porous alumina sample after a 10-min pore widening in 20 g/l CrO_3 and 35 ml/l H_3PO_4 at 60 ºC.

Figure 4-2 shows a SEM image of the surface of the porous alumina covered by WO_3 where it is possible to see that the sputtered sensing layer does not block the pores of the porous alumina template.

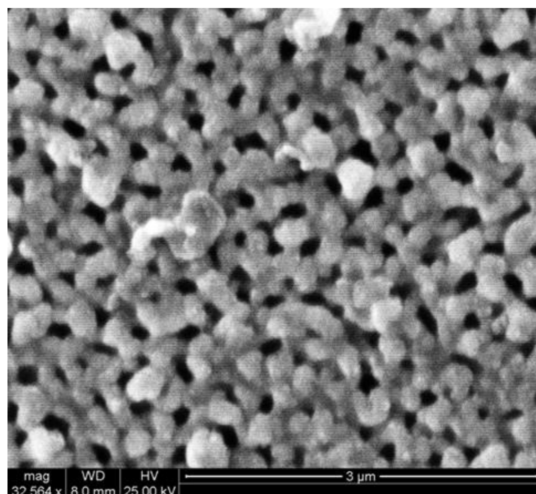

Figure 4-2 SEM surface image of the WO_3 layer sputter-deposited on the pore-widened porous alumina prepared on the micro-hotplate.

UNIVERSITAT ROVIRA I VIRGILI
GAS SENSOR MICROSYSTEMS BASED ON NANOSTRUCTURED LAYERS VIA ANODIC OXIDATION
Raúl Calavia Boldú
Dipòsit Legal: T. 1428-2012

The surface imaging demonstrates that, although the sputtered WO_3 layer does not block the pores on the surface, it does not give information about the continuity of this layer coating the pore walls. In order to further study pore coating an FIB-SEM analysis was performed in which FIB is used to perform a cross-sectional cut of the sample and SEM is then used to image the cut.

Due to the working configuration of FIB-SEM systems, SEM images must be corrected manually if the autocorrection is not enabled (which was the case of our images). The equation to correct them is the following (further explanations can be found in the appendix).

$$Real\ vertical\ size = \frac{Vertical\ size\ measured}{\cos(90º - 52º)} \quad (4\text{-}1)$$

Before starting the cutting process using an FIB it is necessary to deposit a thin layer of gold in all the surface of samples in order to avoid charging effects that would decrease the resolution of SEM analysis (due to the low conductivity of tungsten oxide thin layers). Additionally, in the area to be cut it is necessary to deposit a platinum stub in order to avoid the surface etching of the sample in the area to be cut.

Figure 4-3.b and Figure 4-3.c show SEM images of fragments of the handmade cross fracture and FIB-made cross section of the sensor chip employing the porous-alumina-supported WO_3 layer prepared onto the membrane of the micro-hotplate transducer with the platinum top electrodes. The schematic of Figure 4-3.a points

UNIVERSITAT ROVIRA I VIRGILI
GAS SENSOR MICROSYSTEMS BASED ON NANOSTRUCTURED LAYERS VIA ANODIC OXIDATION
Raúl Calavia Boldú
Dipòsit Legal: T. 1428-2012

out the location of sensor fragment imaged by SEM. On both SEM images, the following sensor elements are identified from the bottom to top: Si_3N_4 membrane, polysilicon heater, SiO_2 isolating layer, titanium layer, porous-alumina-supported WO_3 layer and platinum electrode (Pt stab in the FIB-made section). The fact that, in the SEM images of the FIB-made section, the pores of the PAA-supported WO_3 layer are not seen may result from flattening the morphology of the WO_3-filled alumina layer, partial mixing of Al_2O_3 with WO_3 and the formation of a featureless mixed layer owing to interaction of the gallium ion beam with the nanostructured metal-oxide film. Similarly, under the Ga^+ beam, the SiO_2 mixed with the poly-Si in the vicinity of the SiO_2/poly-Si interface, after which the correct thickness identification for the SiO_2 and poly-Si layers became impossible with the SEM of the FIB-made section. Nevertheless, from the images of Figure 4-3, it is obvious that the porous-alumina-supported WO_3 layer makes a conformal coverage over the surface of the micro-hotplate transducer, without visible discontinuities even on the steps due to the poly-Si micro-heaters.

Using the Image J software, the thickness of the different layers was estimated. Since the automatic compensation was not activated in the image saving process, it was necessary to manually compensate (see Annex) using the equation shown before.

UNIVERSITAT ROVIRA I VIRGILI
GAS SENSOR MICROSYSTEMS BASED ON NANOSTRUCTURED LAYERS VIA ANODIC OXIDATION
Raúl Calavia Boldú
Dipòsit Legal: T. 1428-2012

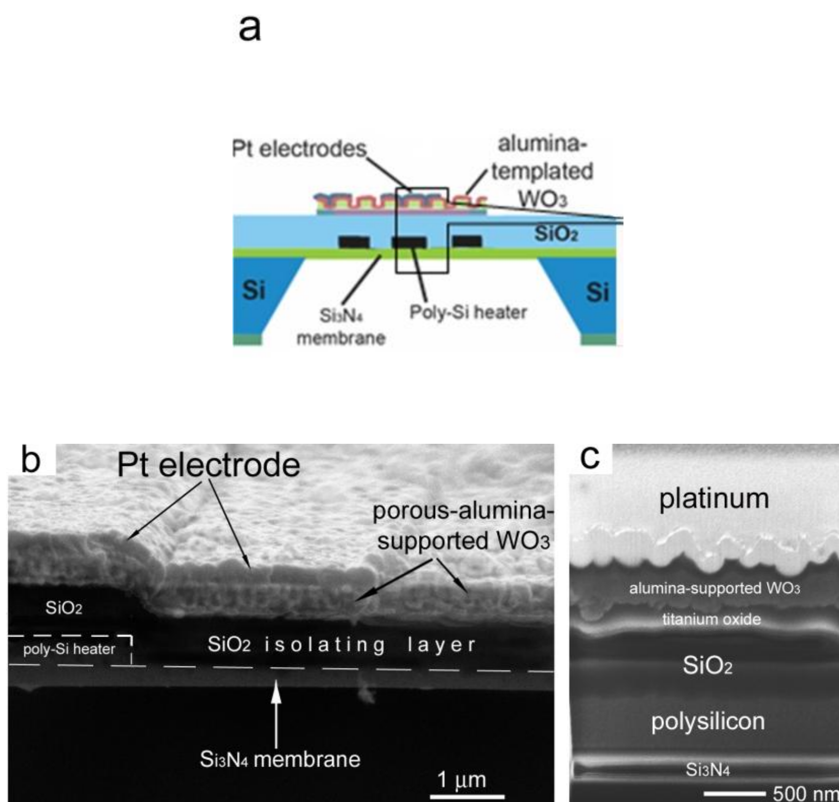

Figure 4-3 Cross section images of the porous-alumina-supported WO_3 layer prepared on the micro-hotplate with the various layers indentified. a) Schematic of points of cutting. b) Handmade fracture. c) FIB-made cut

	Estimated	Theoretical
Alumina-supported WO_3	672 nm	≈600 nm
SiO_2 (isolation)	876 nm	800 nm
Polysilicon (Heater)	487 nm	480 nm
Si3N4 (membrane)	220 nm	300 nm

Table 4-1 Thickness of the layers under the sensing material on the micro-hotplate

UNIVERSITAT ROVIRA I VIRGILI
GAS SENSOR MICROSYSTEMS BASED ON NANOSTRUCTURED LAYERS VIA ANODIC OXIDATION
Raúl Calavia Boldú
Dipòsit Legal: T. 1428-2012

Using the HR-SEM images and the Image J software a study of the dimensions of the pores in the sensing layer was made. The pores were near 140 nm in depth, 262 nm (± 17 nm) in diameter and interpore distance was 417 nm (± 34 nm).

4.1.1.2 WO_3 nanodots derived from the anodised Al/Ti layers

As was reported in Chapter 3, an Al/valve-metal bilayer can be used for nanostructuring the inner valve metal film due to so called porous-alumina-assisted anodising of the underlying metal. In the case of the Al/W bilayer, WO_3 nanodots were successfully synthesised on both a flat dielectric substrate and the micromachined Si_3N_4 membrane (see Figure 4-4), which resulted in the substantially increased surface-to-volume ratio relative to the flat WO_3 layers.

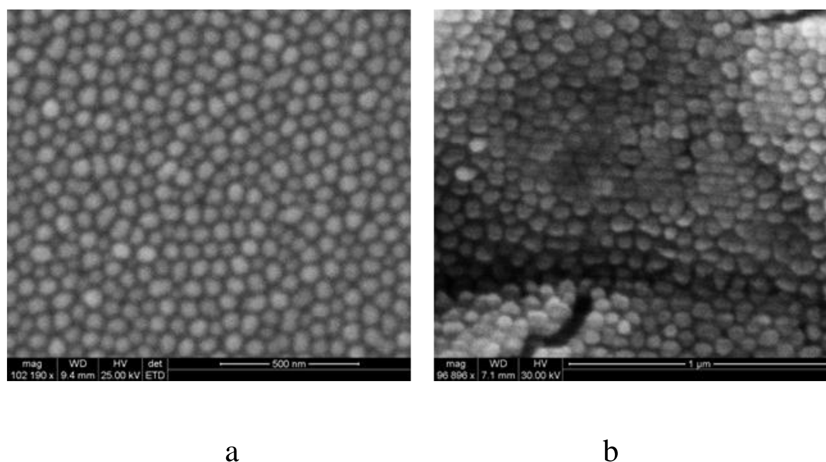

a b

Figure 4-4 ESEM images of the surface of the nanostructured WO_3 layer prepared on different substrates. a) A flat dielectric substrate. b) A micromachined Si_3N_4 membrane

UNIVERSITAT ROVIRA I VIRGILI
GAS SENSOR MICROSYSTEMS BASED ON NANOSTRUCTURED LAYERS VIA ANODIC OXIDATION
Raúl Calavia Boldú
Dipòsit Legal: T. 1428-2012

The big grains, observed in Figure 4-4.b, arise from the developed morphology of the elements (poly-Si heater and SiO_2 isolation layer) formed under the sensing layer. The nanostructured dots of WO_3 themselves looked uniformly distributed and rather closely packed, which is quite a result considering the annealing of the film at 500 ºC. The big grains under the dot-like film are advantageous in that they help to additionally increase the surface of the sensing layer available for interacting with the gas.

With the technology developed, not only the surface of the layers preformed under the titanium film exhibit developed morphology but also the surface of the sputter-deposited aluminium. Figure 4-5.a shows an SEM image of a polycrystalline aluminium layer sputter-deposited to a thickness of 500 nm by RF magnetron method on a flat silicon substrate. Aluminium grains, of submicron sizes, are clearly seen in the image. The morphology of aluminium layer may influence the formation of surface pores, and may affect pore arrangement process at early stages of pore growth, as seen in the image of Figure 4-5.b. If the aluminium film is thin, the pores may reach the buried metal being still disorganized, which may worsen the quality of metal oxide nanodots generated under the pores orientated in different directions. This implies that the quality of surface layer of a sputter-deposited aluminium should receive special attention when it is coupled with another valve metal with the purpose of metal oxide nanodot formation.

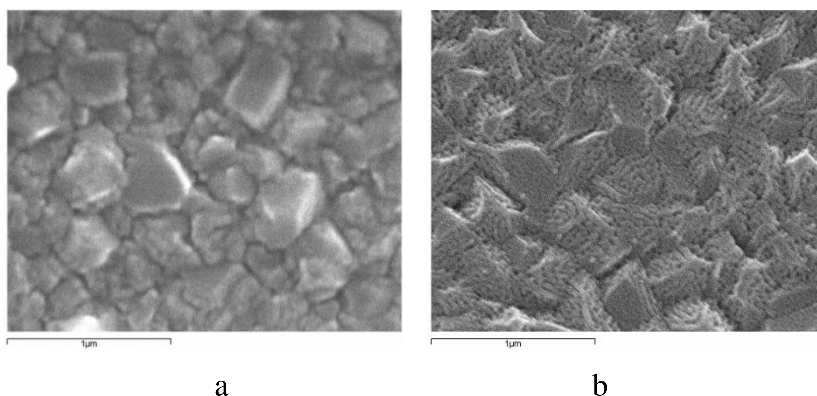

Figure 4-5 SEM images of a 500-nm Al film. a) As sputter-deposited by RF magnetron method. b) After anodising at 27 V in a sulphuric acid solution

Additionally to the SEM imaging of the nanodot film, an AFM analysis was made, using a silicon tip from Budget Sensors Company. The AFM tip used had a resonant frequency at 57 kHz and the scanning type employed was tapping mode. This helped avoiding the damage of the surface because this is a non contact technique. Due to the small size of the nanodots, an open loop tip position control was used. Figure 4-6.a shows a 2D AFM image of the WO_3 nanodot surface where it is possible to see the nanodots and the big grains due to the underlying morphology. A 3D AFM image (Figure 4-6.b) helps identifying the roughness of the layer obtained, which additionally increases the surface-to-volume ratio.

In order to calculate the nanodot height, profiles from different 3D AFM images were analysed. Figure 4-6 c shows the profile of the line shown in Figure 4-6.b. From this profile it is possible to see that the nanodots are very similar in diameter and that the small

UNIVERSITAT ROVIRA I VIRGILI
GAS SENSOR MICROSYSTEMS BASED ON NANOSTRUCTURED LAYERS VIA ANODIC OXIDATION
Raúl Calavia Boldú
Dipòsit Legal: T. 1428-2012

nanodots are growth on an irregular baseline due to the presence of the bigger grains.

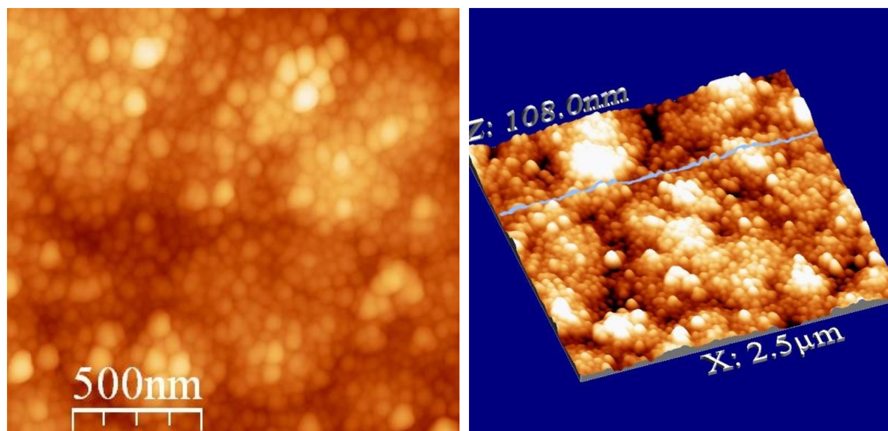

a) b)

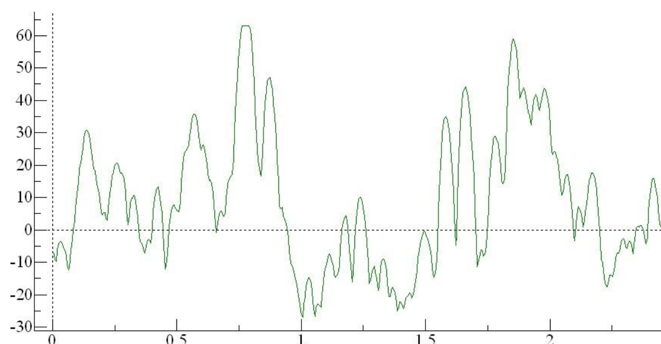

c)

Figure 4-6 AFM Image of a WO_3 nanodot layer prepared on a micromachined hotplate as described in Chapter 3. a) 2D image. b) 3D image. c) Profile of the line marked in the 3D image

UNIVERSITAT ROVIRA I VIRGILI
GAS SENSOR MICROSYSTEMS BASED ON NANOSTRUCTURED LAYERS VIA ANODIC OXIDATION
Raúl Calavia Boldú
Dipòsit Legal: T. 1428-2012

Using the AFM images obtained, the Image J software was used to analyse these images and the Originpro 8 software was employed in the mathematical processing. A statistical diameter study of the WO_3 nanodots was made, employing a population of 150 nanodots for this study.

Figure 4-7 shows the diameter distribution of the nanodots obtained. Maximum frequency is obtained at 55 nm diameter (30 % population), but if we consider the 50 to 60 nm range, then 68 % of population analysed lies in that range. The mean diameter (59.1 nm) and the standard deviation (12.2 nm) of the WO_3 nanodot layer was calculated. The mean distance between nanodots was 9.2 nm, so the nanodot layer density obtained is high and the surface-to-volume ratio is high as well.

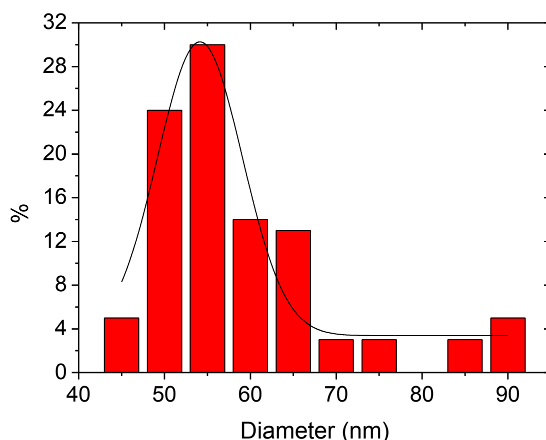

Figure 4-7 Distribution of the diameter of the pores using a population of 150 nanodots. The nanodot film was prepared via anodising an Al/W bilayer on the micro-hotplate at 27 V followed reanodizing to 100 V.

UNIVERSITAT ROVIRA I VIRGILI
GAS SENSOR MICROSYSTEMS BASED ON NANOSTRUCTURED LAYERS VIA ANODIC OXIDATION
Raúl Calavia Boldú
Dipòsit Legal: T. 1428-2012

Since the diameter distribution shown in the bar graph is similar to a Gauss distribution, Origin software was used to make a Gauss fitting for the nanodot diameter frequency. This result was added on the bar graph shown in Figure 4-7.

The mathematical Gauss model employed for this distribution is the following:

$$y = y_0 + \frac{A}{w \cdot \sqrt{\pi/2}} \cdot e^{-2 \cdot \frac{(x-x_C)^2}{w^2}} \quad (4\text{-}2)$$

Where the values obtained after fitting are as follows:

$$y = 3.377 + \frac{333.488}{9.885 \cdot \sqrt{\pi/2}} \cdot e^{-2 \cdot \frac{(x-54.127)^2}{9.885^2}} \quad (4\text{-}3)$$

The correlation obtained using this model is R^2=0.904.

4.2 Elemental and crystallographic analysis

A crystallographic study is very important for any metal oxide material developed for gas sensing applications because the crystalline phases affect sensor reactivity. Therefore, chemical composition and crystallographic analysis were made for films prepared via both approaches, i.e. the porous alumina supported WO_3 layer and the self-organised WO_3 nanodot layer.

4.2.1 Porous alumina supported WO_3 layers

In order to ensure that the layer deposited was tungsten oxide an EDS analysis was made. Figure 4-8 shows an EDS analysis

obtained for a porous alumina supported WO_3 layer prepared by anodising an Al/Ti bilayer on a SiO_2/Si substrate in 0.4 M tartaric acid at 200 V this followed by annealing at 500°C, where INCA software shows the materials detected for every significant pick.

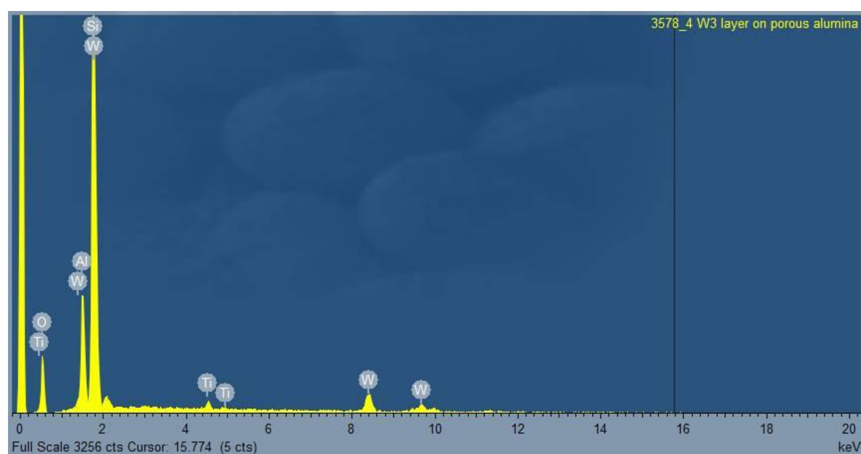

Figure 4-8 EDS microanalysis of a porous alumina supported WO_3 layer prepared on SiO_2/Si substrate. The porous alumina was grown by anodising an Al/Ti bilayer in 0.4 M tartaric acid at 200 V this followed by annealing at 500°C.

Table 4-2 shows the elements and their % weight detected in the EDS analysis. The most concentrated element is tungsten followed by silicon, oxygen and aluminium. This result could be foreseen because the surface should be tungsten oxide and aluminium oxide onto a silicon oxide layer. Titanium weight is very low because we deposited a very thin layer (20 nm) between the alumina and silicon dioxide layer.

Element	Weight %
W	33.95
Si	29.78
O	25.69
Al	9.00
Ti	1.58
Total	*100.00*

Table 4-2 Elements detected by EDS analysis for a porous alumina supported WO_3 layer prepared on SiO_2/Si substrate. The porous alumina was grown by anodising an Al/Ti bilayer in 0.4 M tartaric acid at 200 V this followed by annealing at 500°C.

Once the presence of the expected elements was verified, an XRD analysis was carried out in order to know the crystalline phases in the sensing layer material. Figure 4-9 shows the diffraction pattern recorded in transmission mode on the active area of this sample. It first should be noted that, in the range of 3-50° 2θ, there are no peaks associated with any crystalline phases of Al_2O_3. This confirms that the PAA film supporting the WO_3 layer retains its amorphous structure after being heated to 500ºC. In the range of 20-37° 2θ angles, the marked diffraction peaks are from lattice planes in monoclinic nano-crystalline phase of WO_3 with a P21/n (14) space group defined in the ICDD card number 43-1035. This phase is typically present in a thin tungsten oxide layer deposited by reactive RF sputtering on a smooth substrate [1].

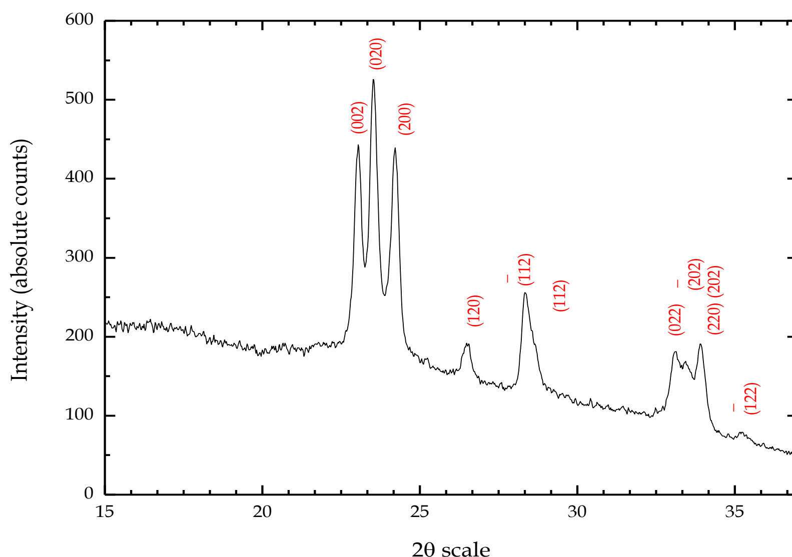

Figure 4-9 XRD pattern recorded for the porous alumina supported WO_3 layer prepared as indicated in Figure 4-8.

The absence of peaks from metallic aluminium in the anodised/annealed Al/Ti bilayer indicates that the aluminium was fully converted into alumina during the anodising and annealing treatments. The absence in the diffraction patterns any peaks associated with crystalline phases of titanium dioxide may be explained either by low content of crystalline phases of titanium in the film composition or by shifting the starting point of titanium crystallisation to a higher temperature range due to the nanostructured morphology of the anodic titanium. The Si_3N_4 is not detected by XRD because CVD silicon nitride is generally amorphous.

Figure 4-10.a and Figure 4-10.b shows the crystal cell (pink colour) image of the crystalline grains, the 001 and 010 orientations are

shown, respectively. The vertexes of the cells are the positions of the oxygen atoms and the tungsten is in the centre of these cells.

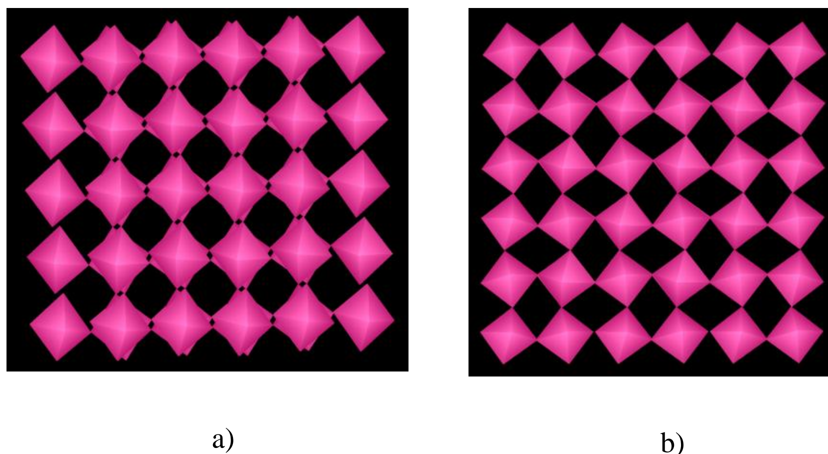

a) b)

Figure 4-10 WO_3 monoclinic crystalline phase obtained for the porous alumina supported tungsten oxide layer prepared as in Figure 4-8. a) 001 orientation image. b) 010 orientation image

4.2.2 WO_3 nanodot film derived from anodised Al/W bilayer

For this trial, the experimental sample was prepared by anodising an Al/W/Ti trilayer formed on the micro-hotplate at 27 V followed by reanodizing to 100 V and annealing at 500°C, as described in detail in Chapter 3. Like in the previous case, the WO_3 nanodot layer was analysed by EDS microanalysis (see Table 4-3), but unlike the previous case, in the nanodot samples the most concentrated element detected was silicon, followed by oxygen and tungsten. The presence of tungsten in the nanodot sample was at lower concentrations than in the previous case. This is because the thickness of the sputter-deposited tungsten film in the initial

UNIVERSITAT ROVIRA I VIRGILI
GAS SENSOR MICROSYSTEMS BASED ON NANOSTRUCTURED LAYERS VIA ANODIC OXIDATION
Raúl Calavia Boldú
Dipòsit Legal: T. 1428-2012

Al/W/Ti sample was very small (50 nm). However, the high concentration of oxygen suggests that the tungsten is oxidised.

Platinum peak appears because this analysis was made after the deposition of platinum electrodes and the area used for the EDS microanalysis included the electrode parts.

Element	Weight %
Si	40.28
O	30.13
W	15.21
Pt	14.38
Total	*100.00*

Table 4-3 EDS analysis for WO_3 nanodot film formed on the micro-hotplate at 27 V followed by reanodizing to 100 V and annealing at 500°C

Figure 4-11 shows XRD pattern recorded from the WO_3 nanodot layer and this diffractogram reveals the presence of three peaks located at 2θ angles of 24°, 28.34° and 33.5° respectively, which correspond to a WO_3 tetragonal crystal phase with space group P4/nmm (ICDD card number 53-434). The absence of peaks from metallic tungsten indicates that it is fully oxidised.

Mean crystal grain size was analysed using XRD, where the value obtained was 8.9±0.3 nm.

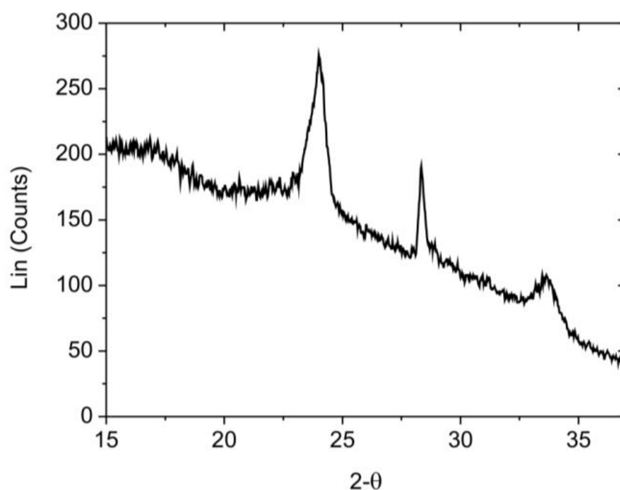

Figure 4-11 XRD pattern recorded for the WO_3 nanodot film formed on the micro-hotplate at 27 V followed by reanodizing to 100 V and annealing at 500°C.

Figure 4-12 shows the 3D image of the crystal structure for the WO_3 grains, divided in plain 001 (Figure 4-12.a) and 010 (Figure 4-12.b). Like in the previous case of alumina supported WO_3 layer, the corners of these pink structures is the location of oxygen atoms and tungsten atoms are located in the centre.

The WO_3 crystalline phase with tetragonal lattice corresponds to a high-temperature WO_3,which is stable even above 740 ºC [2].

UNIVERSITAT ROVIRA I VIRGILI
GAS SENSOR MICROSYSTEMS BASED ON NANOSTRUCTURED LAYERS VIA ANODIC OXIDATION
Raúl Calavia Boldú
Dipòsit Legal: T. 1428-2012

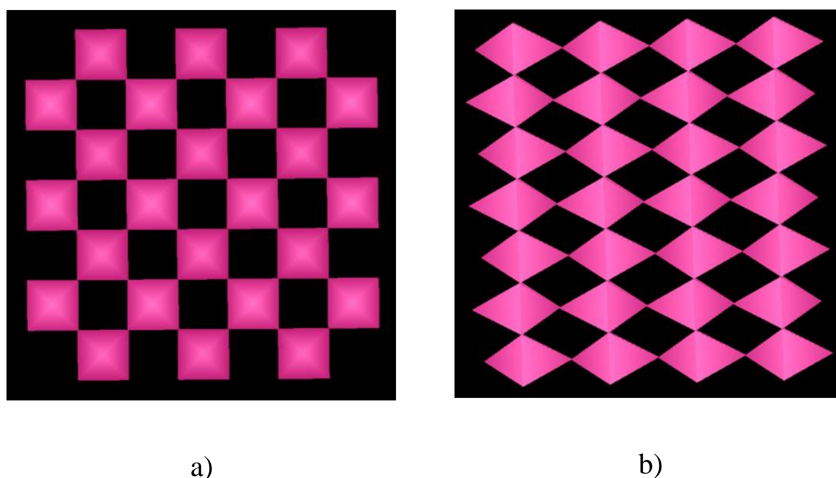

a) b)

Figure 4-12 Crystal images of the WO_3 obtained. a) 001 orientation. b) 010 orientation. The sample is prepared as indicated in Figure 4-11.

Unlike in monoclinic WO_3 crystallites (the most extensively studied WO_3 crystalline structure for gas sensing), which become larger in size as the annealing temperature is raised, the grain size of tetragonal WO_3 grains is insensitive to further heat treatments [3]. Therefore, aggregation of the WO_3 nanodots during annealing and the formation of a continuous WO_3 layer have been avoided and the sensing material retains its distinct dot-like morphology when the sensor chips are assembled.

4.3 Summary

In this chapter we showed the results of morphological, compositional and crystallographic studies of the films synthesised as described in the two approaches successfully implemented in this work for nanostructuring tungsten oxide film, i.e., the porous

UNIVERSITAT ROVIRA I VIRGILI
GAS SENSOR MICROSYSTEMS BASED ON NANOSTRUCTURED LAYERS VIA ANODIC OXIDATION
Raúl Calavia Boldú
Dipòsit Legal: T. 1428-2012

alumina supported WO_3 layer and the self-organised WO_3 nanodot film.

It was found that the porous alumina supported tungsten oxide layer prepared on the micro-hotplate transducer is composed of WO_3 crystalline phase with monoclinic structure with a P21/n (14) space group, so that it may be a proper active layer for gas sensing applications.

The self-organised tungsten oxide nanodot film prepared on the same micro-hotplate was found to be nanocrystalline WO_3 with tetragonal structure with space group P4/nmm, which is rather different from the typical tungsten oxide layers for gas sensing applications prepared by other techniques (i.e. WO_3 phase with monoclinic crystal structure). Nevertheless, the film can potentially be tested as active layer because, most likely, it is nanocrystalline metal oxide semiconductor.

In both cases, the surface-to-volume ratio of the tungsten oxide films has been substantially increased due to the nanostructuring without increasing the area to be heated on the hotplate.

The morphology, chemical composition and crystalline structure of the two types of nanostructured tungsten oxide films prepared on the micro-hotplate transducers have encouraged us to perform a trial to assess gas sensing ability of the new microsensors, the results shown in Chapter 5.

UNIVERSITAT ROVIRA I VIRGILI
GAS SENSOR MICROSYSTEMS BASED ON NANOSTRUCTURED LAYERS VIA ANODIC OXIDATION
Raúl Calavia Boldú
Dipòsit Legal: T. 1428-2012

4.4 Bibliography

[1] Vallejos, S.; Stoycheva, T.; Umek, P.; Navio, C.; Snyders, R.; Bittencourt, C.; Llobet, E.; Blackman, C.; Moniz, S.; Correig, X., Au nanoparticle-functionalised WO3 nanoneedles and their application in high sensitivity gas sensor devices, *Chem. Commun.*, (2011) **47**, 565.
[2] Kehl, W. L.; Hay, R. G.; Wahl, D., The Structure of Tetragonal Tungsten Trioxide, *J. Appl. Phys.*, (1952) **23**, 212.
[3] Solis, J. L.; Heel, A.; Kish, L. B.; Granqvist, C. G.; Saukko, S.; Lantto, V., Gas-sensing properties of nanocrystalline WO3 films made by advanced reactive gas deposition, *J. Am. Ceram. Soc.*, (2001) **84**, 1504.

UNIVERSITAT ROVIRA I VIRGILI
GAS SENSOR MICROSYSTEMS BASED ON NANOSTRUCTURED LAYERS VIA ANODIC OXIDATION
Raúl Calavia Boldú
Dipòsit Legal: T. 1428-2012

Chapter 5

Gas sensing characterisation

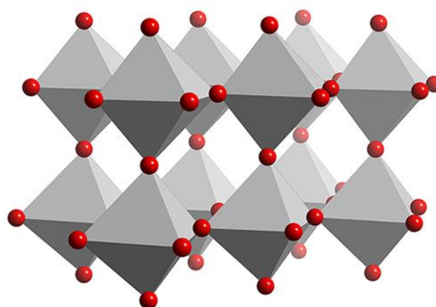

UNIVERSITAT ROVIRA I VIRGILI
GAS SENSOR MICROSYSTEMS BASED ON NANOSTRUCTURED LAYERS VIA ANODIC OXIDATION
Raúl Calavia Boldú
Dipòsit Legal: T. 1428-2012

UNIVERSITAT ROVIRA I VIRGILI
GAS SENSOR MICROSYSTEMS BASED ON NANOSTRUCTURED LAYERS VIA ANODIC OXIDATION
Raúl Calavia Boldú
Dipòsit Legal: T. 1428-2012

5. Gas sensing characterisation

The substantially improved morphologies (drastically enlarged surface-to-volume ratio), appropriate chemical compositions and favourable crystalline structures of the two types of nanostructured tungsten oxide films prepared on the micro-hotplate transducers suggest that gas sensing ability of these films will be substantially improved relative to a smooth, unstructured WO_3 layer formed normally on a flat substrate. The gas sensing characteristics of the nanostructured WO_3 films fabricated on the micromachined transducers have been the subject of investigation done in this work.

5.1 Gas sensing set-up

The system developed for characterisation of gas sensing behaviour of the devices obtained in this work is built up of two parts: the injection of gas and the monitoring of the resistance of the sensing devices.

The gas controlling module is composed of two sub-modules: the gas mixing, using mass flow controllers (MFC), and moisture generating, employing a liquid mass flow controller (LMFC) unit.

All controlling devices used for gas injection are digital devices (from Bronkhorst High-Tech B. V.) and they use a communication standard protocol called FlowBus, which allows for selecting a set

UNIVERSITAT ROVIRA I VIRGILI
GAS SENSOR MICROSYSTEMS BASED ON NANOSTRUCTURED LAYERS VIA ANODIC OXIDATION
Raúl Calavia Boldú
Dipòsit Legal: T. 1428-2012

point and controlling the actual flow of every mass-flow by computer.

Two MFCs mix the dry air used as balance and the gas of interest, called contaminant. This contaminant comes from a calibrated cylinder. By employing the software, it is possible to vary the set points of both MFCs in order to maintain a constant flow in the output, fixed at 100 ml/min, obtaining different contaminant concentrations.

Using the following formula, it is possible to determine the set point of the MFC for the contaminant, expressed in percent of opening (% *cal bot*).

$$\%\,cal\ bot = \frac{Total\ flow\ system \cdot Concentration\ out \cdot 100}{Concentration\ cal\ bot \cdot Max\ flow\ MFC} \tag{5-1}$$

where the *Total flow system* is the flow in the characterisation chamber, the *Concentration out* is the contaminant gas concentration sought, the *Concentration cal bot* is the concentration of the contaminant gas in its calibrated bottle (cylinder) and the *Max flow MFC* is the maximum flow that can control the MFC.

Since the maximum flow that can control the MFC used for the contaminant is 100 ml/min, which equals the value chosen for the flow in the characterisation chamber, the previous equation can be simplified.

$$\%\,cal\ bot = \frac{100 \cdot Concentration\ out}{Concentration\ cal\ bot} \tag{5-2}$$

UNIVERSITAT ROVIRA I VIRGILI
GAS SENSOR MICROSYSTEMS BASED ON NANOSTRUCTURED LAYERS VIA ANODIC OXIDATION
Raúl Calavia Boldú
Dipòsit Legal: T. 1428-2012

The remainder of the flow up to the total flow (i.e., 100 ml/min) is configured as the set point for the MFC connected to the dry air cylinder.

Both the contaminant and balance gases used are dry, so, in order to add humidity, it is necessary to add a relative humidity generating module. This module comprises a liquid mass flow meter from the same company (i.e., Bronkhorst High-Tech B. V.), which is compatible with the same communication protocol (FlowBus). Therefore, all flow controlling systems can be organised and synchronised by the same computer.

The moisture generating system is based on a pressurised (at 1 bar helium) distilled water cylinder. The water arrives pressurised to the inlet of the LMFC (up to 20 gr/hour), which controls the water injected to the gas-water mixing device.

Controlled evaporation and mixing (CEM) is the gas-water mixing device. It works controlling the mixing temperature, because increasing this temperature, which can be computer controlled, results in an improved mixing process. Since the sensor chamber is connected at the output of this device, the tubing distance must be kept as short as possible in order to prevent water condensation.

Configuring the LMFC and CEM parameters is not easy because at low mixing temperatures it is necessary to use very low quantities of water (very precise LMFC controlling) and at high mixing temperatures the probability of water condensation increases (due to temperature drop at the sensor chamber) and, additionally, MOX

UNIVERSITAT ROVIRA I VIRGILI
GAS SENSOR MICROSYSTEMS BASED ON NANOSTRUCTURED LAYERS VIA ANODIC OXIDATION
Raúl Calavia Boldú
Dipòsit Legal: T. 1428-2012

gas sensors respond to gas temperature (sensor surface heating by gas flow). Therefore, there must be a compromise between the mixing temperature and the water injected in the gas flow.

The third parameter affecting the configuration of the moisture generation and mixing is the gas flow set point. The higher the gas flow is, the more water is necessary to obtain the moisture level sought and this can be better dealt with by the LMFC.

In summary, for this study it was necessary to obtain moisture levels that ranged from 0 to 80 % RH (relative humidity) employing as low as possible mixing temperature (CEM temperature) and using a flow rate as similar as possible to 100 ml/min.

In the Bronkhorst [1] web page, there is an application that calculates the water that must be introduced into the system (in grams per hour) in order to obtain the RH sought. System parameters are the gas flow rate, room temperature, water pressure, water temperature, CEM temperature…).

Using this web page application, the optimal flow rate and CEM temperature were finally set to 200 ml/min and 56.7ºC, respectively.

UNIVERSITAT ROVIRA I VIRGILI
GAS SENSOR MICROSYSTEMS BASED ON NANOSTRUCTURED LAYERS VIA ANODIC OXIDATION
Raúl Calavia Boldú
Dipòsit Legal: T. 1428-2012

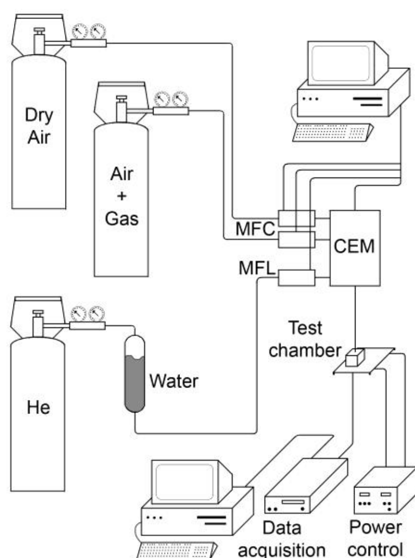

Figure 5-1 Completed monitoring set-up for gas sensor characterisation

Table 5-1 shows the parameters introduced in the Bronkhorst application and Table 5-2 shows the grams per hour of water that are necessary to be input in the system in order to obtain a RH ranging from 0 to 80 %.

Water pressure	1 bar
Water temperature	20 ºC
Mixing temperature	56.7 ºC
Gas pressure	1 bar
Gas temperature	20 ºC
Gas flow	200 ml/min
Accuracy of LMFC	±0.075 gr/hour

Table 5-1 Parameters for the calculation of the LMFC set-points

UNIVERSITAT ROVIRA I VIRGILI
GAS SENSOR MICROSYSTEMS BASED ON NANOSTRUCTURED LAYERS VIA ANODIC OXIDATION
Raúl Calavia Boldú
Dipòsit Legal: T. 1428-2012

Relative Humidity (%)	Water injection (gr/hour)
0	0
10	0.17
20	0.34
30	0.52
40	0.71
50	0.90
60	1.10
70	1.31
80	1.53

Table 5-2 Water injection to obtain various relative humidity values for the conditions indicated in Table 5-1

Measurements were performed as follows. The test vapour was flown into a stainless steel test chamber housing the gas sensors. Since the baseline resistance of the sensors in dry air was rather high (TΩ level at room temperature), the sensor test chamber was placed inside a Faraday cell-like structure and 3 way coaxial cables were used in order to counteract the effect produced by external noise on the data acquired. Sensor resistance was monitored with a 6517A model Keithley equipment (Keithley Instruments Inc., USA). A low current scanner card (6521 model, Keithley Instruments Inc., USA) was used for realising sensors connections. Data acquisition was performed at a sampling rate of 1 sample per second by a program written in LabView. The operating temperature of the sensors was set by applying a constant voltage to their heating elements.

5.2 Sensor employing porous alumina supported WO_3 active layer

Characterisation of the micro-hotplate sensors employing nanostructured porous-alumina-supported WO_3 active layers was performed using the system described in Figure 5-1. The study was focused on hydrogen detection. Figure 5-2 shows sensor response to a 1000 ppm H_2 atmosphere at 150 ºC working temperature. As the sensor resistance dropped by 3 orders of magnitude, it was necessary to set a logarithmic Y axis.

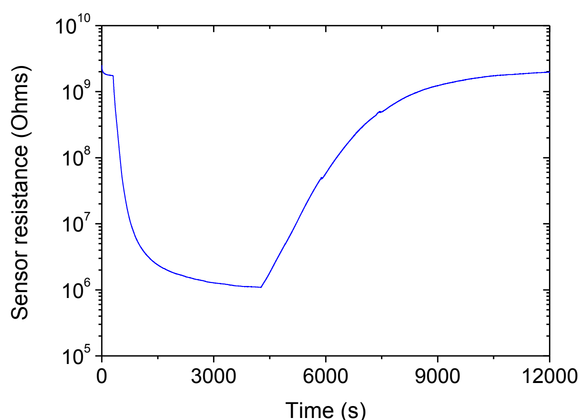

Figure 5-2 Response of a micro-hotplate sensor employing nanostructured porous-alumina-supported WO_3 active layer to 1000 ppm of H_2 at 150 ºC

As seen from Figure 5-2, the sensor exhibits huge response to hydrogen and this response is well reproducible as shown in Figure 5-3. This figure demonstrates the sensor response to 1000 ppm of H_2 at operating temperature of 300 ºC for 3 cycles of the response and recovery. It is possible to verify that the initial and final baseline values are nearly identical in each cycle.

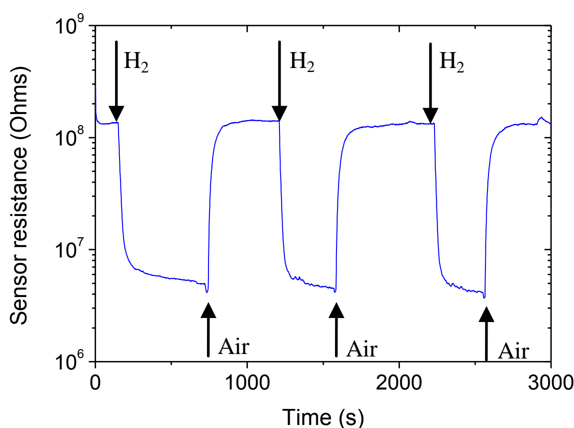

Figure 5-3 Sensor response to 1000 ppm H_2 at 300°C. The sensor was fabricated as indicated in Figure 5-2.

Figure 5-4 shows the sensor response (defined in Equation 5-3) for 1000 ppm H_2 at different operating temperatures.

$$Sensor\ Response = \frac{R_{air}}{R_{gas}} \quad (5\text{-}3)$$

The sensor response versus the working temperature was fitted using a Gaussian approximation. The formula used for this fitting is the following:

$$y = y_0 + \frac{A}{w \cdot \sqrt{\pi/2}} \cdot e^{-2 \cdot \frac{(x - x_C)^2}{w^2}} \quad (5\text{-}4)$$

Employing Origin software, the Gauss fitted equation is obtained as follows:

$$y = 15.294 + \frac{130633.32}{81.043 \cdot \sqrt{\pi/2}} \cdot e^{-2 \cdot \frac{(x - 146.034)^2}{81.043^2}} \quad (5\text{-}5)$$

where the correlation determined with this model was: R^2=0.998

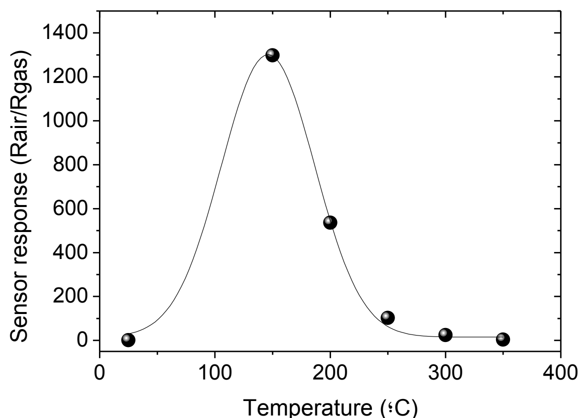

Figure 5-4 Response of the sensor to 1000 ppm of H_2 at different operating temperatures. The sensor was fabricated as indicated in Figure 5-2.

The sensor response was studied at various working temperatures, ranging from room temperature to 350 ºC. Typically, the nanostructured WO_3 films appeared to have their maximum response to hydrogen at an operating temperature of 150 ºC. From 100 ºC (theoretical) to 200 ºC (measured), the sensor shows a response to 1000 ppm H_2 that is higher than 500, so it can be used in all this operating temperature range with high response.

Typically for MOX based gas sensors, the response time drops when the operating temperature is decreased because reaction kinetics are faster at higher temperatures.

Figure 5-5 shows the sensor response and recovery times, defined as the time necessary to reach 90 % of the final response value, for 1000 ppm H_2. In this figure it is possible to see that these time

spans increase exponentially when the operating temperature is lowered. At 150 ºC, the response time was 1000 seconds and the recovery time was near 13,000 seconds. Since the response time was too high, conducting a study at room temperature was unreasonable, and the sensor having such a long recovery time would not find any practical application. Therefore, higher operating temperatures are required for the sensor produced.

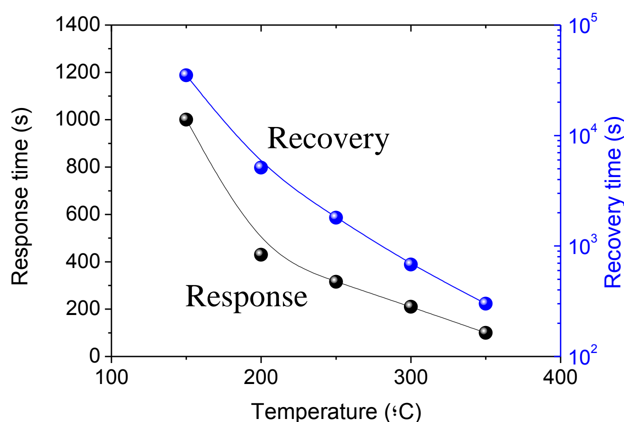

Figure 5-5 Response and recovery times for the sensor to 1000 ppm of H_2 at different operating temperatures. The sensor was fabricated as indicated in Figure 5-2.

Evaluating the results obtained for the sensor response (Figure 5-4) and the response and recovery times (Figure 5-5) obtained at different working temperatures, we decided that the optimal working temperature range was from 200 ºC to 250 ºC because the response for 1000 ppm H_2 remains above 100 and the response and recovery times are lower than 400 and 5000 seconds, respectively.

In the gas sensing characterisation of these micro-hotplate sensors employing nanostructured porous-alumina-supported WO_3 active

UNIVERSITAT ROVIRA I VIRGILI
GAS SENSOR MICROSYSTEMS BASED ON NANOSTRUCTURED LAYERS VIA ANODIC OXIDATION
Raúl Calavia Boldú
Dipòsit Legal: T. 1428-2012

layers, the response to 1000 ppm of propane at 250 ºC was studied as well (Figure 5-6). Figure 5-6 shows the response obtained for this gas, where it is possible to see that the response time is very short (near 20 seconds) but the recovery is rather long (about 10,000 seconds). The sensor response value obtained for this gas is 45. This shows that the sensor can be used for the detection of flammable gases because for the particular case in which a continuous monitoring of a potentially explosive atmosphere is to be performed, high response and low response time are more important than recovery time.

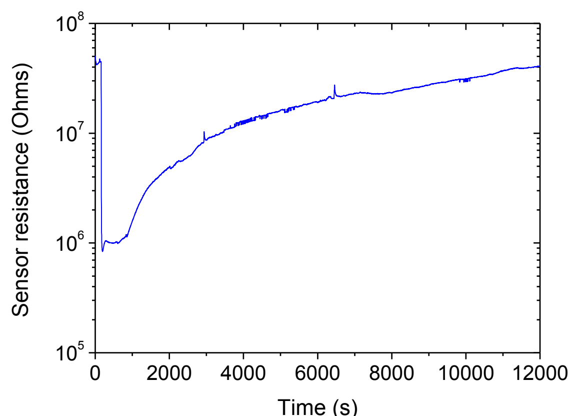

Figure 5-6 Response for 1000 ppm of propane at 250 ºC. The sensor was micro-hotplate sensors employing nanostructured porous-alumina-supported WO_3 active layer.

5.3 Sensor with WO_3 nanodot active layer

In this work, gas sensing characterisation was done to the second sensor type - a micro-hotplate sensor employing self-organised

WO_3 nanodot film as active layer - like in the previous trial, for hydrogen detection.

Figure 5-7 shows the sensor response to 1000 ppm of H_2 at 250 ºC. As in the previous case, the response is very high and the Y-axis is configured in logarithmic scale. The initial resistance value for this sensor is extremely high (tens of GOhm at 250 ºC), so their monitoring must be made carefully in order to measure them properly.

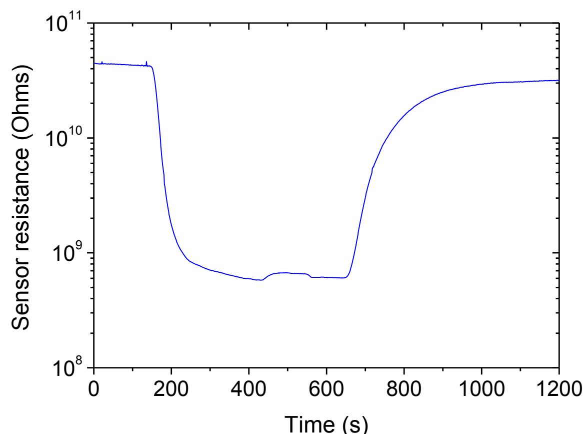

Figure 5-7 Sensor response to 1000 ppm H_2 at 250 ºC. The sensor was a micro-hotplate sensor employing self-organised WO_3 nanodot film as active layer.

The response/operating temperature characterisation was studied for this sensor type (Figure 5-8) and, like in the previous case, the experimental data points were fitted using the following Gauss mathematical model:

$$y = y_0 + A \cdot e^{\left(-\frac{(x-x_C)^2}{2 \cdot w^2}\right)} \qquad (5\text{-}6)$$

The Origin software was used for fitting the data obtaining the following final mathematical model for the response/operating temperature:

$$y = 10 + 93 \cdot e^{\left(-\frac{(x-150)^2}{2 \cdot 54.87^2}\right)} \quad (5\text{-}7)$$

The correlation coefficient obtained for this Gaussian curve fitting was r^2=0.999, so there is a very high correlation level.

The maximum experimentally measured response was obtained at 150 ºC, while the Gaussian fitting predicts the maximum response to be at 165 ºC.

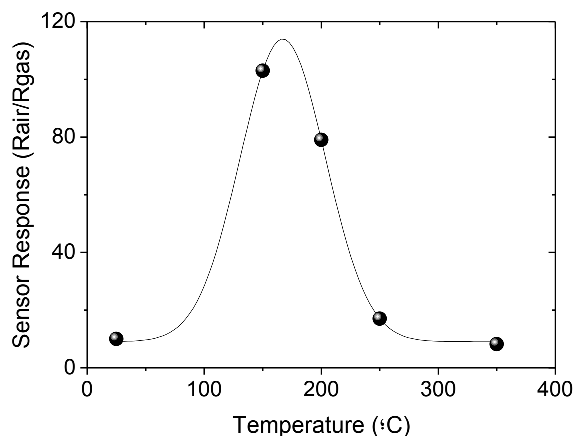

Figure 5-8 Sensitivity vs temperature for 1000 ppm of H_2. The sensor was as indicated in Figure 5-7.

The response and recovery times decrease when the temperature is raised (Figure 5-9). Although these are higher at room temperature, at 200 ºC the response and recovery times are of 100 and 500 seconds, respectively. At this temperature, the response value is

UNIVERSITAT ROVIRA I VIRGILI
GAS SENSOR MICROSYSTEMS BASED ON NANOSTRUCTURED LAYERS VIA ANODIC OXIDATION
Raúl Calavia Boldú
Dipòsit Legal: T. 1428-2012

about 80. Therefore, it can be concluded that, as a compromise, 200ºC is a suitable operating temperature.

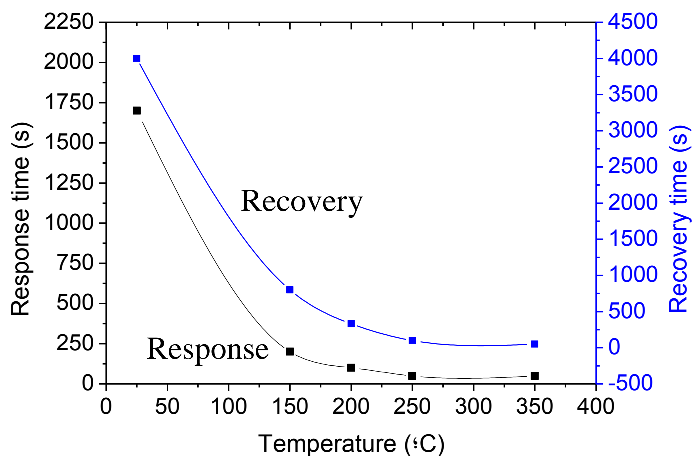

Figure 5-9 Response and recovery times to 1000 ppm of H_2 at different operating temperatures. The sensor was as indicated in Figure 5-7.

Figure 5-10 shows the sensor response for low hydrogen concentrations (5, 10, 15 and 20 ppm) at 200 ºC. The obtained responses have good signal-to-noise ratio. The response time for these low hydrogen concentrations is short as well.

UNIVERSITAT ROVIRA I VIRGILI
GAS SENSOR MICROSYSTEMS BASED ON NANOSTRUCTURED LAYERS VIA ANODIC OXIDATION
Raúl Calavia Boldú
Dipòsit Legal: T. 1428-2012

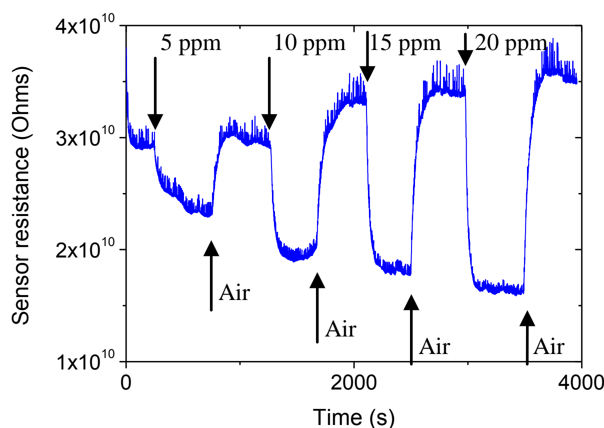

Figure 5-10 Response for 5, 10, 15 and 20 ppm H_2 at 200 ºC. The sensor was as indicated in Figure 5-7.

The sensor response defined in Equation 5-3 for low hydrogen concentrations shows a linear concentration dependence (see Figure 5-11). Again, the Origin software was used to calculate a linear fitting for the actual sensor responses (employing five repetitions of every concentration in the mathematical calculation). The results were added to Figure 5-11 in red colour. The following equation shows the linear fitting obtained where x is the hydrogen concentration in ppm and y the estimated sensor response. The correlation coefficient obtained was r^2=0.994 indicating that the sensor response for low concentrations of hydrogen is linear.

$$y = 0.05x + 1 \quad (5\text{-}8)$$

UNIVERSITAT ROVIRA I VIRGILI
GAS SENSOR MICROSYSTEMS BASED ON NANOSTRUCTURED LAYERS VIA ANODIC OXIDATION
Raúl Calavia Boldú
Dipòsit Legal: T. 1428-2012

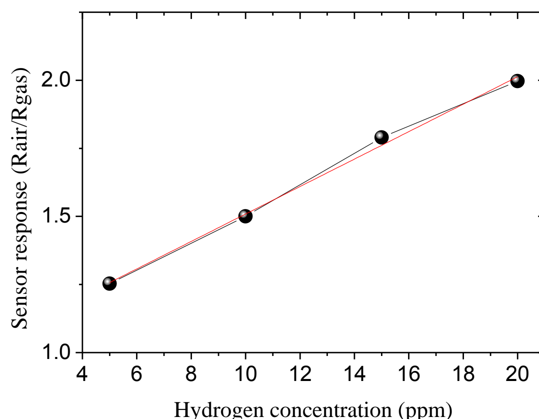

Figure 5-11 Linear fitting of the sensor response for low concentrations of H_2 at 200 ºC. The sensor was as indicated in Figure 5-7.

For this type of sensors, the response to other gases, such as 8000 ppm ethanol at 200 ºC was also studied. Ethanol response is shown in Figure 5-12. In this figure it is possible to see that the response and recovery times are short (several seconds) and that the response value for the given gas and concentration was about 85.

MOX gas sensors shown, in general, large responses to ethanol, so the response of 85 is not considered as high, especially if we consider the very high concentration value tested (i.e., 8000 ppm).

UNIVERSITAT ROVIRA I VIRGILI
GAS SENSOR MICROSYSTEMS BASED ON NANOSTRUCTURED LAYERS VIA ANODIC OXIDATION
Raúl Calavia Boldú
Dipòsit Legal: T. 1428-2012

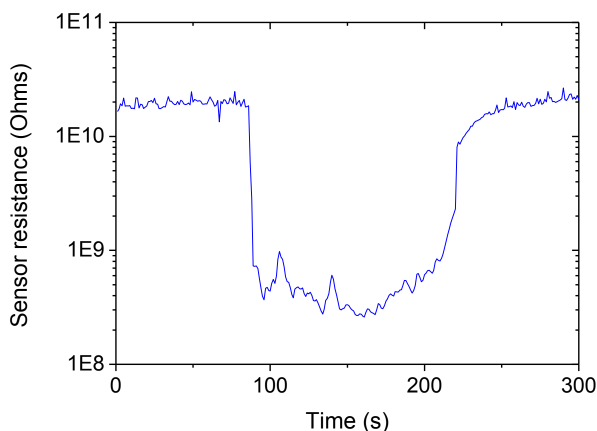

Figure 5-12 Response for 8000 ppm of ethanol at 200 ºC. The sensor was as indicated in Figure 5-7.

Figure 5-13 shows the response for 2 cycles of synthetic air and 600 ppm C_2H_4 at 200 ºC. It is possible to see that the response is repeatable with a response value of 7.5 and a response time of just a few seconds.

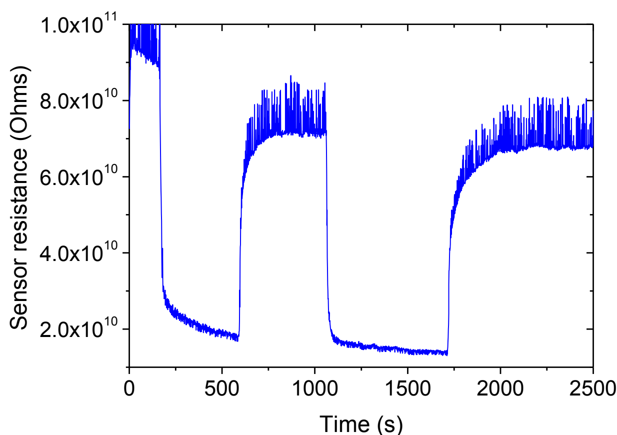

Figure 5-13 Response for 600 ppm of C_2H_4 at 200 ºC. The sensor was as indicated in Figure 5-7.

UNIVERSITAT ROVIRA I VIRGILI
GAS SENSOR MICROSYSTEMS BASED ON NANOSTRUCTURED LAYERS VIA ANODIC OXIDATION
Raúl Calavia Boldú
Dipòsit Legal: T. 1428-2012

These sensors have been characterised for different gases and we can conclude that they are quite selective for hydrogen, because the response is several times higher for this gas than for the other gases.

The findings of this work may be considered as first steps towards improving the selectivity, not only sensitivity, of tungsten oxide based gas sensors.

Figure 5-14 shows the sensor response to changes in the ambient RH. The moisture effect is high for moisture levels lower than 50 % RH, but at higher concentrations the effect decreases. For this reason, these sensors can be operated in environments either without a humidity or at the humidity levels higher than 50 % RH, like, for example, in a fuel cell.

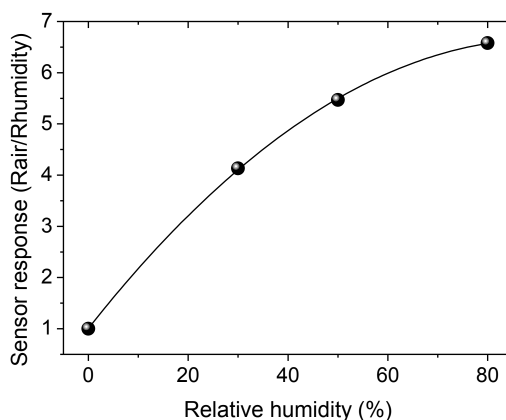

Figure 5-14 Response to different RH at 150 ºC. The sensor was as indicated in Figure 5-7.

UNIVERSITAT ROVIRA I VIRGILI
GAS SENSOR MICROSYSTEMS BASED ON NANOSTRUCTURED LAYERS VIA ANODIC OXIDATION
Raúl Calavia Boldú
Dipòsit Legal: T. 1428-2012

5.4 Comparison between the planar and nanostructured WO_3 layers

The main objective of this thesis is increasing the response of micromachined gas sensors via nanostructuring their active layer. Figure 5-15 shows the response and the response time for a micro-hotplate sensor employing a flat, sputtered-deposited, WO_3 sensing layer, to 1000 ppm of H_2 at various operating temperatures. In these sensors, the same deposition conditions were employed on micro-hotplate substrates that were identical to the ones used for the nanostructured sensors described above

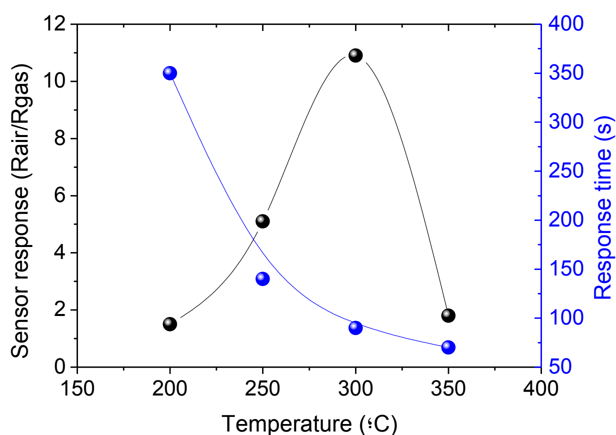

Figure 5-15 Sensor response and response time to 1000 ppm H_2 for a traditional planar WO_3 active layer fabricated on a micromachined transducer at different operating temperatures

In this work, two types of nanostructured WO_3 layers have been prepared on the micromachined transducers, and, in both cases, the highest responses to hydrogen was obtained at about 150 ºC. The

UNIVERSITAT ROVIRA I VIRGILI
GAS SENSOR MICROSYSTEMS BASED ON NANOSTRUCTURED LAYERS VIA ANODIC OXIDATION
Raúl Calavia Boldú
Dipòsit Legal: T. 1428-2012

response time of the sensors at such a low operating temperature was high, but a good trade-off between the sensor response (high) and the response time (short) was obtained at 200 ºC.

The maximum response to hydrogen for the flat WO_3 sensing layer on the same micro-transducer was obtained at 300 ºC, so our new gas sensing devices need a significantly lower operating temperature.

In the case of porous-alumina-supported WO_3 sensing layer, the maximum sensor response to 1000 ppm of H_2 was 1300 (at 150 ºC) and 500 (at 200 ºC). At 150 ºC and 200 ºC, the response time was 1000 and 450 seconds, respectively.

For the case of self-organised WO_3 nanodot film, the maximum sensor response obtained for 1000 ppm of H_2 was 110 at 150 ºC and 80 at 200 ºC. The response times were 200 and 125 seconds at 150 ºC and 200 ºC, respectively.

The sensor response for the nanostructured WO_3 sensing layers is several times higher than for the planar WO_3 layer. This is especially true for the case of porous alumina supported WO_3 active layer.

Obviously, the response time of the nanostructured sensors at the optimal operating temperature is larger than that of the flat sensors. However, since the nanostructured sensors exhibit an extremely high response, it is possible to increase their operating temperature

UNIVERSITAT ROVIRA I VIRGILI
GAS SENSOR MICROSYSTEMS BASED ON NANOSTRUCTURED LAYERS VIA ANODIC OXIDATION
Raúl Calavia Boldú
Dipòsit Legal: T. 1428-2012

above the optimal in order to decrease the response time without jeopardising the gain in sensitivity.

5.5 Gas sensing mechanism

It is known that the working mechanism of tungsten trioxide film lies in a change of the resistance of the oxide, which is dependent on the free electron density in the space charge layer. Hydrogen is a typical reducing gas, increasing the conductivity of a metal oxide upon interaction. During the chemisorptions process, the analyte dissociates onto the film surface by injecting electrons. These free electrons reduce the surface depletion region (thereby increase the surface conductivity), whose electron concentration is mainly determined by the concentration of stoichiometric defects such as oxygen vacancies present in the material.

From the sensor responses to the different gases obtained in the present work, the nanostructured tungsten oxide behaves as an *n*-type metal oxide semiconductor.

Molecular hydrogen dissociates on the surface of the platinum electrodes giving hydrogen ions and electrons. Like explained in the state of the art chapter, in a WO_3 lattice the main oxidation state is W^{6+}. The hydrogen ions adsorbed on the surface reduce the tungsten oxidation state to W^{5+} by the electrons generated in the hydrogen decomposition reaction, and the sensor resistance drops.

UNIVERSITAT ROVIRA I VIRGILI
GAS SENSOR MICROSYSTEMS BASED ON NANOSTRUCTURED LAYERS VIA ANODIC OXIDATION
Raúl Calavia Boldú
Dipòsit Legal: T. 1428-2012

The combination of H^+ with surface bound O^{2-} ions produced by the reduction of W^{6+} forms H_2O molecules, which adsorb on, and readily escape from, the WO_3 layer at elevated temperature.

When the hydrogen gas is purged from the chamber by dry air flow, the stoichiometry of the affected part of the tungsten oxide film is gradually restored, and the resistance returns to its initial value.

At room temperature, the H_2O molecules generated by the tungsten reduction reaction are all adsorbed on the film surface, and this suppresses the response of the sensor to hydrogen gas. However, at 150 ºC, the water begins to evaporate and the diffusion of the adsorbed oxygen species and the adsorption rate of H_2 gas on the device active layer get strongly enhanced, generating more charge carriers resulting in the increased sensor response. As the oxidation-reduction reaction is endothermic, the excess water is expected to escape until equilibrium is reached with the humidity of the surrounding atmosphere.

However, further rise in the operating temperature, accompanying by the greatly enhanced water evaporation, depresses the equilibrium of the adsorption/desorption reactions and reduces the number of active adsorption sites, which is associated with the weakening of the sensor response at temperatures above 150 ºC.

The similarity in the temperature-dependent behaviour of the responses obtained from the two types of nanostructured WO_3 films

UNIVERSITAT ROVIRA I VIRGILI
GAS SENSOR MICROSYSTEMS BASED ON NANOSTRUCTURED LAYERS VIA ANODIC OXIDATION
Raúl Calavia Boldú
Dipòsit Legal: T. 1428-2012

suggests that the structuring of the tungsten oxide active layer at the nanoscale is the key factor that controls the behaviour.

5.6 Summary

In this chapter the gas sensing studies have been performed for the two different sensor types, employing however the same micro-hotplate transducers, prepared in accord with the two approaches developed in this thesis for nanostructuring tungsten oxide film, namely, the porous-alumina-supported WO_3 film and the self-organised WO_3 nanodot film as active layers.

In the trial for porous-alumina-supported WO_3 sensors (first type), a high sensor response (1300 to 1000 ppm H_2 at 150 ºC) and a long response time (1000 seconds) have been obtained.

For the WO_3 nanodot sensor (second type), the sensor response time in 1000 ppm of H_2 at 150 ºC was 110 and a 200 second only, which is obviously better than for the first sensor type. However, these sensors exhibited relatively lower sensitivity to 1000 ppm H_2 (~100 to at 150 ^{o}C).

The difference is because the second type sensor is considered as two-dimensional, limiting the response kinetics to the sensitive film surface, while the first type sensor is three-dimensional since the diffusion of chemical species within the nanotubes and their interaction with the tube walls play an important role in the detection mechanism.

UNIVERSITAT ROVIRA I VIRGILI
GAS SENSOR MICROSYSTEMS BASED ON NANOSTRUCTURED LAYERS VIA ANODIC OXIDATION
Raúl Calavia Boldú
Dipòsit Legal: T. 1428-2012

All the nanostructured WO_3 layers developed in this work appeared to be substantially, by orders of magnitude, more sensitive to the gas than the standard flat WO_3 layer.

The advantages are due to the nanostructured morphologies of sensor active layers complemented by the substantially enlarged film surface area and, hence, the surface-to-volume ratio.

5.7 Bibliography

[1] Bronkhorst, www.bronkhorst.com, In.

Chapter 6

Conclusions and future work

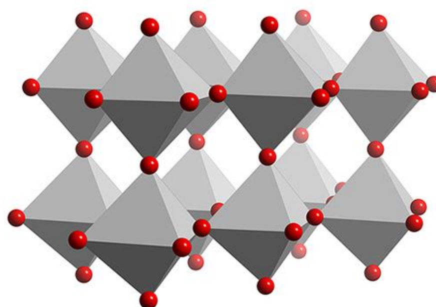

UNIVERSITAT ROVIRA I VIRGILI
GAS SENSOR MICROSYSTEMS BASED ON NANOSTRUCTURED LAYERS VIA ANODIC OXIDATION
Raúl Calavia Boldú
Dipòsit Legal: T. 1428-2012

UNIVERSITAT ROVIRA I VIRGILI
GAS SENSOR MICROSYSTEMS BASED ON NANOSTRUCTURED LAYERS VIA ANODIC OXIDATION
Raúl Calavia Boldú
Dipòsit Legal: T. 1428-2012

6 Conclusions and future work

Major conclusions derived from the entire work are formulated below. New challenges and directions for future work arisen from the findings of this thesis are given then.

6.1 Conclusions

(1) In the present work, integral technologies have been developed for tungsten oxide gas sensors on silicon-based micro-hotplates, having a substantially increased sensitivity, due to nanostructuring the sensing layers. As the key material, porous anodic alumina films (layers) have been synthesised and employed as either templates or parts of electrochemical systems for growing porous-anodic-alumina-supported WO_3 layers or self-organized WO_3 nanodot films as sensor's active layers.

With the original experimental setup developed and integrated with relevant instrumentation and controlling software for anodising metal layers onto silicon wafers, experiments on anodising thin layers of Al and Al/Ti bilayers have been performed and the conditions have been optimised for growing the porous alumina templates and performing porous-alumina-assisted anodising of the underlying tungsten metal.

(2) The facile, one-step method has been developed and experimentally justified for preparing nanoporous alumina templates suitable for being used as supporting layers for tungsten

UNIVERSITAT ROVIRA I VIRGILI
GAS SENSOR MICROSYSTEMS BASED ON NANOSTRUCTURED LAYERS VIA ANODIC OXIDATION
Raúl Calavia Boldú
Dipòsit Legal: T. 1428-2012

oxide sputter-deposition. Alternatively, a modified, one-step version of anodising the Al/W metal bilayer has been developed to grow an array of tungsten oxide nanodots for being used as gas sensing film having significantly enlarged surface-to-volume ratio.

(3) Two original approaches have been successfully implemented based on a lift-off patterning process for synthesising two principle types of nanostructured tungsten oxide layers using porous alumina as (1) supporting template for magnetron sputter-deposition of WO_3 layers and (2) as part of the electrochemical system that provided the growth of self-organised WO_3 nanodots. Gas sensor chips have been fabricated on 100-mm silicon wafers in accordance with the technologies developed and packaged.

(4) The results of analytic studies performed in this thesis have shown that the porous-alumina-supported tungsten oxide layer prepared on the micro-hotplate transducer is composed of WO_3 crystalline phase with monoclinic structure while the self-organised tungsten oxide nanodot film prepared on the micro-hotplate is nanocrystalline WO_3 with tetragonal structure. In both cases, the surface-to-volume ratio of the tungsten oxide films has been substantially increased due to the nanostructuring without increasing the area to be heated on the hotplate.

(5) Gas sensing studies have been performed for the two sensor types, employing however the same micro-hotplate transducers, prepared in accord with the two approaches developed in this thesis for nanostructuring tungsten oxide film, namely, the porous-

UNIVERSITAT ROVIRA I VIRGILI
GAS SENSOR MICROSYSTEMS BASED ON NANOSTRUCTURED LAYERS VIA ANODIC OXIDATION
Raúl Calavia Boldú
Dipòsit Legal: T. 1428-2012

alumina-supported WO_3 film (first type) and the self-organised WO_3 nanodot film (second type) as active layers.

In hydrogen atmosphere, the first type sensor exhibited a very high response (1300 to 1000 ppm H_2 at 150 ºC) but a long response time (1000 seconds). For the second type, the sensor response time in 1000 ppm of H_2 at 150 ºC was as short as 110 and 200 seconds, which is enormously faster than for the first type sensor. However, the second type sensor exhibited relatively lower sensitivity to 1000 ppm H_2 (~100 to at 150 ^{o}C).

Thus, although the response time for the sensor employing the porous-alumina-supported WO_3 layer is rather long, the response value is very high, so that it seems reasonable to increase the operating temperature to some 200°C to obtain a good trade-off between the response time and response value.

The second type sensors have been characterised for more gases (ethylene, ethanol) and we can conclude that they are quite selective for hydrogen, because the response is several times higher for this gas than for the other gases. The findings of this work may be considered as first steps towards improving the selectivity, not only sensitivity, of tungsten oxide based gas sensors.

The difference between the two sensor types arises because the second type sensor is considered as two-dimensional, limiting the response kinetics to the sensitive film surface, while the first type sensor is three-dimensional since the diffusion of chemical species within the nanotubes and their interaction with the tube walls play

UNIVERSITAT ROVIRA I VIRGILI
GAS SENSOR MICROSYSTEMS BASED ON NANOSTRUCTURED LAYERS VIA ANODIC OXIDATION
Raúl Calavia Boldú
Dipòsit Legal: T. 1428-2012

an important role in the detection mechanism. Additionaly and importantly, the effective surface area in the first type sensor is relatively larger than that in the second type sesnor.

All the nanostructured WO_3 layers developed in this work appeared to be substantially (on orders of magnitude) more sensitive to the gas than the standard flat WO_3 layer.

(6) The findings revealed in this thesis have proved that the advantages of the technologies developed are due to the nanostructured morphologies of the sensor active layers, accompanied by the substantially enlarged film surface and the reduced power consumption of the end devices, as well as due to the successfully making the anodizing processes and relevant materials compatible with standard silicon-based technology for micro-hotplate transducer fabrication.

Conclusively, the goal of the present thesis – to develop integral technologies for tungsten oxide gas sensors on silicon-based micro-hotplates, having a substantially increased sensitivity, due to nanostructuring the sensing layers through the application of porous anodic alumina films as templates and parts of electrochemical systems for growing porous-anodic-alumina-supported and self-organized nanostructured tungsten oxide layers – has been achieved.

UNIVERSITAT ROVIRA I VIRGILI
GAS SENSOR MICROSYSTEMS BASED ON NANOSTRUCTURED LAYERS VIA ANODIC OXIDATION
Raúl Calavia Boldú
Dipòsit Legal: T. 1428-2012

6.2 Future work

6.2.1 Effect of surface roughness of sputter-deposited aluminium

For porous anodising of aluminium, it is important to start from a good-quality, microscopically flat surface of the aluminium layer. In case of thick metal layers, electropolishing is commonly used to obtain a flat and reproducible aluminium surface. However, when it goes to thin metal layers sputter-deposited onto silicon wafers, electropolishing cannot be carried out.

A magnetron device of a sputtering-deposition machine works either at a constant voltage (DC) or at an alternating voltage (RF), and for the same power applied during the deposition, the thickness of a film is bigger for DC sputter-deposition due to relatively higher sputtering rates. However, the quality of the deposited layers is better for the RF mode from the grain size point of view. The deposition rate for aluminium (Table 6-1) is lower than that for other materials like platinum, so it is necessary to use longer deposition times and, under these conditions, the temperature of the substrate inevitably increases during the sputtering. The typical thickness for the aluminium layer ranges from 400 nm to 1000 nm, so the deposition time at 200 W by DC magnetron ranges between 4000 and 10000 seconds, respectively. Since the deposition time is rather long, the temperature of the silicon wafer rises significantly and the grains of aluminium within the film grow bigger,

UNIVERSITAT ROVIRA I VIRGILI
GAS SENSOR MICROSYSTEMS BASED ON NANOSTRUCTURED LAYERS VIA ANODIC OXIDATION
Raúl Calavia Boldú
Dipòsit Legal: T. 1428-2012

protruding over the film surface in the form of hillocks of submicrometer sizes (Figure 6-1).

	Ti		Al		W		Pt	
Power (W)	DC	RF	DC	RF	DC	RF	DC	RF
100	0.4		0.5	0.3	0.7	0.4	1.4	0.7
150	0.5	0.3	0.7	0.4	1.0	0.5	2.0	1.0
200	0.7	0.4	1	0.6	1.3	0.7	2.7	1.3
250	0.8	0.6	1.2	0.75	1.6	0.8	3.3	1.5
300	1		1.6		1.8		3.9	

Table 6-1 Deposition rates in Angstroms per second at a pressure of 3 mTorr and 20 sccm of argon at a distance of 35 mm between the target and the sample for a sputtering ATC Orion 8-HV. AJA International

Figure 6-1 shows SEM images of a 500-nm thick aluminium layer obtained in a single sputter-deposition step and in a number of interruptions of sputtering process. In the left column, SEM views show the sample obtained by the single sputter-deposition, in which a number of big grains (≈500 nm size) are clearly seen. Contrarily, such grains are not observed in the right column images of the surfaces prepared with interruptions because the lower substrate temperature, due to the interruptions, helps to maintain the grain size smaller.

UNIVERSITAT ROVIRA I VIRGILI
GAS SENSOR MICROSYSTEMS BASED ON NANOSTRUCTURED LAYERS VIA ANODIC OXIDATION
Raúl Calavia Boldú
Dipòsit Legal: T. 1428-2012

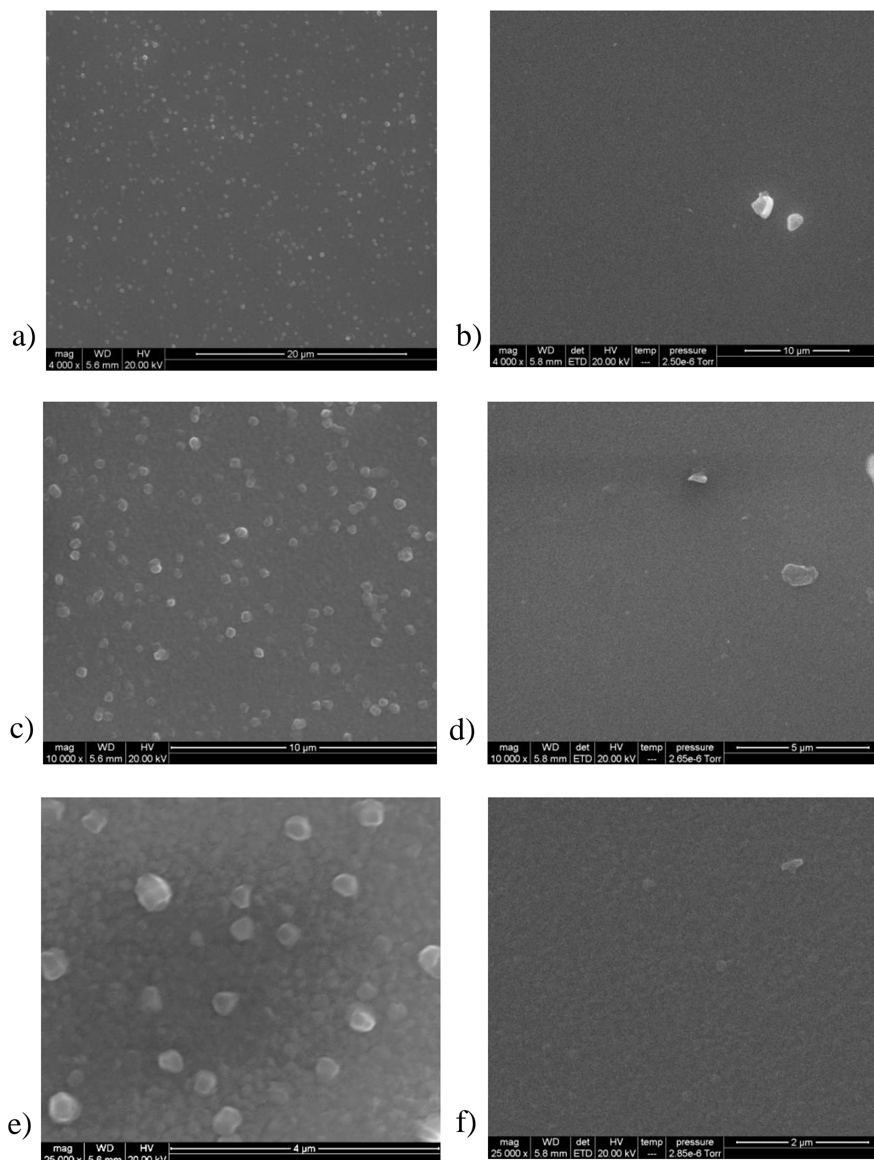

Figure 6-1 SEM images of the surface of a 500-nm thick aluminum layer sputter-deposited on silicon wafer by DC magnetron technique at 200 W, 35 mm of distance and 3 mTorr using an ATC Orion 8-HV. AJA International sputtering machine in a single deposition step a) 4000 x c) 10000 x e) 25000 x and with interruptions b) 4000 x d) 10000 x f) 25000 x. The scale bar on all images is the same

UNIVERSITAT ROVIRA I VIRGILI
GAS SENSOR MICROSYSTEMS BASED ON NANOSTRUCTURED LAYERS VIA ANODIC OXIDATION
Raúl Calavia Boldú
Dipòsit Legal: T. 1428-2012

These grains observed on the surface of the one-step sputter-deposited film worsens the quality of porous anodic film (see Figure 4-5 and Figure 6-2), which then is transformed to the Al/valve-metal interface making the dot-like oxide less ordered.

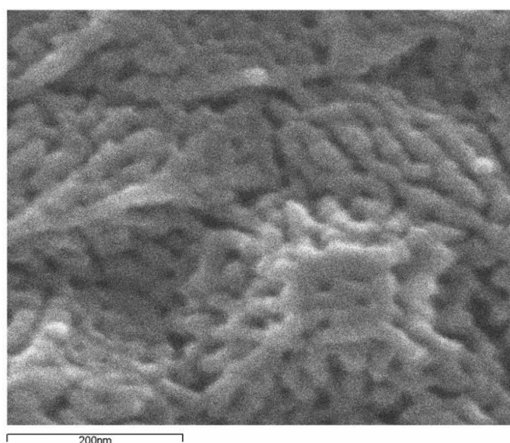

Figure 6-2 ESEM image of a porous alumina film obtained by anodising of a 500-nm thick one-step sputter-deposited aluminium layer at 27 V in 0.2 M sulphuric acid

The interruptions in the sputter-deposition process limit the maximum temperature reached by the substrate during the deposition process. For instance, interrupting the aluminium deposition every 10 minutes results in a temperature of the substrate, which effectively decreases the grain size in the aluminium layer.

Figure 6-3 shows the differences in the aluminum layers deposited by sputtering. Figure 6-3.a shows a photograph of the 500-nm thick aluminium layer obtained by DC sputtering at 200 W in the usual way (one-step deposition step) and Figure 6-3.b shows a photo of two silicon wafer pieces with a 500-nm thick aluminum layer on top obtained by DC sputtering at 200 W with interruptions of the

UNIVERSITAT ROVIRA I VIRGILI
GAS SENSOR MICROSYSTEMS BASED ON NANOSTRUCTURED LAYERS VIA ANODIC OXIDATION
Raúl Calavia Boldú
Dipòsit Legal: T. 1428-2012

deposition process. While in the sample obtained with interruptions the aluminium layer has a mirror-like surface, the sample obtained in a single deposition step scatters the light, which indicates that the surface of the sample grown with interruptions is definitely flatter and, importantly, does not contain crystals protruding over the surface.

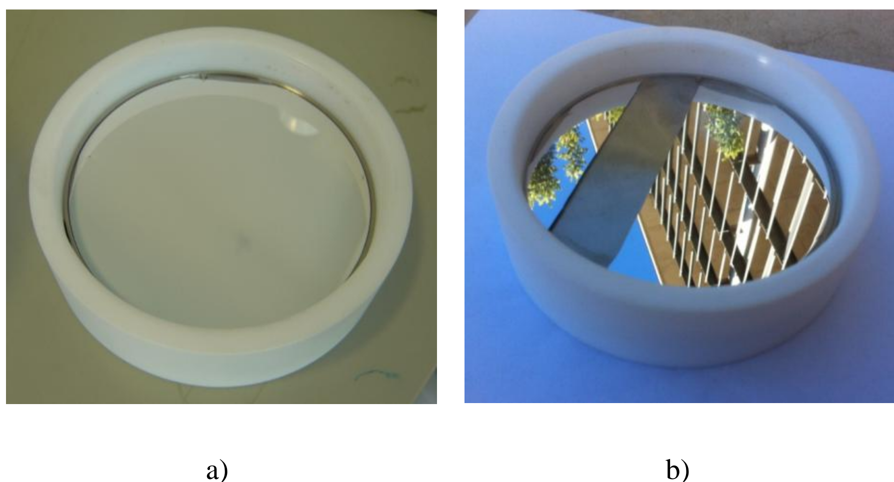

a) b)

Figure 6-3 Aluminium sputter-deposited on a silicon substrate to a thickness of 500-nm using 200 W DC magnetron. a) Single deposition step. b) Interruptions during the deposition.

Figure 6-4.a shows a 2 x 2 μm AFM image of the sample grown with interruptions. Figure 6-4.b shows a profile across the sample in Figure 6-4.a and the mean height of the grains was calculated using a population of 100 particles. The mean height obtained was 29 nm, so the surface produced is very flat. The AFM images were processed by the WSxM program [5] and using the free software ImageJ. While the mean size of the grains in the sample obtained by one step deposition process is 404 nm, this size of the film prepared with interruptions is 264 nm, which is about twice as

smaller. Thus, the future challenge associated with anodizing aluminium or Al-containing multilayers will be the preparation of aluminium layers by sputter-deposition with interruptions and growth of anodic films on such layers and under the layers on other valve metals.

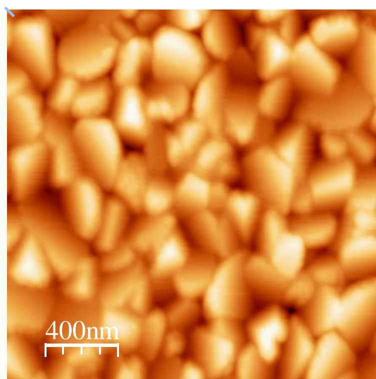

a)

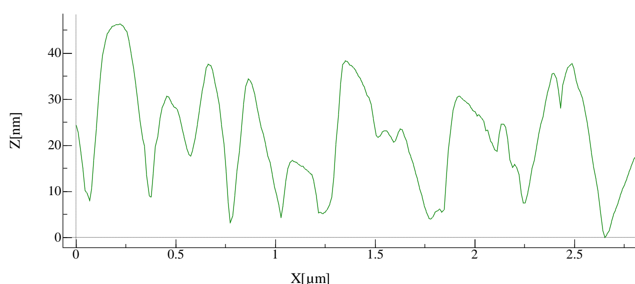

b)

Figure 6-4 AFM image of aluminium layer obtained by DC magnetron method with interruptions. a) AFM image with the line of the profile extracted. b) Profile of the line marked in the AFM image

UNIVERSITAT ROVIRA I VIRGILI
GAS SENSOR MICROSYSTEMS BASED ON NANOSTRUCTURED LAYERS VIA ANODIC OXIDATION
Raúl Calavia Boldú
Dipòsit Legal: T. 1428-2012

6.2.2 Effect of the aspect ratio of porous-alumina-assisted tungsten oxide nanostructures on their gas sensing properties

The sensitivity for the WO_3 nanodot layer may further increase due to increasing the aspect ratio of the nanostructures, i.e. by growing them longer. However, the process of making platinum electrodes of top of the film having longer column-like nanostructures by sputter-deposition and lift-off technique needs to be carefully investigated and optimized before putting it in practice. Alternatively, the electrodes may be formed not above but under the anodic film, if such an architecture may be suitable for anodizing. These aspects may be the subject of future work.

6.2.3 Employing other read-out techniques like pseudorandom sequences for temperature modulation

Using different measuring techniques it is possible to increase the sensitivity and the selectivity of a sensor and it is interesting to use these techniques in order to try improving these parameters. Modulating the operating temperature of the sensors has been reported to result in selectivity improvements. Pseudorandom sequences can be used to optimise the temperature modulation in micro-hotplate sensors.

UNIVERSITAT ROVIRA I VIRGILI
GAS SENSOR MICROSYSTEMS BASED ON NANOSTRUCTURED LAYERS VIA ANODIC OXIDATION
Raúl Calavia Boldú
Dipòsit Legal: T. 1428-2012

Appendix

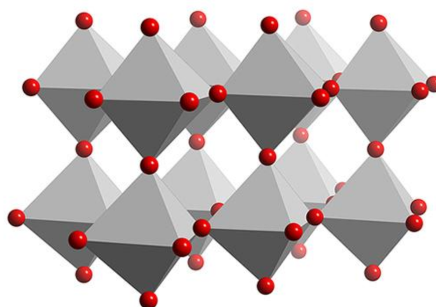

UNIVERSITAT ROVIRA I VIRGILI
GAS SENSOR MICROSYSTEMS BASED ON NANOSTRUCTURED LAYERS VIA ANODIC OXIDATION
Raúl Calavia Boldú
Dipòsit Legal: T. 1428-2012

UNIVERSITAT ROVIRA I VIRGILI
GAS SENSOR MICROSYSTEMS BASED ON NANOSTRUCTURED LAYERS VIA ANODIC OXIDATION
Raúl Calavia Boldú
Dipòsit Legal: T. 1428-2012

Appendix

Calculation of image corrections for FIB

FIB uses an ion beam in order to perform a deposition or etching on the surface of the sample. The deposition (Figure 1) is based on a precursor and a focused beam of ions, which breaks the precursor molecules. These broken molecules deposit on the surface of the sample the material sough and the residual species are pumped away. The quality of the layers obtained by this method is not very good because impurities remain on the sample from the ion beam and precursor by-products not fully pumped away.

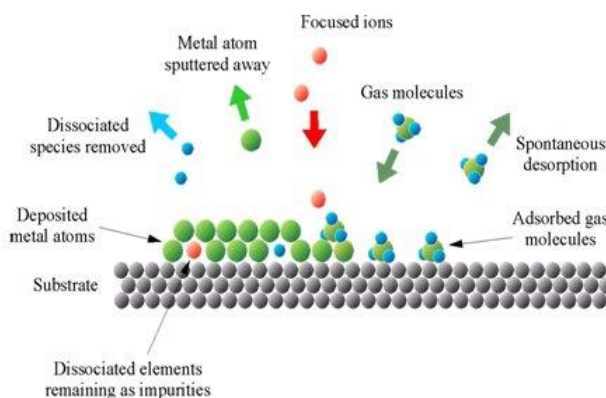

Figure 1 Deposition using FIB

Etching by FIB (Figure 2) employs a focused beam of ions for promoting the reaction of a gas inserted in the chamber with the surface of the sample. The reaction species are in gas phase at room temperature and these are pumped away. Therefore, the surface of the sample is thinned, layer by layer, and the system can, eventually, cut the sample.

UNIVERSITAT ROVIRA I VIRGILI
GAS SENSOR MICROSYSTEMS BASED ON NANOSTRUCTURED LAYERS VIA ANODIC OXIDATION
Raúl Calavia Boldú
Dipòsit Legal: T. 1428-2012

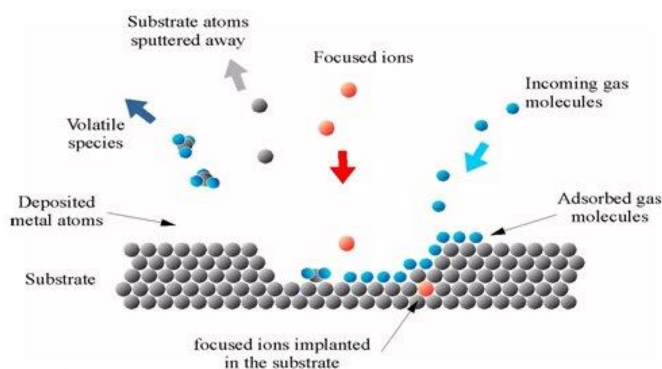

Figure 2 Etching using FIB

FIB-SEM have two beam types, ions (deposition and etching) and electrons (low-speed deposition and imaging), so if the two beams have a known angle (Figure 3) the image measurements can be corrected.

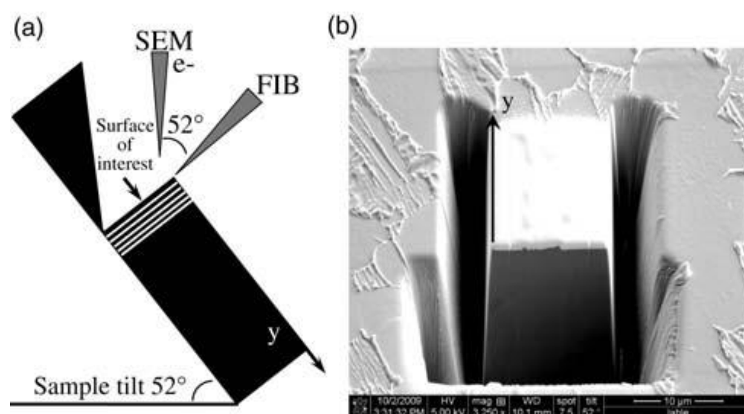

Figure 3 FIB-SEM schematic for the incidating angles [1]

If the sample is tilted the same degrees of the angle formed by the electron and ion beams, the cutting obtained is perpendicular to the surface of the sample (Figure 3).

UNIVERSITAT ROVIRA I VIRGILI
GAS SENSOR MICROSYSTEMS BASED ON NANOSTRUCTURED LAYERS VIA ANODIC OXIDATION
Raúl Calavia Boldú
Dipòsit Legal: T. 1428-2012

In the FIB-SEM used the angle from both beams is 52º, so the sample is tilted this angle for cutting. Electron beam is tilted the complementary angle from the sample tilted (i.e, 38º).

Since the SEM e-beam is tilted 38º, in the image obtained the vertical size of objects does not show actual values and, therefore, it needs to be corrected using a rectangle triangle as the one shown in Figure 4.

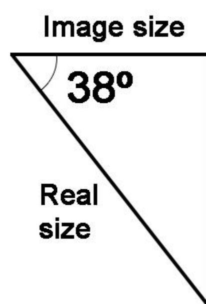

Figure 4 Tilt correction for SEM image

Since the substrate is tilted 52º and the image obtained has not auto tilt correction enabled, the size in vertical measurements must be calculated manually using the rectangle triangle shown in Figure 4. Using trigonometry basics, the final equation for size correction is as follows:

$$Real\ vertical\ size = \frac{Vertical\ size\ measured}{\cos(90º - 52º)} \quad (1)$$

UNIVERSITAT ROVIRA I VIRGILI
GAS SENSOR MICROSYSTEMS BASED ON NANOSTRUCTURED LAYERS VIA ANODIC OXIDATION
Raúl Calavia Boldú
Dipòsit Legal: T. 1428-2012

Bibliography

[1] Ding, R. G.; Jones, I. P., An FIB-SEM slice-and-view study of three-dimensional beta phase distribution in Ti-6Al-4V, *J. Electron Microsc.*, (2011) **60**, 149.